



universität
wien

DISSERTATION

Titel der Dissertation

Functional analyses of chlorite dismutase-like proteins from
Listeria monocytogenes and *Nitrobacter winogradskyi*

angestrebter akademischer Grad

Doktorin der Naturwissenschaften (Dr. rer.nat.)

Verfasserin:	Mag. Stephanie Füreder
Matrikel-Nummer:	9825649
Dissertationsgebiet (lt. Studienblatt):	Ökologie
Betreuer:	Univ.-Prof. Dr. Michael Wagner

Wien, im September 2009

የክፍል ስም

Index

Section A	General Introduction and Outline	7
Section B	Characterisation of the chlorite dismutase homologue of <i>Listeria monocytogenes</i>	23
Section C	The true function of the putative chlorite dismutase from <i>L. monocytogenes</i> remains concealed	61
Section D	The truncated chlorite dismutase of <i>Nitrobacter winogradskyi</i> is a fully functional chlorite degrading enzyme	97
Appendix		
	Minimal Medium for <i>L. monocytogenes</i>	119
	Abbreviations	122
	Zusammenfassung /Summary	124
	Acknowledgements	130
	Curriculum Vitae	132

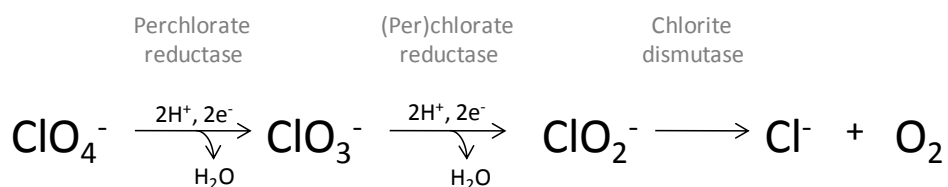
Section A

General Introduction and Outline

Dissimilatory reduction of (per)chlorate

Oxochlorates are of general interest as environmental contamination by them can be a serious health and environmental problem. Perchlorate (ClO_4^-), mainly resulting from anthropogenic pollution, can be ubiquitously found in different environments like soil, vegetation, groundwater and surface water. Besides this it is also known from a few natural sources e.g. in Texas, New Mexico, Utah and Chile (29, 32). Perchlorate is mainly used as oxidizer in flares, pyrotechnics, explosives, and numerous other applications. The recent detection of environmental contamination has primarily been associated with its use in rocket propellants and missile motors. If high amounts of perchlorate are ingested by human, it interferes with iodine uptake by the thyroid gland leading to serious health problems (32). Other oxochlorates like chlorate (ClO_3^-), chlorite (ClO_2^-), hypochlorite (HOCl), and chlorine dioxide (ClO_2) are used or released as by-products of bleaching processes in textile, paper and pulp industries, as disinfectants and herbicides. However, the natural occurrence of oxochlorates is limited and therefore does not explain the high diversity of (per)chlorate reducing bacteria (PCRB) (7).

Bioremediation of (per)chlorate is an important aspect in removal of anthropogenic pollution with these compounds. The complete reduction of ClO_4^- under anaerobic conditions occurs in three steps involving at least two enzymes (7, 38). $\text{ClO}_4^-/\text{ClO}_3^-$ thereby act as alternative electron acceptors:



Equation 1: according to (35)

Perchlorate reductase (Pcr) is a molybdopterin-dependent enzyme of the DMSO reductase family, capable of catalyzing the first two steps from ClO_4^- to ClO_2^- , thereby producing one water

molecule at each step (4, 23). In mere chlorate reducers like *Ideonella dechloratans*, chlorate reductase, an enzyme belonging to the same family as the Pcr, is responsible for the production of chlorite (38).

Initially, chlorate reduction has primarily been associated with nitrate-respiring organisms, where chlorate was assumed to be a competitive substrate for nitrate reductase (34). However, the end product of chlorate reduction is toxic chlorite and there was no evidence that these bacteria could utilize this compound (7). Since the discovery of PCRb, it was shown that many, but not all of these organisms, are capable of nitrate respiration (2, 6, 15, 42, 43). Interestingly, in 2002, it was shown for the PCRb *Dechloromonas suillum* that the concomitant presence of perchlorate and nitrate in the medium, generally induced nitrate reduction prior to perchlorate reduction. Only when all nitrate was consumed, perchlorate reduction and also chlorite dismutase activity was detectable. This demonstrates an important link between the nitrate and perchlorate reduction pathways in this organism (6). A slightly different picture was shown by Giblin *et al.* (15). In strain per1ace, perchlorate and nitrate reduction occur simultaneously if both substrates are present. The rate of reduction was only marginally reduced with both substrates present compared to the presence of only one of these electron acceptors. Thus, the authors suggested the presence of two different reductases involved.

Chlorite dismutase – a ubiquitous chlorite degrading enzyme?

The last step in the reduction pathway from toxic ClO_2^- to harmless Cl^- and O_2 is catalyzed by chlorite dismutase (Cld). The name “chlorite dismutase” is misleading as the reaction is not a dismutation or disproportionation of chlorite, but an intramolecular redox reaction. The correct name should therefore be chloride:oxygen oxidoreductase or chlorite O₂-lyase (EC1.13.11.49) as suggested by Hagendoorn *et al.* (18). However, to be in conformance with broadly established nomenclature, throughout this thesis, the name chlorite dismutase will be used.

Section A

The first report about a chlorite dismutase was published by van Ginkel *et al.* in 1996 (39) characterizing the Cld of strain GR-1 (now *Azospira oryzae* GR-1). Since then, six other *cld* genes from validated PCRBs as well as other known bacteria followed. These comprise Cld from the PCRBs *I. dechloratans* (33, 37), *Dechloromonas agitata* (3, 6, 27), *Dechloromonas aromatica* RCB (35) and *Pseudomonas chloritidismutans* (26) as well as the extremely thermophilic bacterium *Thermus thermophilus* HB8 (11) and the nitrite-oxidizer '*Candidatus Nitrospira defluvii*' (25). Furthermore, for *Moorella perchloratireducens* (2) and *Alicyclyphilus denitrificans* Strain BC (41), chlorite degradation could be shown but no experimental and/or sequence data about *cld* was provided.

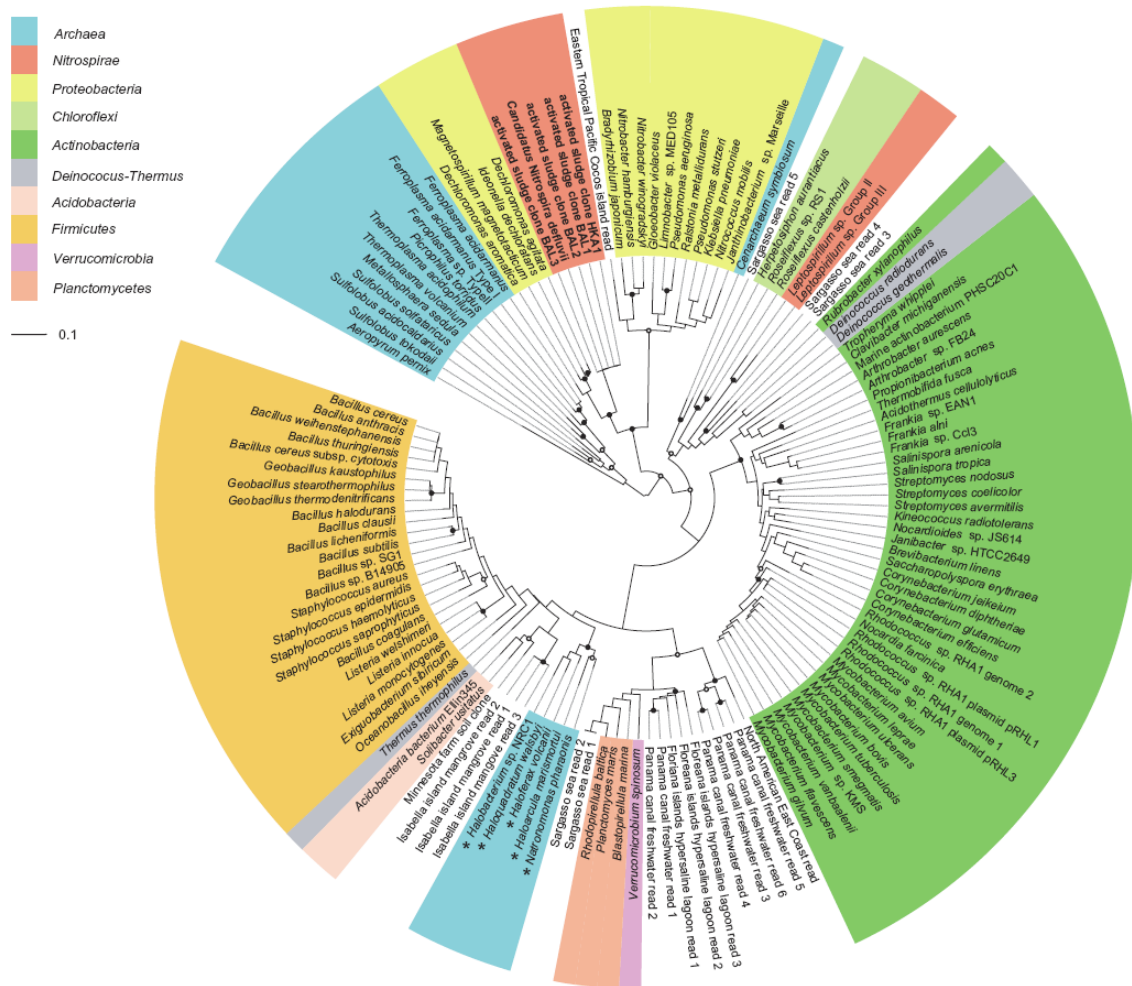


Fig. A.1: Maximum likelihood tree based on amino acid sequences of Cld-like proteins. Colours depict the affiliations of the respective organisms with bacterial and archaeal phyla according to 16S rRNA-based phylogeny. Sequences marked with an asterisk are Cld-like domains in fusion proteins. White circles represent quartet puzzling reliability values $\geq 70\%$. Black circles symbolize additional high parsimony bootstrap support ($\geq 90\%$) based on 100 iterations. The scale bar depicts 0.1 substitutions per residue (with permission from (24)).

Section A

Recently, extensive sequence analysis revealed a large number of genes encoding proteins with similarities to known chlorite dismutases (25). These sequences derive from known and sequenced organisms as well as from metagenomic reads, thereby revealing a huge protein family. Surprisingly, the majority of the sequences belonged to different members of *Bacteria* and *Archaea* not known to respire on (per)chlorate. Cld-based phylogenies also suggested lateral gene transfer of *cld* genes occurring not only within *Bacteria* and *Archaea* but also between these two domains (Fig. A.1 (25)). This ubiquitous distribution of *cld* genes also raises the question if all of these genes really encode functional chlorite dismutases (25). Maixner *et al.* hypothesised that the specialization of Cld in the (per)chlorate reduction pathway might be a relatively recent event in terms of evolution, since chlorite is mainly an industrial contaminant. The association of Cld with an antibiotic monooxygenase domain in *H. volcanii* (1) might also indicate the importance of oxygen formation by Cld to allow further crucial reactions in the cell under oxygen-limited conditions. This is further supported by observations of Coates *et al.* (8). In their study, chlorite degradation by *D. agitata* strain CKB enabled hydrocarbon-oxidizing bacteria to degrade hydrocarbons under anaerobic conditions. Another interesting observation about *cld* was made in the non-PCRB *Staphylococcus aureus*. Ji *et al.* showed that *cld* is a gene essential for growth in *S. aureus* by applying a genome-wide antisense RNA approach (22). This was the first report about a *cld*-like gene being essential, which is remarkable because all known and validated Clds derive from organisms that are not - or only with difficulties - genetically modifiable.

All so far validated Clds share common features like the homo-multimeric structure of the active enzyme with a mean subunit size of 28.5 kDa. All of them are assumed to be located in the periplasm as indicated by signal peptide prediction. The characteristic Soret peak indicated an iron protoheme IX ligand suggested to be a heme b. The optimal temperatures of the validated Clds are between 25°C-30°C and the pH optimum is about pH 6 (26). Reports about the expression of *cld* are controversial. Some studies show a dependence of *cld* expression on low oxygen concentrations and the presence of (per)chlorate (3, 6, 27), whereas others state a basal or even

constitutive *clt* expression under aerobic conditions (7, 25, 42) even without the addition of (per)chlorate.

Thirteen years after the first study of a chlorite dismutase, the mechanism of chlorite degradation was proposed by Lee *et al.* (24). The authors suggest an O-O bond forming mechanism similar to photosystem II. Thereby, compound I results from the transfer of an oxygen atom from chlorite to the ferric heme. The oxygen atoms from compound I and from the generated hypochlorite recombine again to yield O₂ and Cl⁻ (Fig. A.2).

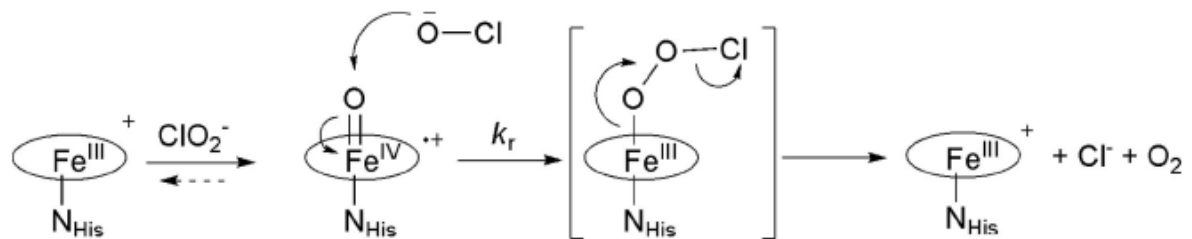


Fig. A.2: Reaction pathway of chlorite degradation by Cld as proposed by Lee *et al.* (with permission from (24))

This mechanism was highly supported by the crystal structure of Cld from *A. oryzae* GR-1 (10) revealing important residues for heme coordination and ligand binding (see section B).

Listeria monocytogenes

As described above, many *clt* or *clt*-like sequences found in the available databases derive from various organisms. The abundance of *clt* in organisms not capable of (per)chlorate reduction was surprising and raised several questions: why do these organisms harbour a chlorite dismutase gene and does the gene product of *clt* really function as a chlorite degrading enzyme in these organisms or does it have a different function? To answer these questions we chose to investigate the putative chlorite dismutase gene of *L. monocytogenes*. This microorganism appeared to be a very suitable candidate to characterize a gene with unknown function due to various reasons: (i) fully sequenced genome available (16), (ii) established lab techniques allow a wide range of different experiments (21), (iii) capability of survival in diverse environments like soil, silage and

sludge (12, 28) as well as intracellularly in different host cells (13, 17, 30) and (iv) well described physiology and pathogenesis (17, 19).

The genus *Listeria* belongs to the phylum *Firmicutes* together with the genera *Bacillus*, *Clostridium*, *Enterococcus*, *Streptococcus* and *Staphylococcus*. *Listeria* spp. are described as non-spore-forming, motile, rod shaped, facultatively-anaerobic, Gram-positive bacteria that can grow over a broad range of pH (pH 4.5 – 9) and temperature (0-45°C) conditions (19). The six species belonging to this genus comprise *Listeria monocytogenes*, *Listeria ivanovii*, *Listeria innocua*, *Listeria seeligeri*, *Listeria welshimeri*, and *Listeria grayi* (31). Only *L. monocytogenes* and *L. innocua* are known pathogens able to cause diseases in humans and/or animals.

L. monocytogenes was first described by E.G.D. Murray in 1926 following an epidemic affecting rabbits and guinea pigs in animal care houses in Cambridge (England) (Fig. A.3). The first human cases were confirmed in 1929 (9).

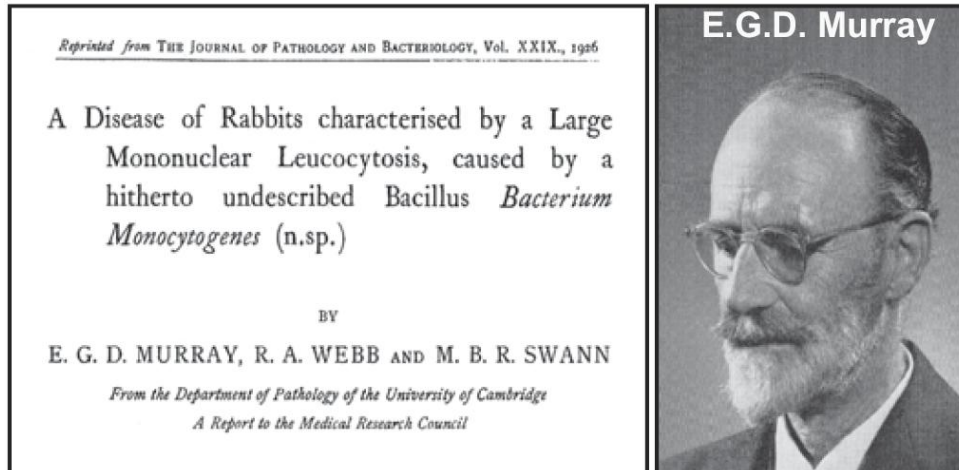


Fig. A.3: First report of *L. monocytogenes* causing an epidemic in rabbits by E.G.D. Murray. *Bacterium monocytogenes* was later on renamed to *Listeria monocytogenes* (taken from (9)).

L. monocytogenes is a food-borne pathogen, thus indicating that ingestion of a high dose of bacteria is necessary to cause a listeriosis outbreak. After oral entry into the human host, *L. monocytogenes* is able to cross the main barriers in the human body: the intestinal, the blood-brain and the placental barrier. Once the bacteria overcome the host immune system, listeriosis manifests as gastroenteritis, meningitis, encephalitis, mother-to-fetus infections and septicaemia

(40). Newborns, elderly and immunocompromised people show the highest risk of this severe infection leading to death in 25-30% of the cases despite an occurrence of only 2-15 cases per million people per year (19, 20, 36).

The survival and growth of *L. monocytogenes* inside various host cells has been extensively investigated. As shown in Figure A.4., *L. monocytogenes* can either force its entry into the host cell by the internalins *inlA* and *inlB* or they are actively phagocytosed by professional phagocytes such as macrophages. These cells of the immune system recognize lipoteichoic acid, a component of the gram-positive bacterial cell wall. Once the bacteria entered the cells they are trapped inside a vacuole called phagosome. To escape into the cytoplasm, the phagosomal membrane is disrupted by the secreted two phospholipases, PlcA and PlcB, and the pore-forming toxin listeriolysin O. Escape from the phagosome and further the phagolysosome, a fusion product of phagosome and bactericidal lysosome, is crucial to protect *L. monocytogenes* from being killed. When bacteria are released into the cytoplasm, they multiply and start to polymerize actin, as observed by the presence of the characteristic actin tails. Actin polymerization allows bacteria to pass into a neighbouring cell by forming protrusions in the plasma membrane. On entry into the neighbouring cell, bacteria are present in a double-membraned vacuole, from which they can escape to perpetuate the cycle (13, 20, 30) (Fig. A.4).

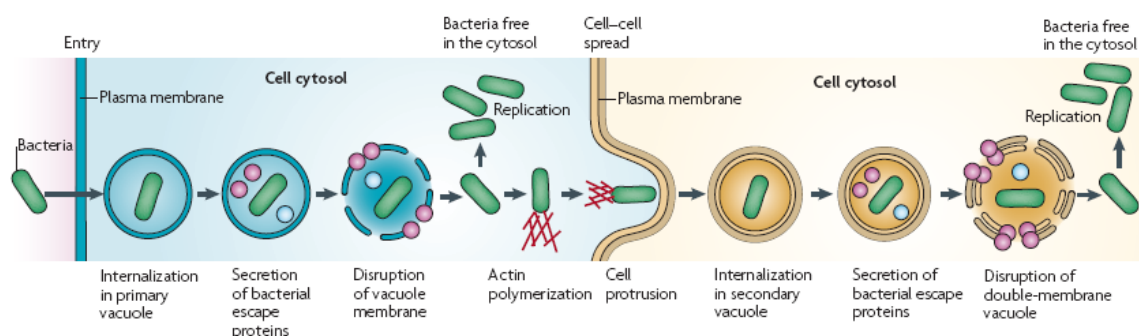


Fig. A.4: The intracellular lifestyle of *Listeria monocytogenes* (with permission from (30))

Inside the phagolysosome, *L. monocytogenes* encounters different microbicidal features that attack the defense mechanism of the bacteria comprising acidification of the vacuole, production

of various antimicrobial proteins and peptides and the generation of different reactive oxygen species (ROS) and reactive nitrogen species (RNS). ROS can result from electron transfer from cytosolic NADPH to molecular oxygen, releasing O_2^- into the phagosomal lumen. Within the phagosome, O_2^- can dismutate to H_2O_2 which can further react to hydroxyl radicals and singlet oxygen. H_2O_2 can also be converted by myeloperoxidases into highly reactive hypochlorous acid (HOCl) and chloramines. RNS occur by the synthesis of reactive NO^\cdot in the cytosol which can then diffuse across the phagosomal membrane. Together with certain ROS, NO^\cdot can convert into nitrogen dioxide, peroxyxynitrite, dinitrogen trioxide and further compounds. ROS and RNS together exert highly toxic effects as they interact with various cellular targets such as thiols, metal centers, nucleic acids and lipids (for a review see (13)).

As already mentioned, chlorite is a highly toxic compound due to its high oxidation potential and could therefore be considered as a ROS. Thus, it is tempting to speculate that Cld could be involved in bacterial survival inside the phagosome by degrading other, closely related compounds. However, in a microarray study by Camejo *et al.* (5), the putative *cld*-gene *Imo2113* of *L. monocytogenes* was not upregulated during infection. This could indicate that Cld either is not necessary during infection or it is already constitutively expressed in sufficient amounts.

Besides the described pathogenic lifestyle of *L. monocytogenes*, this organism is also able to survive and grow in soil, silage, groundwater, and decaying vegetation where it is thought to live as a saprophyte (14). Unfortunately, only very little is known about its environmental lifestyle (for review see (14, 17)). However, the publication of the genome sequence (16) together with previously published physiological studies give a good overview over listerial behaviour and physiology in its inside and outside environment (19).

Considering all available data, it is difficult to answer the question why *Listeria* would need a functional chlorite degrading enzyme. A major aim of this thesis was therefore to elucidate the function of *cld* in *L. monocytogenes* by deletion of the *cld*-homolog *Imo2113* and the subsequent

Section A

phenotypic characterization of the mutant and wild type strains. Furthermore, functional characterization of heterologously expressed and purified Cld (as described by Maixner *et al.* (25)), should be performed to analyze the chlorite degrading properties of Cld (see section B). Based on evidence for a possible regulatory influence of the two-component system ResDE on Cld (see section C) the Cld protein expression profile under anaerobic and aerobic conditions as well as in rich BHI medium and in minimal medium was monitored. To further investigate a putative influence of Cld on the pathogenicity of *L. monocytogenes* and *S. typhimurium*, infection assays with RAW264.7 macrophages were performed. The heterologous expression of *cld* in *E. coli* revealed a highly increased OD₆₀₀, similar to the expression of hemoglobins in *E. coli*. This effect was further investigated concerning a comparable function of these two proteins. Another interesting aspect was a possible peroxidase or catalase function of Cld as already mentioned by Ebihara *et al.* (11) and Lee *et al.* (24). Using different spectroscopic methods, compound I formation of Cld was monitored using different substrates as described in section B and C.

A truncated chlorite dismutase from *Nitrobacter winogradskyi*

Besides the chlorite dismutase gene from the non-PCRB *Listeria monocytogenes*, we were also interested in another unusual chlorite dismutase. *Nitrobacter winogradskyi* is a nitrite-oxidizing alphaproteobacterium encoding a rather short version of Cld of only 184 aa compared to the 250-300 aa long validated Clds. As shown in section D, it lacks the N-terminus and therefore it was interesting to test if the missing part is important for the overall chlorite-degrading activity of the enzyme. Furthermore, we wanted to compare the characteristics of the Cld from *N. winogradskyi* with the Cld of another nitrite-oxidizing bacterium, '*Candidatus Nitrospira defluvii*', published by Maixner *et al.* (25).

References

1. **Bab-Dinitz, E., H. Shmueli, J. Maupin-Furlow, J. Eichler, and B. Shaanan.** 2006. *Haloferax volcanii* PitA: an example of functional interaction between the Pfam chlorite dismutase and antibiotic biosynthesis monooxygenase families? *Bioinformatics* **22**:671-5.
2. **Balk, M., T. van Gelder, S. A. Weelink, and A. J. Stams.** 2008. (Per)chlorate reduction by the thermophilic bacterium *Moorella perchloratireducens* sp. nov., isolated from underground gas storage. *Appl Environ Microbiol* **74**:403-9.
3. **Bender, K. S., S. M. O'Connor, R. Chakraborty, J. D. Coates, and L. A. Achenbach.** 2002. Sequencing and transcriptional analysis of the chlorite dismutase gene of *Dechloromonas agitata* and its use as a metabolic probe. *Appl Environ Microbiol* **68**:4820-6.
4. **Bender, K. S., C. Shang, R. Chakraborty, S. M. Belchik, J. D. Coates, and L. A. Achenbach.** 2005. Identification, characterization, and classification of genes encoding perchlorate reductase. *J Bacteriol* **187**:5090-6.
5. **Camejo, A., C. Buchrieser, E. Couve, F. Carvalho, O. Reis, P. Ferreira, S. Sousa, P. Cossart, and D. Cabanes.** 2009. In vivo transcriptional profiling of *Listeria monocytogenes* and mutagenesis identify new virulence factors involved in infection. *PLoS Pathog* **5**:e1000449.
6. **Chaudhuri, S. K., S. M. O'Connor, R. L. Gustavson, L. A. Achenbach, and J. D. Coates.** 2002. Environmental factors that control microbial perchlorate reduction. *Appl Environ Microbiol* **68**:4425-30.
7. **Coates, J. D., and L. A. Achenbach.** 2004. Microbial perchlorate reduction: rocket-fueled metabolism. *Nat Rev Microbiol* **2**:569-80.
8. **Coates, J. D., R. A. Bruce, and J. D. Haddock.** 1998. Anoxic bioremediation of hydrocarbons. *Nature* **396**:730.
9. **Cossart, P.** 2007. Listeriology (1926-2007): the rise of a model pathogen. *Microbes Infect* **9**:1143-6.
10. **de Geus, D. C., E. A. J. Thomassen, P. Hagedoorn, N. S. Pannu, E. van Duijn, and J. P. Abrahams.** 2009. Crystal structure of chlorite dismutase, a detoxifying enzyme producing molecular oxygen. *Journal of Molecular Biology* **387**:192-206.
11. **Ebihara, A., A. Okamoto, Y. Kousumi, H. Yamamoto, R. Masui, N. Ueyama, S. Yokoyama, and S. Kuramitsu.** 2005. Structure-based functional identification of a novel heme-binding protein from *Thermus thermophilus* HB8. *J Struct Funct Genomics* **6**:21-32.
12. **Fenlon, D. R.** 1999. *Listeria monocytogenes* in the natural environment. **2nd ed.** Marcel Dekker, New York, N. Y.:21-38.
13. **Flannagan, R. S., G. Cosio, and S. Grinstein.** 2009. Antimicrobial mechanisms of phagocytes and bacterial evasion strategies. *Nat Rev Microbiol* **7**:355-66.
14. **Freitag, N. E., G. C. Port, and M. D. Miner.** 2009. *Listeria monocytogenes* - from saprophyte to intracellular pathogen. *Nat Rev Microbiol* **7**:623-8.

15. **Giblin, T., and W. T. Frankenberger, Jr.** 2001. Perchlorate and nitrate reductase activity in the perchlorate-respiring bacterium *perclace*. *Microbiol Res* **156**:311-5.
16. **Glaser, P., L. Frangeul, C. Buchrieser, C. Rusniok, A. Amend, F. Baquero, P. Berche, H. Bloecker, P. Brandt, T. Chakraborty, A. Charbit, F. Chetouani, E. Couve, A. de Daruvar, P. Dehoux, E. Domann, G. Dominguez-Bernal, E. Duchaud, L. Durant, O. Dussurget, K. D. Entian, H. Fsihi, F. Garcia-del Portillo, P. Garrido, L. Gautier, W. Goebel, N. Gomez-Lopez, T. Hain, J. Hauf, D. Jackson, L. M. Jones, U. Kaerst, J. Kreft, M. Kuhn, F. Kunst, G. Kurapkat, E. Madueno, A. Maitournam, J. M. Vicente, E. Ng, H. Nedjari, G. Nordsiek, S. Novella, B. de Pablos, J. C. Perez-Diaz, R. Purcell, B. Remmel, M. Rose, T. Schlueter, N. Simoes, A. Tierrez, J. A. Vazquez-Boland, H. Voss, J. Wehland, and P. Cossart.** 2001. Comparative genomics of *Listeria* species. *Science* **294**:849-52.
17. **Gray, M. J., N. E. Freitag, and K. J. Boor.** 2006. How the bacterial pathogen *Listeria monocytogenes* mediates the switch from environmental Dr. Jekyll to pathogenic Mr. Hyde. *Infect Immun* **74**:2505-12.
18. **Hagedoorn, P. L., D. C. De Geus, and W. R. Hagen.** 2002. Spectroscopic characterization and ligand-binding properties of chlorite dismutase from the chlorate respiring bacterial strain GR-1. *Eur J Biochem* **269**:4905-11.
19. **Hain, T., S. S. Chatterjee, R. Ghai, C. T. Kuenne, A. Billion, C. Steinweg, E. Domann, U. Karst, L. Jansch, J. Wehland, W. Eisenreich, A. Bacher, B. Joseph, J. Schar, J. Kreft, J. Klumpp, M. J. Loessner, J. Dorscht, K. Neuhaus, T. M. Fuchs, S. Scherer, M. Doumith, C. Jacquet, P. Martin, P. Cossart, C. Rusniok, P. Glaser, C. Buchrieser, W. Goebel, and T. Chakraborty.** 2007. Pathogenomics of *Listeria* spp. *Int J Med Microbiol* **297**:541-57.
20. **Hamon, M., H. Bierne, and P. Cossart.** 2006. *Listeria monocytogenes*: a multifaceted model. *Nat Rev Microbiol* **4**:423-34.
21. **Higgins, D. E., Buchrieser C., Freitag N.E.** 2006. Genetic tools for use with *Listeria monocytogenes*. In J.J. Ferreti et al. (ed.), *Gram-positive pathogens*, 2nd ed. ASM Press, Washington D.C.:620 - 633.
22. **Ji, Y., B. Zhang, S. F. Van, Horn, P. Warren, G. Woodnutt, M. K. Burnham, and M. Rosenberg.** 2001. Identification of critical staphylococcal genes using conditional phenotypes generated by antisense RNA. *Science* **293**:2266-9.
23. **Kengen, S. W., G. B. Rikken, W. R. Hagen, C. G. van Ginkel, and A. J. Stams.** 1999. Purification and characterization of (per)chlorate reductase from the chlorate-respiring strain GR-1. *J Bacteriol* **181**:6706-11.
24. **Lee, A. Q., B. R. Streit, M. J. Zdilla, M. M. Abu-Omar, and J. L. DuBois.** 2008. Mechanism of and exquisite selectivity for O-O bond formation by the heme-dependent chlorite dismutase. *Proc Natl Acad Sci U S A* **105**:15654-9.
25. **Maixner, F., M. Wagner, S. Lucker, E. Pelletier, S. Schmitz-Esser, K. Hace, E. Spieck, R. Konrat, D. Le Paslier, and H. Daims.** 2008. Environmental genomics reveals a functional chlorite dismutase in the nitrite-oxidizing bacterium '*Candidatus Nitrospira defluvi*'. *Environ Microbiol* **10**:3043-56.

26. **Mehboob, F., A. F. Wolterink, A. J. Vermeulen, B. Jiang, P. L. Hagedoorn, A. J. Stams, and S. W. Kengen.** 2009. Purification and characterization of a chlorite dismutase from *Pseudomonas chloritidismutans*. *FEMS Microbiol Lett* **293**:115-21.
27. **O'Connor, S. M., and J. D. Coates.** 2002. Universal immunoprobe for (per)chlorate-reducing bacteria. *Appl Environ Microbiol* **68**:3108-13.
28. **Paillard, D., V. Dubois, R. Thiebaut, F. Nathier, E. Hoogland, P. Caumette, and C. Quentin.** 2005. Occurrence of *Listeria* spp. in effluents of French urban wastewater treatment plants. *Appl Environ Microbiol* **71**:7562-6.
29. **Rao, B., T. A. Anderson, G. J. Orris, K. A. Rainwater, S. Rajagopalan, R. M. Sandvig, B. R. Scanlon, D. A. Stonestrom, M. A. Walvoord, and W. A. Jackson.** 2007. Widespread natural perchlorate in unsaturated zones of the southwest United States. *Environ Sci Technol* **41**:4522-8.
30. **Ray, K., B. Marteyn, P. J. Sansonetti, and C. M. Tang.** 2009. Life on the inside: the intracellular lifestyle of cytosolic bacteria. *Nat Rev Microbiol* **7**:333-40.
31. **Schmid, M. W., E. Y. Ng, R. Lampidis, M. Emmerth, M. Walcher, J. Kreft, W. Goebel, M. Wagner, and K. H. Schleifer.** 2005. Evolutionary history of the genus *Listeria* and its virulence genes. *Syst Appl Microbiol* **28**:1-18.
32. **Srinivasan, A., and T. Viraraghavan.** 2009. Perchlorate: health effects and technologies for its removal from water resources. *Int J Environ Res Public Health* **6**:1418-42.
33. **Stenklo, K., H. D. Thorell, H. Bergius, R. Aasa, and T. Nilsson.** 2001. Chlorite dismutase from *Ideonella dechloratans*. *J Biol Inorg Chem* **6**:601-7.
34. **Stewart, V.** 1988. Nitrate respiration in relation to facultative metabolism in enterobacteria. *Microbiol Rev* **52**:190-232.
35. **Streit, B. R., and J. L. DuBois.** 2008. Chemical and steady-state kinetic analyses of a heterologously expressed heme dependent chlorite dismutase. *Biochemistry* **47**:5271-80.
36. **Swaminathan, B., and P. Gerner-Smidt.** 2007. The epidemiology of human listeriosis. *Microbes Infect* **9**:1236-43.
37. **Thorell, H. D., J. Karlsson, E. Portelius, and T. Nilsson.** 2002. Cloning, characterisation, and expression of a novel gene encoding chlorite dismutase from *Ideonella dechloratans*. *Biochim Biophys Acta* **1577**:445-51.
38. **Thorell, H. D., K. Stenklo, J. Karlsson, and T. Nilsson.** 2003. A gene cluster for chlorate metabolism in *Ideonella dechloratans*. *Appl Environ Microbiol* **69**:5585-92.
39. **van Ginkel, C. G., G. B. Rikken, A. G. Kroon, and S. W. Kengen.** 1996. Purification and characterization of chlorite dismutase: a novel oxygen-generating enzyme. *Arch Microbiol* **166**:321-6.
40. **Vazquez-Boland, J. A., M. Kuhn, P. Berche, T. Chakraborty, G. Dominguez-Bernal, W. Goebel, B. Gonzalez-Zorn, J. Wehland, and J. Kreft.** 2001. *Listeria* pathogenesis and molecular virulence determinants. *Clin Microbiol Rev* **14**:584-640.

Section A

41. **Weelink, S. A., N. C. Tan, H. ten Broeke, C. van den Kieboom, W. van Doesburg, A. A. Langenhoff, J. Gerritse, H. Junca, and A. J. Stams.** 2008. Isolation and characterization of *Alicyclophilus denitrificans* strain BC, which grows on benzene with chlorate as the electron acceptor. *Appl Environ Microbiol* **74**:6672-81.
42. **Xu, J., J. J. Trimble, L. Steinberg, and B. E. Logan.** 2004. Chlorate and nitrate reduction pathways are separately induced in the perchlorate-respiring bacterium *Dechlorosoma* sp. KJ and the chlorate-respiring bacterium *Pseudomonas* sp. PDA. *Water Res* **38**:673-80.
43. **Zhang, H., M. A. Bruns, and B. E. Logan.** 2002. Perchlorate reduction by a novel chemolithoautotrophic, hydrogen-oxidizing bacterium. *Environ Microbiol* **4**:570-6.

Section B

Characterization of the chlorite dismutase homologue of *Listeria monocytogenes*

submitted to Applied and Environmental Microbiology

Characterization of the chlorite dismutase homologue of *Listeria monocytogenes*

Stephanie Füreder^{1,2}, Michael Wagner¹, Paul G. Furtmüller³, Katharina F. Ettwig⁴, Nancy E. Freitag⁵, Thomas Decker², Angela Witte², Holger Daims^{1*} and Emmanuelle Charpentier^{2,6*}

Department of Microbial Ecology, Vienna Ecology Centre, University of Vienna, Althanstrasse 14, A-1090 Vienna, Austria¹; Max F. Perutz Laboratories, Department of Microbiology, Immunobiology and Genetics, University of Vienna, Dr. Bohrgasse 9, A-1030 Vienna, Austria²; Division of Biochemistry, Department of Chemistry, University of Natural Resources and Applied Life Sciences, Muthgasse 18, A-1190 Vienna, Austria³; Department of Microbiology, Institute for Water and Wetland Research, Radboud University Nijmegen, Nijmegen, The Netherlands⁴; Department of Microbiology and Immunology, University of Illinois at Chicago College of Medicine, Chicago, Illinois⁵; The Laboratory for Molecular Infection Medicine Sweden (MIMS), Umeå University, S-90187 Umeå, Sweden⁶

Running title: Characterization of the Cld homologue of *L. monocytogenes*

Key words: *Listeria monocytogenes*, chlorite dismutase, heme protein, essential gene.

* Contributed equally to the work.

For correspondence: Holger Daims, Phone: (+43) 1 4277 54392, Fax: (+43) 1 4277 54389, E-mail: daims@microbial-ecology.net

Abstract

Chlorite dismutase (Cld) is a key enzyme in bacteria that gain energy by reducing perchlorate (ClO_4^-) or chlorate (ClO_3^-) to chlorite (ClO_2^-). In this process, Cld detoxifies the respiration product, chlorite, to Cl^- and O_2 . Remarkably, genomic and phylogenetic analyses revealed the widespread presence of *cld* homologues in various prokaryotic lineages, for which no (per)chlorate-reducing phenotype has been demonstrated to date. Here we analyzed the expression and function of the Cld homologue in the food-borne human gram-positive pathogen *Listeria monocytogenes*. We show that the *cld*-like gene (*lmo2113*) is transcribed as monocistronic and bi-cistronic transcripts outside the eukaryotic host. Expression analysis on the protein level demonstrated that the Cld-like protein of *L. monocytogenes* is cytosolic, shows a high degree of stability, is constitutively expressed *in situ* throughout growth at 28°C and 37°C, and that its expression is upregulated under anaerobic growth conditions. Interestingly, no chlorite degradation but a weak catalase activity was detected with the purified recombinant Cld homologue. To uncover a possible other physiological role for the Cld homologue, construction of a deficient mutant was initiated and indicated that *lmo2113* is a previously unrecognized essential gene of *L. monocytogenes*. The results of this study lend support to the hypothesis that the Cld-like protein family contains enzymes with various, mostly yet to be determined functions and that only a sublineage of this family evolved into canonical Cld.

Introduction

Chlorite dismutase (Cld) is a key enzyme of (per)chlorate-reducing bacteria (PCRB) (3, 47). Under anoxic conditions, these heterotrophic microbes respire using (per)chlorate instead of oxygen as terminal electron acceptor. During this process, perchlorate (ClO_4^-) or chlorate (ClO_3^-) is reduced to toxic chlorite (ClO_2^-), which must be eliminated to prevent cell damage. Chlorite is detoxified by Cld that converts chlorite to harmless chloride (Cl^-) and oxygen (O_2) and is one of the very few known biocatalysts, which promote the synthesis of oxygen by the formation of O-O bonds. So far, the biochemistry of this reaction has only partially been resolved. The Cld of *Ideonella dechloratans* has been described as a periplasmic homotetrameric heme protein with characteristics distinct from those of other heme enzymes such as catalases and peroxidases. Chlorite is produced most probably via an O-O bond forming mechanism (4, 17, 20, 31, 32, 34, 37). In addition, the water-soluble iron porphyrin system was shown to serve alone as catalyst for the conversion of chlorite to Cl^- and O_2 , thus implying a crucial function of the heme cofactor in the reaction catalyzed by Cld (38).

Clearly, the function of chlorite dismutase is of central importance for (per)chlorate degradation by PCRB and for the bioremediation of these industrial contaminants. However, in-depth phylogenetic analyses recently revealed a much wider distribution of *cld* homologues in prokaryotic genomes and metagenomes than previously anticipated (20). Interestingly, the organisms harbouring these genes form a heterogeneous group of microbes from a large number of bacterial and archaeal phyla. They represent a great variety of physiological types and lifestyles, some of which are markedly different from the known heterotrophic PCRB. For example, the recent discovery of a highly active chlorite dismutase in the nitrite-oxidizing bacterium "*Candidatus Nitrospira defluvii*" extended the known distribution of this enzyme to a group of chemolithoautotrophic nitrifiers (20). As *Nitrospira* are not known to be (per)chlorate reducers, the physiological role of Cld in these organisms is less obvious than in PCRB. The degree

Section B

of sequence divergence among Cld homologues and the ecophysiological diversity of the respective organisms lead to the question of whether all Cld-like proteins actually possess a chlorite dismutase function. Indeed, the Cld-like protein of *T. thermophilus* displays only a low chlorite dismutase activity. This enzyme also has a low catalase activity and was suggested, based on structural similarities to peroxidases, to function as a novel heme peroxidase in a pathway downstream of superoxide dismutase to protect the cell from harmful reactive oxygen intermediates (ROI) (12). In the halophilic archaeon *Haloferax volcanii*, a functional link between the Cld homologue and an antibiotic biosynthesis monooxygenase (ABM) was proposed by *in silico* analyses, whereby the Cld-like protein would provide oxygen for the ABM reaction in a hypoxic environment or would neutralize ROI produced by ABM (2).

Among the bacterial species carrying *cld*-like genes, it was surprising to find members of the *Firmicutes* that are well-known human pathogens, i.e. *Staphylococcus aureus*, *Bacillus anthracis*, and *Listeria monocytogenes*. The latter was chosen as model in this study to investigate the function of Cld homologues in these putatively non-(per)chlorate reducing pathogenic bacteria. *L. monocytogenes* is a facultatively intracellular gram-positive bacterium responsible for severe opportunistic infections in humans, e.g. gastroenteritis, meningitis, encephalitis, mother-to-fetus infections and septicaemia (7, 14). Based on the lifestyle of this pathogen, different functions of its Cld homologue can be hypothesized. *L. monocytogenes* is widely found in the environment (e.g. soil, silage and sludge) (7) and the Cld homologue could act as a chlorite dismutase to help *L. monocytogenes* survive in (per)chlorate or chlorite-contaminated environments. As a human pathogen, *L. monocytogenes* can reside and replicate intracellularly in host cells (14) where the bacterium can be exposed to oxidative bursts having listericidal effects. Therefore, it is tempting to speculate that the Cld homologue might confer a certain degree of resistance against oxidative stress, e.g. by scavenging ROI or reactive nitrogen intermediates (RNI), and thus contributes to intracellular survival and pathogenicity. Here, the expression of the Cld homologue of *L.*

monocytogenes was analyzed at the transcriptional and translational levels, and genetic as well as biochemical experiments were performed in an attempt to reveal its function.

Materials and Methods

Bacterial strains and growth conditions

A list of bacterial strains used in this study is presented in Table S1 in the supplementary material. *Escherichia coli* was cultured at 37°C in Luria-Bertani (LB) medium either in liquid with agitation (150 rpm) or on agar supplemented (if required) with the following antibiotics used at the indicated concentrations: ampicillin [100 µg/ml], kanamycin (Km) [100 µg/ml] and carbenicillin [50-100 µg/ml]. *L. monocytogenes* L028 was grown routinely at 37°C (unless otherwise stated) in Brain Heart Infusion (BHI) (Becton Dickinson GmbH) liquid medium under aerobic conditions with agitation (150 rpm) or on BHI agar plates. For growth of *L. monocytogenes* in liquid medium under anoxic conditions, sterile BHI medium was divided in sterile bottles, which were sealed and flushed with N₂ gas until complete removal of oxygen. In these experiments, bacterial inoculation and sampling were performed using a syringe. *L. monocytogenes* was grown anaerobically on agar plates in an anaerobic pot using Anaerocult A (Merck GmbH) to generate a CO₂-based anaerobic atmosphere and Anaerotest (Merck GmbH) to verify that conditions were anaerobic. If required, the medium was amended with the antibiotics chloramphenicol (Cm) [10 µg/ml] and Km [50 µg/ml]. Bacterial growth was monitored at regular time intervals by measuring the optical density of culture aliquots at 600 nm using a standard spectrophotometer (U-2800A, Hitachi) or at 620 nm using a microplate reader (SLT Spectra Reader).

DNA manipulations

Plasmids used in this study are listed in Table S2 in the supplementary material. DNA amplification by PCR, digestion with restriction endonucleases, ligation, and analysis by agarose gel electrophoresis were carried out essentially as described by Sambrook *et al.* (29). Genomic DNA

from *L. monocytogenes* L028 was prepared as described elsewhere (26). PCR fragments were obtained using either Pwo polymerase (Roche Diagnostics GmbH) for further use in cloning or GoTaq[®] Green Master Mix (Promega GmbH) for screening purposes. All restriction enzymes were obtained from Fermentas (Fermentas Life Sciences). Plasmids, PCR products, and digested and agarose gel-extracted DNA fragments were purified using kits from PEQLAB (PeqLab Biotechnologie GmbH) or QIAGEN (QIAGEN VertriebsGmbH) according to the manufacturers' instructions. Oligonucleotides used as primers are listed in Table S3 in the supplementary material. All newly generated plasmids were analyzed by restriction digestion. PCR amplicons and plasmid inserts were Sanger-sequenced using an ABI 3130 XL genetic analyzer (Applied Biosystems).

RNA manipulations

Total RNA was isolated, according to a previously described protocol (15), from *L. monocytogenes* culture samples harvested at different time points during growth. RNA preparations were treated with DNase I (Fermentas) and the RNA concentration was determined using a NanoDrop UV/VIS spectrophotometer (ND-1000, PeqLab Biotechnologie GmbH). Northern blot analysis was carried out as described elsewhere (15). Blots were hybridized with α -³²P-dATP labelled DNA probes specific to *Imo2113* (the *cld*-like gene). For this, PCR-generated DNA fragments internal to the genes of interest were labelled using the DECA-prime II random priming DNA labeling kit (Ambion). For reverse transcriptase (RT)-PCR, the reverse transcription was performed using reverse primer OSF13 and RevertAid[™] First Strand cDNA Synthesis Kit (Fermentas Life Sciences) according to the manufacturer's instructions. This was followed by a PCR reaction using the generated cDNA as template, OSF13 or OSF33 as forward primer, OSF18 as reverse primer and GoTaq[®] Green Master Mix (Promega GmbH). Equal amounts of total RNA and genomic DNA were used as template controls in the PCR reactions.

Cloning, heterologous expression and purification of recombinant Lmo2113

The coding sequence of *cld* homologue (ORF annotated as *Lmo2113* in EGD-e genome, accession no. NC003210) was PCR-amplified using genomic DNA of *L. monocytogenes* L028 as template and primers OSF17 and OSF18. After purification and digestion with *Nde*I and *Xho*I, the PCR fragment was cloned into the expression system pET21b(+), which contains a promoter for T7 RNA polymerase and a C-terminal His-tag (Novagen), thus generating plasmid pSF24. Plasmid pSF24 was then introduced into *E. coli* C43(DE3). For Lmo2113 overexpression, recombinant *E. coli* C43(DE3) harbouring pSF24 was grown at 37°C in phosphate-buffered LB medium (pH 6.8) to reach the logarithmic phase, when the inducer IPTG was added at a final concentration of 1 mM. To facilitate formation of the recombinant Lmo2113 holoenzyme, hemin was added at a final concentration of 50 mg/l at the time of induction. After 4 hrs of induction, cells were harvested by centrifugation, sonicated, and the His-tagged Lmo2113 protein was purified using appropriate amounts of Ni-NTA agarose according to the manufacturer's instructions (QIAGEN). Purified His-tagged Lmo2113 was analysed by SDS-PAGE for molecular mass determination and quality controls. For further use in assays for chlorite dismutase activity, the protein preparation was dialysed overnight against phosphate buffer (200 mM, pH 6.8). The absorption spectrum of the purified Lmo2113 was recorded using a NanoDrop UV/VIS spectrophotometer (ND-1000, PeqLab Biotechnologie GmbH).

A slightly different protocol was used to prepare recombinant Lmo2113 for catalase activity assays. *E. coli* harbouring plasmid pSF24 was grown at 37°C in LB medium supplemented with 100 µg/ml carbenicillin until an optical density (at 600 nm) of 0.8 was reached. Subsequently, the temperature was lowered to 20°C and protein expression was induced by adding 0.1 mM IPTG. After 12 hrs, cells were harvested by centrifugation (4,000 x g, 20 min, 4°C) and frozen in liquid nitrogen. The thawed biomass was resuspended in 35 ml of lysis buffer (50 mM HEPES (4-(2-hydroxyethyl)-1-piperazineethanesulfonic acid), 250 mM NaCl, 5% glycerol, 1 mM PMSF (phenylmethylsulfonylfluorid), 142 µM hemin, 20 mM imidazole pH 7.4) and sonicated to disrupt

Section B

the cells. Cell debris was removed by centrifugation (45,000 x g, 20 min, 4°C). After equilibrating a 20 ml HisTrap FF crude column (GE Healthcare) with 5 column volumes of “buffer 1” (50 mM HEPES pH 7.4, 150 mM NaCl, 20 mM imidazole, 5% glycerol), the supernatant of the protein preparation was loaded onto the column. After washing the column with 5 volumes of “buffer 2” (50 mM HEPES pH 7.4, 150 mM NaCl, 40 mM imidazole, 5% glycerol), the protein was eluted with a step gradient of 50 mM HEPES (pH 7.4), 150 mM NaCl, 500 mM imidazole, and 5% glycerol. Collected fractions were pooled and dialysed overnight in 20 mM HEPES (pH 7.4). Quality and concentration of the protein preparation were determined as described above.

Protein extraction from *L. monocytogenes*

For the preparation of total cell lysates, cultures of *L. monocytogenes* were harvested by centrifugation at different time points during growth. The cell pellets were resuspended in 200 mM Na-phosphate buffer, pH 6.8, and the suspension was sonicated to lyse the cells. For the extraction of exoproteins, supernatants of *L. monocytogenes* LO28 cultures were collected at the late-logarithmic growth phase, filter sterilized (0.2 µm cellulose-acetate membrane filters, Ivaki), and proteins were precipitated by adding 100% trichloroacetic acid and vigorous mixing. After a 30 min ice-cold incubation, precipitated exoproteins were harvested by centrifugation and washed with ice-cold acetone. The air-dried protein pellet was resuspended with appropriate amounts of 200 mM Na-phosphate buffer, pH 6.8. The protein concentration was determined using the “Protein assay dye reagent concentrate” (Bio-Rad Laboratories Inc.) according to the manufacturer’s instructions, and 10 µg of extracted protein was analyzed by SDS-PAGE. All gels were stained using colloidal Coomassie staining.

Western blot analysis

Polyclonal antibodies against the recombinant His-tagged Lmo2113 were commercially produced and used in dilutions of 1:2500 to 1:5000 in the primary antibody hybridization reaction. As controls, listeriolysin O (LLO) (Diatheva s.r.l.) and the ribosomal protein S9 were detected by using

specific antibodies in dilutions of 1:500 and 1:10,000, respectively. The secondary antibody mixture consisted of the horseradish peroxidase (HRP)-coupled anti-rabbit IgG antibody (GE Healthcare) for detecting Lmo2113 and LLO, and anti-goat IgG antibody (Dianova s.r.l.) for detecting S9. The antigen-antibody complex was detected using the Super Signal West Pico Chemiluminescent Substrate (Pierce). Band intensities were quantified by digital image analysis by using the software ImageQuant (GE Healthcare). In order to check for equal amounts of all samples in Western Blot analyses, a SDS-PAGE was loaded in parallel and stained with Coomassie blue.

Determination of protein stability

To determine Lmo2113 protein stability, the protein synthesis inhibitor spectinomycin was added to a final concentration of 100 µg/ml to cultures of *L. monocytogenes* LO28 at the mid-logarithmic growth phase. Samples were collected at different time points. Total proteins were then extracted and analyzed by SDS-PAGE and Western blot as described above.

Functional assays with Lmo2113

Oxygen production by Lmo2113 in presence of sodium chlorite (NaClO₂) was measured using a Clark-type oxygen sensor (Unisense) (27), which was calibrated using oxygen-saturated water and an anoxic 100 mM ascorbate/100 mM NaOH solution. First, 300 mM Na-phosphate buffer (pH 6, which is the optimum pH of bona fide Cld (23)) was flushed with helium to remove oxygen present in the system, thus facilitating the measurement of oxygen formation during the enzymatic reaction. A glass cuvette containing a micro-magnetic stirrer was filled with the prepared buffer (avoiding air bubble formation), closed, and incubated in a water bath at 23°C. The oxygen sensor was introduced into the cuvette while the buffer was constantly being stirred. To start the reaction, purified recombinant Lmo2113 protein was added to a final concentration of 100 nM, followed by the addition of 10 mM NaClO₂ using a glass syringe. Oxygen formation was monitored using a picoammeter (Unisense) and the measured values were recorded using the

program sensortrace (Unisense). As positive control for the assays, oxygen formation from chlorite by purified Cld from “*C. N. defluvii*” (19) was measured under the same conditions.

Catalase activity of recombinant Lmo2113 was determined using a Clark type oxygen electrode (YSI 5331 Oxygen Probe). For this purpose, 5 ml of 50 mM phosphate buffer (pH 7) was flushed with N₂ gas to remove dissolved oxygen. Then 100 μM H₂O₂ and 5 μM purified Lmo2113 were added under constant stirring and oxygen formation was determined. All measurements were performed at room temperature.

Non-conditional and conditional *lmo2113* gene inactivation strategies

(i) In-frame gene deletion. Briefly, a thermosensitive shuttle plasmid (pSF26) was constructed, which includes a thermo-sensitive origin of replication (*repFts*) specific for gram-positive bacteria (35), the ColE1 replicon, a kanamycin resistance cassette (*aphIII*) and a multiple-cloning site (21). For this purpose, a 1,045 bp fragment upstream (*lmo2113up*) and a 1,156 bp fragment downstream (*lmo2113dw*) of the *lmo2113* coding sequence were amplified using L028 genomic DNA as template and primer pairs OLEC253/OLEC254 and OLEC255/OLEC256, respectively. After digestion with appropriate restriction enzymes, the fragments were cloned into pEC84, a thermo-sensitive vector containing the origin of replication *repA_{ts}*, thus generating pSF25. To exchange *repA_{ts}* with *repF_{ts}* in pSF25, the 1,420 bp cassette *repF_{ts}* was released from pEC64 by digestion with *ApaI* and *NarI* and then cloned into *ApaI/NarI* digested pSF25 devoid of *repA_{ts}*, thus resulting in plasmid pSF26. For the in-frame deletion of *lmo2113*, the recombinant plasmid pSF26 was introduced into *L. monocytogenes* L028 by electroporation (24) and the cells were incubated at the permissive temperature (28°C). A temperature shift to the non-permissive temperature (37°C) in the presence of Km promoted integration of the plasmid into the chromosome via a single crossover event. Shifting the temperature back to 28°C, the cells were grown without Km to stimulate a second recombination event leading to the excision of the plasmid from the chromosome. In principle, the final recombination should lead to the production of a mixture of

Km^S isolates with the wild-type *Imo2113* allele and Km^S mutants without the target gene (*Imo2113*) (21).

(ii) Gene replacement. A chloramphenicol cassette, *cat194*, including its own promoter without a transcriptional terminator, was amplified using pEC38 as DNA template and primers OSF31/OSF32. After digestion with appropriate enzymes, the *cat194* cassette was inserted between the *Imo2113*_{up} and *Imo2113*_{dw} fragments in the temperature-sensitive shuttle plasmid pSF26 described above, thus generating pSF6. To facilitate screening for plasmid loss during the temperature shifts, a β -galactosidase cassette allowing blue-white selection was amplified using vector pMAD (1) as DNA template and primers OLEC644/OLEC645. After digestion with appropriate enzymes, the β -galactosidase cassette was introduced downstream of the cassette *aphIII* in pSF6, leading to plasmid pSF7. pSF7 was then introduced into electro-competent L028 cells, which were incubated at 28°C to allow plasmid replication. The strategy of gene replacement was the same as described above for the in-frame deletion, but with two additional selective advantages: selection of white colonies having lost the plasmid after the temperature shifts and subsequent selection of Km^S and Cm^R mutants.

(iii) Conditional in-frame gene deletion. With this strategy (11), *Imo2113* gene deletion is performed by the method described above (see approach i), under conditions when *Imo2113* is expressed under the control of an IPTG-inducible promoter from a multi-copy plasmid. For this purpose, the *Imo2113* gene including the ribosome binding site (RBS) was amplified using L028 genomic DNA as template and primers OSF43/OSF44. After digestion with appropriate enzymes, the fragment was cloned downstream of the IPTG-inducible promoter at the *Xba*I site in vector pLIV1 (9), thus resulting in plasmid pSF9. The whole expression cassette was excised using *Kpn*I, digested with T4 DNA polymerase to create blunt ends, and cloned into the high-copy plasmid pAM401 (36) digested with *Eco*RV, thus creating pSF11 (18). The conditional in-frame *Imo2113* deletion strategy then consisted of introducing plasmid pSF11 into electro-competent cells of

strain L028, which already contained pSF5, and performing the in-frame deletion as described for strategy (i) in presence of IPTG.

(iv) Gene silencing by an inducible anti-sense RNA approach. To construct a plasmid for *lmo2113* anti-sense RNA (asRNA) expression, the *lmo2113* gene including the RBS was cloned in anti-sense orientation in the backbone vector pAM401 using the same cloning approach as described for the creation of pSF11, thus generating pSF10. To construct the plasmid for *llo* (encoding listeriolysin O) asRNA expression, primers OSF48/OSF49 were used with genomic DNA of strain L028 as template to amplify a 1,614 bp fragment including the *llo* RBS. After digestion with appropriate enzymes, the PCR fragment was then cloned into pAM401, resulting in plasmid pSF15. Plasmids were introduced into electro-competent L028 cells. Expression of *lmo2113* or *llo* in L028 strains, which were also expressing *lmo2113* asRNA or *llo* asRNA from pSF10 or pSF15, was analyzed by Western blot (*lmo2113*) or by RT-PCR (*llo*) and hemolysis assays (LLO).

(v) Gene disruption by plasmid integration. This approach allows the assessment of essentiality of a gene by determining whether gene disruption is lethal. Here, an internal 450 bp fragment of *lmo2113* was amplified using strain L028 genomic DNA as template and primers OSF54/OSF55. After digestion with appropriate enzymes, the PCR fragment was cloned into the thermo-sensitive plasmid pKSV7 (25, 30). Previously described pKSV7 variants containing internal fragments of the *actA*, *gap* and *rpoB* genes were used as controls (25). Plasmids were introduced into electro-competent L028 cells followed by incubation at 28°C. Cultures of strains harbouring the plasmids were shifted from 28°C to 37°C in BHI containing Cm to promote plasmid integration into the chromosome. After 3 days of passaging at 37°C, cultures were diluted in fresh BHI medium and culture aliquots were spotted onto BHI agar containing Cm. After overnight incubation at 37°C under aerobic or anaerobic conditions, the agar plates were checked for growth of the *Listeria* spots (25) (Fig. B. 8B).

Sequence analyses and phylogeny

Nucleic acid and amino acid sequences were obtained from public databases using BLAST (<http://blast.ncbi.nlm.nih.gov/Blast.cgi>) and the Joint Genome Institute Integrated Microbial Genomes web-based interface (<http://img.jgi.doe.gov/pub/main.cgi>). Putative signal peptides in amino acid sequences were searched using SignalP (5). For prediction of promoter and terminator sequences, BPROM (<http://linux1.softberry.com/berry.phtml>) was used. Sequence analysis and annotation were done using Vector NTI (Invitrogen). The phylogeny of selected Cld-like proteins was studied by maximum-likelihood analysis (PhyML (13)) using the ARB software package (19) as described by Maixner *et al.* (20).

Results and Discussion

Phylogeny of the *cld* homologues of *Firmicutes*

Screening all available genomes of organisms belonging to the *Firmicutes* revealed a striking separation of lineages harbouring and not harbouring a *cld* homologue. A *cld*-like gene was detected in all available genomes from the order *Bacillales* except in the draft genome of *Pasteuria nishizawae* (strain North America). In contrast, none of the available *Lactobacillales*, *Clostridiales* and *Mollicutes* genomes contain *cld* homologues. In *Moorella perchloratireducens* (*Thermoanaerobacterales*) chlorite dismutase activity has been detected, but neither the genome of this organism nor the Cld protein sequence is available (3).

Interestingly, the presence of a *cld*-like gene seems not to be linked to any obvious group-specific lifestyle difference. The *Bacillales* are ecologically diverse and contain free-living or intracellular, non-pathogenic or pathogenic, aerobic or (facultatively) anaerobic, and spore forming or non-spore forming members. Each of these features is found at least in one of the other three groups (*Lactobacillales*, *Clostridiales*, *Mollicutes*) that lack *cld*-like genes. The phylogeny of the Cld homologues of *Bacillales* was studied by maximum likelihood analysis of selected Cld-like

sequences (Fig. B.1). All analyzed *Bacillales* Cld-like proteins cluster together and are clearly distinct from the validated chlorite dismutases of PCRB and of “*C. N. defluvii*” (Fig. B.1). Notably, the Cld-like protein of the *Deinococcus-Thermus* phylum member *Thermus thermophilus* (12) is relatively closely related to the Cld-like sequences of *Bacillales* (Fig. B.1), indicating lateral gene transfer and possibly also similar functions of these proteins (amino acid identity to Lmo2113, the Cld-like protein of *L. monocytogenes*: 46.9%, amino acid similarity: 73.3%).

Genomic context of the *cld* homologue (*Imo2113*) in *L. monocytogenes*

In the available sequenced genome of *L. monocytogenes* strain EGDe, the 756 bp-long coding sequence of the *cld*-like gene (*Imo2113*) is located downstream of two genes involved in sugar metabolism (*Imo2108*, *Imo2110*), a gene encoding a putative hydrolase/acyltransferase belonging to the esterase/lipase superfamily (*Imo2109*) and a gene encoding a putative FMN (flavin mononucleotide)-containing NADPH-linked flavin/nitro reductase gene (*Imo2111*) (Fig. B.2). Downstream of the *cld* homologue are genes encoding a putative ATP-binding protein (*Imo2114*) and a putative permease (*Imo2115*), both belonging to the ABC transporter family, as well as two genes coding for hypothetical proteins of unknown function (*Imo2116*, *Imo2117*). Interestingly, the gene *Imo2112* located directly upstream of *Imo2113* shows homology to a putative DNA-binding domain of the excisionase family. Excisionase-like genes usually are located on temperate phages, plasmids or transposons, and are involved in excisive genomic recombination (33). The described *Imo2113* neighbourhood is conserved in the five complete genome sequences of *L. monocytogenes* and *L. innocua* available to date (data not shown). The only published complete genome sequence of *L. welshimeri* (strain SLCC 5334), however, lacks the genes *Imo2108* and *Imo2109*. In the draft genome of *L. grayi*, only a homologue to the *cld*-like gene *Imo2113* was detected, whereas homologues to any other genes in the region between *Imo2108*-*Imo2117* were not found in the available sequence data from this organism. Based on the combined occurrence of homologues to *Imo2112* and *Imo2113* in all sequenced *Listeria* spp., it is tempting to speculate that mobile genetic elements might have been involved in the acquisition of the *cld* homologue by

this genus. Comparative analysis of the region around *lmo2113* to the genomic context of *clt*-like genes in other organisms than *Listeria* did not reveal any shared synteny and thus provided no clue regarding similar functions of Lmo2113 and other Clt-like proteins. Consistent with this observation, the Clt-like proteins from different bacteria and archaea display only low sequence similarity, indicating a functional diversification within this protein family (20).

Transcription analysis of *lmo2113* in *L. monocytogenes* LO28

Sequence analysis of the *lmo2113* locus in the sequenced genome of *L. monocytogenes* strain EGD-e revealed two putative promoters for this *clt*-like gene, one located directly upstream of *lmo2113* and a second one located upstream of the excisionase-like sequence *lmo2112* (Fig. B.3A). These two promoters, and a terminator downstream of *lmo2113*, are conserved in all 24 finished and unfinished *L. monocytogenes* genomes. The absence of a putative transcriptional terminator in the intergenic region between the two sequences suggested that *lmo2113* is expressed from a monocistronic and/or a bicistronic transcript. Accordingly, Northern blot analysis of *L. monocytogenes* LO28 total RNA using a *lmo2113*-specific probe demonstrated the presence of two transcripts, the size of which corresponded to the expected sizes of the putative monocistronic and bicistronic transcripts (data not shown). This finding was confirmed by an additional RT-PCR analysis (Fig. B.3B). The observed co-transcription of the putative DNA binding domain of the excisionase family with *lmo2113* supports further the above suggestion that mobile genetic elements might have been implicated in the acquisition or dissemination of the *clt*-like gene.

Expression and subcellular localization of Lmo2113

Western blot analysis of *L. monocytogenes* LO28 cell lysates using a Lmo2113-specific polyclonal antibody revealed that Lmo2113 is expressed *in vivo* as a protein of about 29 kDa, which is in accordance with the predicted molecular weight (MW) of 28.85 kDa (251 amino acid residues) (Fig. B.4A). Validated chlorite dismutases have a similar MW, e.g. 25 kDa [*Ideonella dechloratans*,

(31)] or about 30 kDa [“*C. N. defluvii*” (20)]. Further analysis demonstrated constitutive expression of Lmo2113 during growth at 37°C (Fig. B.4A) or 28°C (data not shown).

A protein synthesis inhibition assay was performed to assess the stability of Lmo2113, showing that this protein was stable up to 2 hrs post-inhibition, whereas its concentration decreased markedly at 4 hrs post-inhibition (Fig. B.4B). To investigate the localization of Lmo2113 in *L. monocytogenes* cells, separate Western blot analyses of whole cell lysates and of culture supernatants prepared from cultures at the late logarithmic growth phase were performed. Unlike the secreted listeriolysin O (LLO), Lmo2113 was detected only in the cell lysate fraction (Fig. B.4C). The same result was obtained for the cytosolic ribosomal protein S9 used as control in these experiments (Fig. B.4C). This result is in accordance with the lack of a putative signal peptide in the N-terminal part of Lmo2113 (data not shown). The cytosolic localization of Lmo2113 is in contrast to the periplasmic localization of the validated chlorite dismutases of the PCB *Ideonella dechloratans* (31) and *Dechloromonas aromatica* (32). The lack of a LPXTG motif or transmembrane helices in the Lmo2113 sequence indicated that the protein is not associated to the cell wall or integrated in the cytoplasmic membrane. Taken together, the Cld homologue of *L. monocytogenes* is a cytosolic protein showing a relatively high stability and constitutive expression during growth at 28°C and 37°C.

Lmo2113 expression in *L. monocytogenes* LO28 under anaerobic conditions

Anaerobic conditions are known to be important for the expression of Cld in the facultatively anaerobic PCB (6, 8, 28, 32). As *L. monocytogenes* is a facultative anaerobe, the question of whether Lmo2113 expression is influenced by anaerobic growth conditions was addressed. Western blot analyses of aerobically or anaerobically grown *L. monocytogenes* cultures showed that anaerobiosis led to a 4.9-fold increased level of Lmo2113 (Fig. B.5). Consistent with this observation, an increased expression of the *cld* homologue *ywfI* in *B. subtilis*, another member of the *Bacillales*, under anaerobic conditions was previously demonstrated (22). Thus, in contrast to

PCRB, high levels of the Cld-like proteins of these *Firmicutes* are present under both aerobic and anaerobic growth conditions, but these enzymes might be more functionally important or more stable in the absence of oxygen.

Functional analysis of Lmo2113

To determine whether Lmo2113 may act as a chlorite dismutase in *L. monocytogenes*, we tested whether the enzyme was able to convert chlorite to chloride and oxygen. Recombinant Lmo2113 was expressed in the heterologous host *E. coli*, purified, and first characterized with regard to its heme binding properties. When *E. coli* expressing Lmo2113 was grown without hemin in the medium, the purified enzyme did not show the red colour that is typical of highly concentrated Cld preparations (20, 32). In contrast, the addition of hemin to the growth medium resulted in a reddish Lmo2113 preparation, indicating that Lmo2113 is a heme-binding enzyme. Indeed, UV/VIS spectrophotometrical analysis of purified recombinant Lmo2113 was consistent with predominant five-coordinate high-spin heme, with the Soret band at 412 nm and Q-bands at 540 and 570 nm highly similar to those reported for validated heme-containing chlorite dismutases (data not shown) (20, 31, 34). Subsequently, purified recombinant Lmo2113 was analyzed with regard to O₂ production in presence of chlorite. Although a sensitive oxygen sensor was used (lower detection limit 0.3 µM), no O₂ production was detected under the tested conditions (Fig. B.6). In contrast, recombinant Cld of “*C. N. defluvii*”, which was used as control in parallel experiments, showed a strong chlorite dismutase activity as O₂ production was clearly observed (Fig. B.6). The apparent absence of Cld activity could be caused by structural differences between the recombinant Lmo2113 and its native form in *L. monocytogenes*, and/or the lack of important post-translational processing steps in the heterologous host *E. coli*. Alternatively, Lmo2113 is not a functional chlorite dismutase although comparative sequence analysis and phylogeny clearly showed that Lmo2113 and Cld are distantly affiliated homologues. So far, no member of the genus *Listeria* has been reported to use (per)chlorate as electron acceptor and thus there seems to be no requirement for a functional chlorite dismutase activity in these organisms. The purified Cld-like

protein of *T. thermophilus*, which is similar to Lmo2113 and also only distantly related to the highly efficient Clds of PCRB and of *Nitrospira*, shows only a very weak Cld activity (12). As this enzyme possesses a weak catalase activity *in vitro*, it has been proposed to be involved in the protection from reactive oxygen species *in vivo* (12). Therefore, we tested a putative catalase function of Lmo2113 by monitoring the release of O₂ after addition of H₂O₂ to the recombinant enzyme. Interestingly, a weak production of O₂ was observed (Fig. B.7), indicating that also Lmo2113 might function as a catalase. However, due to the presence of a canonical catalase in *L. monocytogenes* (16) it seems unlikely that H₂O₂ degradation is the primary function of Lmo2113 *in vivo*. Whereas the Cld-like protein of *T. thermophilus* was suggested to be a peroxidase based on structural features (12), additional tests did not reveal a peroxidase activity of Lmo2113 (data not shown).

Comparative analysis of key residues in Lmo2113 and chlorite dismutases

Recently, de Geus *et al.* (10) determined the crystal structure of the chlorite dismutase of the PCRB *Azospira oryzae* strain GR-1. Several amino acid residues in close proximity to the heme group were proposed to be important for heme binding, coordination of iron binding, and charge separation. Four amino acids (Asn117, Tyr118, Ile119, Trp155) form hydrogen bonds with two propionate groups of the heme (10). In addition, Trp155 was identified as electron donor for the reduction of the intermediate products “compound I” and “compound II” during chlorite degradation (17). The iron of the heme is coordinated by His170, which is highly conserved in Cld-like proteins (20). Analysis of the Lmo2113 sequence revealed that all these key residues except Ile119, which is replaced by leucine, are also present in *L. monocytogenes*. Furthermore, de Geus *et al.* (10) proposed an important role for Arg183 in substrate positioning and activation. Interestingly, this positively charged arginine is conserved in the validated chlorite dismutases of PCRB and of “*C. N. defluvii*”, but is replaced by the neutral amino acid glutamine in Lmo2113. This change of a key amino acid at the active site of the enzyme could explain why Lmo2113 did not show chlorite-degrading activity in our experiments.

Imo2113* is a novel essential gene of *L. monocytogenes

In order to determine the biological role of *Imo2113*, we attempted to create an *Imo2113*-deficient mutant of *L. monocytogenes* strain L028 using the five different strategies described in the Materials and Methods section as strategies (i) to (v). Subsequent analyses of such a mutant were planned to investigate phenotypic differences compared to the wild type. However, the in-frame deletion approaches (i) and (ii) were unsuccessful as no *Imo2113*-deficient mutants were identified even after screening of about 3,000 clones. This observation led to the hypothesis that *Imo2113* might be an essential gene of *L. monocytogenes*. Consequently, the conditional knock-out strategy (iii) was applied, which combined in-frame gene deletion of *Imo2113* with the concomitant expression of a plasmid-encoded *Imo2113* copy from an IPTG-inducible promoter. Again, no *Imo2113*-deficient mutant was obtained. We assume that this approach failed due to a very low extra-chromosomal expression of *Imo2113* from the IPTG-inducible promoter, which was not sufficient to compensate the loss of the chromosomal *Imo2113* copy. Strategy (iv) (silencing of *Imo2113* expression by an inducible as-RNA) was not successful either. Western blot analysis showed that the level of Lmo2113 protein was not reduced in cells transformed with vector pSF10 carrying the *Imo2113* as-RNA (data not shown). Most likely the cellular level of as-RNA was too low to achieve a complete silencing of *Imo2113* expression. Control experiments carried out with *llo* as-RNA showed that LLO activity was not reduced in as-RNA expressing cells either, suggesting that strategy (iv) did not work as expected in our setup. Finally, gene disruption by plasmid integration (strategy (v) described in the Materials and Methods section; Fig. B.8A), was used to determine whether *Imo2113* is an essential gene. As controls, the known essential genes *gap* and *rpoB* and the non-essential gene *actA* were disrupted in parallel experiments. In addition, the backbone integrative vector was used in a control experiment to validate the correct experimental setup. Interestingly, under aerobic and anaerobic conditions the disruption of *Imo2113* resulted in a phenotype identical to that observed for the disrupted essential genes *gap* and *rpoB* (suppressed growth), whereas disruption of *actA* did not have this effect (Fig. B.8B).

Thus, the outcome of strategy (v) strongly suggests that *lmo2113* is an essential gene under the tested growth conditions, and this also explains why our attempts to create a deletion mutant were not successful. This finding correlates well with a study of Li *et al.* (18), who applied a genome-wide screening approach to identify genes important or essential for the growth of *Staphylococcus aureus* and found the *clt* homologue of this Gram-positive organism to be essential, too. Notably, no (per)chlorate or chlorite was present in any of these experiments performed with *L. monocytogenes* or *S. aureus*. This feature of *clt* homologues in *Firmicutes* seems to be in sharp contrast to the chlorite dismutase genes of PCRB, for which an essential role has only been demonstrated for growth under anaerobic conditions and in simultaneous presence of (per)chlorate.

Conclusions

Cld serves a crucial role in PCRB during respiration with (per)chlorate as electron acceptor, but the functions of Cld homologues in other bacteria remain to be determined. Their wide distribution among the prokaryotes suggests that Cld-like proteins are an ancient protein family and one could speculate that the ancestral function was the degradation of chlorite. However, the source of chlorite is mostly anthropogenic and therefore this compound is unlikely to have been the main substrate of Cld-like proteins prior to industrialization (20). According to a more plausible hypothesis, these enzymes have been involved in the removal of toxic by-products of bacterial metabolism such as free radicals, ROI, and RNI (12, 20). This study revealed that the Cld homologue of *L. monocytogenes* (Lmo2113) differs in key aspects from the chlorite dismutases of PCRB. It is located in the cytoplasm, is constitutively expressed in presence or absence of atmospheric O₂, and seems not to take chlorite as substrate. Like for a closely related enzyme of *T. thermophilus* (12), a weak catalase activity of Lmo2113 was observed which is unlikely to be the primary function of this enzyme. Furthermore, evidence was collected that *lmo2113* is a previously unrecognized essential gene of *L. monocytogenes*. Based on these findings, we propose

that Lmo2113 has an important house-keeping function in this facultative pathogen and possibly also in the other *Firmicutes* harbouring homologous proteins. A challenging task will now be to identify this biological role. From a more applied perspective, Cld homologues in human and animal pathogens including *Listeria*, *Staphylococcus*, *Bacillus*, *Mycobacterium*, and *Tropheryma* species, if indeed essential, might be interesting targets for new antimicrobials because homologues of Cld seem to be absent from eukaryotes.

Acknowledgements

We thank Darren Higgins for providing plasmid pLIV1, Michel Débarbouillé for providing plasmid pMAD, and Isabella Moll for providing S9 antibodies. We are grateful to Mike Jetten and Marc Strous for hosting S.F. in their laboratory during a research visit at the Department of Microbiology, Radboud University Nijmegen, Netherlands. We thank Frank Maixner and Thomas Rattei for help with comparative sequence analyses, and Christian Baranyi and Georg Mlynek for excellent technical assistance. This work was funded by the University Research Focus “Symbiosis research and molecular principles of recognition” of the University of Vienna (project no. FS573001 “Molecular Interactions between intracellular bacteria and their eukaryotic cells” to E.C., H.D., T.D. and M.W.).

References

1. **Arnaud, M., A. Chastanet, and M. Debarbouille.** 2004. New vector for efficient allelic replacement in naturally nontransformable, low-GC-content, gram-positive bacteria. *Appl. Environ. Microbiol.* **70**:6887-6891.
2. **Bab-Dinitz, E., H. Shmueli, J. Maupin-Furlow, J. Eichler, and B. Shaanan.** 2006. *Haloferax volcanii* PitA: an example of functional interaction between the Pfam chlorite dismutase and antibiotic biosynthesis monooxygenase families? *Bioinformatics* **22**:671-675.
3. **Balk, M., T. van Gelder, S. A. Weelink, and A. J. Stams.** 2008. (Per)chlorate reduction by the thermophilic bacterium *Moorella perchloratireducens* sp. nov., isolated from underground gas storage. *Appl. Environ. Microbiol.* **74**:403-409.
4. **Bender, K. S., S. M. O'Connor, R. Chakraborty, J. D. Coates, and L. A. Achenbach.** 2002. Sequencing and transcriptional analysis of the chlorite dismutase gene of *Dechloromonas agitata* and its use as a metabolic probe. *Appl Environ. Microbiol.* **68**:4820-4826.
5. **Bendtsen, J. D., H. Nielsen, G. von Heijne, and S. Brunak.** 2004. Improved prediction of signal peptides: SignalP 3.0. *J. Mol. Biol.* **340**:783-795.
6. **Bruce, R. A., L. A. Achenbach, and J. D. Coates.** 1999. Reduction of (per)chlorate by a novel organism isolated from paper mill waste. *Environ. Microbiol.* **1**:319-329.
7. **Buchrieser, C.** 2007. Biodiversity of the species *Listeria monocytogenes* and the genus *Listeria*. *Microbes Infect.* **9**:1147-1155.
8. **Coates, J. D., U. Michaelidou, R. A. Bruce, S. M. O'Connor, J. N. Crespi, and L. A. Achenbach.** 1999. Ubiquity and diversity of dissimilatory (per)chlorate-reducing bacteria. *Appl. Environ. Microbiol.* **65**:5234-5241.
9. **Dancz, C. E., A. Haraga, D. A. Portnoy, and D. E. Higgins.** 2002. Inducible control of virulence gene expression in *Listeria monocytogenes*: temporal requirement of listeriolysin O during intracellular infection. *J. Bacteriol.* **184**:5935-5945.
10. **de Geus, D. C., E. A. J. Thomassen, P. Hagedoorn, N. S. Pannu, E. van Duijn, and J. P. Abrahams.** 2009. Crystal structure of chlorite dismutase, a detoxifying enzyme producing molecular oxygen. *J. Mol. Biol.* **387**:192-206.
11. **Dubail, I., A. Bigot, V. Lazarevic, B. Soldo, D. Euphrasie, M. Dupuis, and A. Charbit.** 2006. Identification of an essential gene of *Listeria monocytogenes* involved in teichoic acid biogenesis. *J. Bacteriol.* **188**:6580-6591.
12. **Ebihara, A., A. Okamoto, Y. Kousumi, H. Yamamoto, R. Masui, N. Ueyama, S. Yokoyama, and S. Kuramitsu.** 2005. Structure-based functional identification of a novel heme-binding protein from *Thermus thermophilus* HB8. *J. Struct. Funct. Genomics* **6**:21-32.
13. **Guindon, S., and O. Gascuel.** 2003. A simple, fast, and accurate algorithm to estimate large phylogenies by maximum likelihood. *Syst. Biol.* **52**:696-704.

14. **Hamon, M., H. Bierne, and P. Cossart.** 2006. *Listeria monocytogenes*: a multifaceted model. *Nat. Rev. Microbiol.* **4**:423-434.
15. **Herbert, S., P. Barry, and R. P. Novick.** 2001. Subinhibitory clindamycin differentially inhibits transcription of exoprotein genes in *Staphylococcus aureus*. *Infect. Immun.* **69**:2996-3003.
16. **Leblond-Francillard, M., J. L. Gaillard, and P. Berche.** 1989. Loss of catalase activity in Tn1545-induced mutants does not reduce growth of *Listeria monocytogenes* in vivo. *Infect. Immun.* **57**:2569-2573.
17. **Lee, A. Q., B. R. Streit, M. J. Zdilla, M. M. Abu-Omar, and J. L. DuBois.** 2008. Mechanism of and exquisite selectivity for O-O bond formation by the heme-dependent chlorite dismutase. *Proc. Natl. Acad. Sci. U S A* **105**:15654-15659.
18. **Li, Z., X. Zhao, D. E. Higgins, and F. R. Frankel.** 2005. Conditional lethality yields a new vaccine strain of *Listeria monocytogenes* for the induction of cell-mediated immunity. *Infect. Immun.* **73**:5065-5073.
19. **Ludwig, W., O. Strunk, R. Westram, L. Richter, H. Meier, Yadhukumar, A. Buchner, T. Lai, S. Steppi, G. Jobb, W. Forster, I. Brettske, S. Gerber, A. W. Ginhart, O. Gross, S. Grumann, S. Hermann, R. Jost, A. Konig, T. Liss, R. Lussmann, M. May, B. Nonhoff, B. Reichel, R. Strehlow, A. Stamatakis, N. Stuckmann, A. Vilbig, M. Lenke, T. Ludwig, A. Bode, and K. H. Schleifer.** 2004. ARB: a software environment for sequence data. *Nucleic Acids Res.* **32**:1363-1371.
20. **Maixner, F., M. Wagner, S. Lucker, E. Pelletier, S. Schmitz-Esser, K. Hace, E. Spieck, R. Konrat, D. Le Paslier, and H. Daims.** 2008. Environmental genomics reveals a functional chlorite dismutase in the nitrite-oxidizing bacterium '*Candidatus Nitrospira defluvii*'. *Environ. Microbiol.* **10**:3043-3056.
21. **Mangold, M., M. Siller, B. Roppenser, B. J. Vlamincx, T. A. Penfound, R. Klein, R. Novak, R. P. Novick, and E. Charpentier.** 2004. Synthesis of group A streptococcal virulence factors is controlled by a regulatory RNA molecule. *Mol. Microbiol.* **53**:1515-1527.
22. **Marino, M., T. Hoffmann, R. Schmid, H. Mobitz, and D. Jahn.** 2000. Changes in protein synthesis during the adaptation of *Bacillus subtilis* to anaerobic growth conditions. *Microbiology* **146 (Pt 1)**:97-105.
23. **Mehboob, F., A. F. Wolterink, A. J. Vermeulen, B. Jiang, P. L. Hagedoorn, A. J. Stams, and S. W. Kengen.** 2009. Purification and characterization of a chlorite dismutase from *Pseudomonas chloritidismutans*. *FEMS Microbiol. Lett.* **293**:115-121.
24. **Park, S. F., and G. S. Stewart.** 1990. High-efficiency transformation of *Listeria monocytogenes* by electroporation of penicillin-treated cells. *Gene* **94**:129-132.
25. **Port, G. C., and N. E. Freitag.** 2007. Identification of novel *Listeria monocytogenes* secreted virulence factors following mutational activation of the central virulence regulator, PrfA. *Infect. Immun.* **75**:5886-5897.
26. **Poyart-Salmeron, C., P. Trieu-Cuot, C. Carlier, A. MacGowan, J. McLauchlin, and P. Courvalin.** 1992. Genetic basis of tetracycline resistance in clinical isolates of *Listeria monocytogenes*. *Antimicrob. Agents Chemother.* **36**:463-466.

Section B

27. **Revsbach, N. P.** 1989. An oxygen microsensor with a guard cathode. *Limnol. Oceanogr.* **34**:474 - 478.
28. **Rikken, G. B., A. G. Kroon, and C. G. van Ginkel.** 1996. Transformation of (per)chlorate into chloride by a newly isolated bacterium: reduction and dismutation. *Appl. Microbiol. Biotechnol.* **45**:420-426.
29. **Sambrook, J., Fritsch, E.F., and Maniatis, T. .** 1989. *Molecular cloning. A laboratory manual.* Cold Spring Harbor Laboratory, Cold Spring Harbor, New York.
30. **Smith, K., and P. Youngman.** 1992. Use of a new integrational vector to investigate compartment-specific expression of the *Bacillus subtilis* spoIIM gene. *Biochimie* **74**:705-711.
31. **Stenklo, K., H. D. Thorell, H. Bergius, R. Aasa, and T. Nilsson.** 2001. Chlorite dismutase from *Ideonella dechloratans*. *J. Biol. Inorg. Chem.* **6**:601-607.
32. **Streit, B. R., and J. L. DuBois.** 2008. Chemical and steady-state kinetic analyses of a heterologously expressed heme dependent chlorite dismutase. *Biochemistry* **47**:5271-5280.
33. **Swalla, B. M., E. H. Cho, R. I. Gumpport, and J. F. Gardner.** 2003. The molecular basis of co-operative DNA binding between lambda integrase and excisionase. *Mol. Microbiol.* **50**:89-99.
34. **van Ginkel, C. G., G. B. Rikken, A. G. Kroon, and S. W. Kengen.** 1996. Purification and characterization of chlorite dismutase: a novel oxygen-generating enzyme. *Arch. Microbiol.* **166**:321-326.
35. **Villafane, R., D. H. Bechhofer, C. S. Narayanan, and D. Dubnau.** 1987. Replication control genes of plasmid pE194. *J. Bacteriol.* **169**:4822-4829.
36. **Wirth, R., F. Y. An, and D. B. Clewell.** 1986. Highly efficient protoplast transformation system for *Streptococcus faecalis* and a new *Escherichia coli*-*S. faecalis* shuttle vector. *J. Bacteriol.* **165**:831-836.
37. **Xu, J., and B. E. Logan.** 2003. Measurement of chlorite dismutase activities in perchlorate respiring bacteria. *J. Microbiol. Methods* **54**:239-247.
38. **Zdilla, M. J., A. Q. Lee, and M. M. Abu-Omar.** 2008. Bioinspired dismutation of chlorite to dioxygen and chloride catalyzed by a water-soluble iron porphyrin. *Angew. Chem. Int. Ed. Engl.* **47**:7697-7700.

Figures

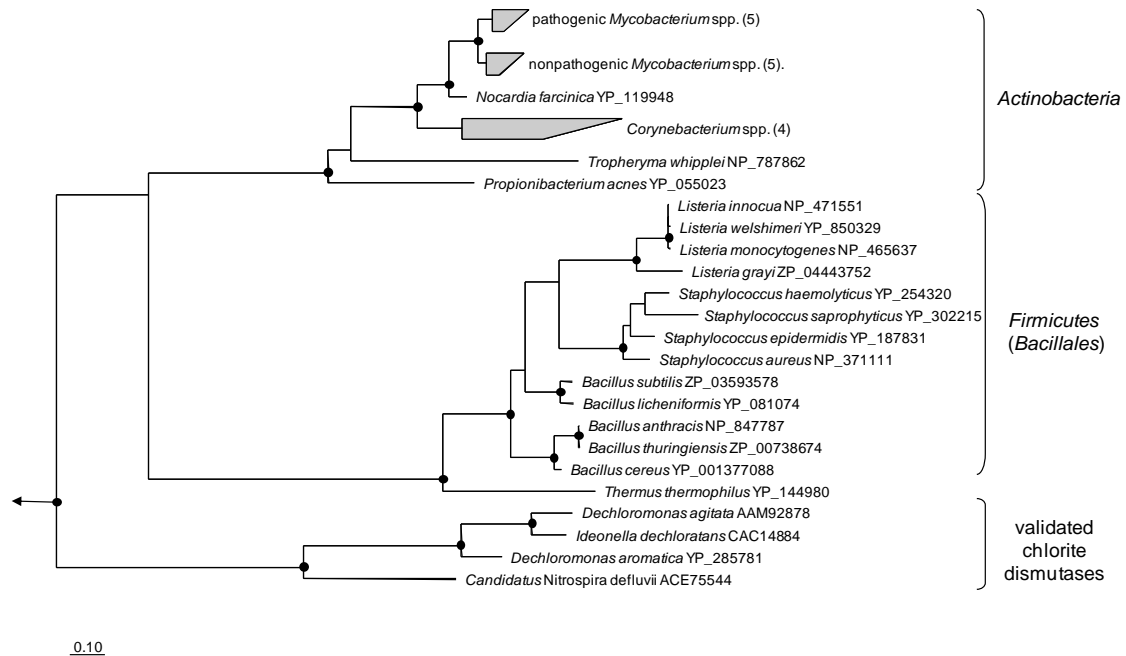


Fig. B.1: Phylogenetic and sequence analysis of Cld homologues. Maximum likelihood tree based on amino acid sequences of validated chlorite dismutases and selected Cld-like proteins from *Firmicutes* and *Actinobacteria*. Black circles symbolize high parsimony bootstrap support ($\geq 90\%$) based on 100 iterations.

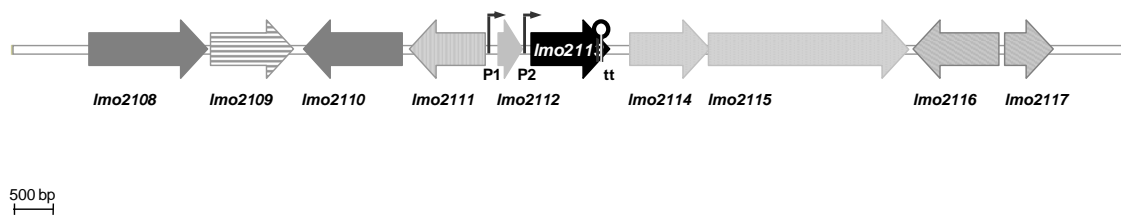


Fig. B.2: Genetic organization of the *Imo2113* locus in *L. monocytogenes*. Schematic representation of the genomic neighbourhood of the identified *cld* homologue, *Imo2113*, in *L. monocytogenes*. Putative functions of the adjacent genes are as follows: *Imo2108*, putative N-acetylglucosamine-6-phosphate deacetylase; *Imo2109*, putative hydrolase or acyltransferase; *Imo2110*, putative mannose 6-phosphate isomerase; *Imo2111*, putative FMN-containing NADPH-linked nitro/flavin reductase; *Imo2112*, putative DNA binding domain of excisionase family; *Imo2113*, *cld* orthologue; *Imo2114*, putative ABC transporter (ATP-binding protein); *Imo2115*, putative ABC transporter (permease); *Imo2116*, hypothetical protein; *Imo2117*, putative acyltransferase. Arrows indicate the direction of translation of the genes. P1 and P2, predicted promoters of *Imo2113*. tt, predicted transcription terminator of *Imo2113*. The gene annotation and names refer to those of the genome sequence of *L. monocytogenes* strain EGD-e (accession no. NC003210). The genome region is drawn to scale.

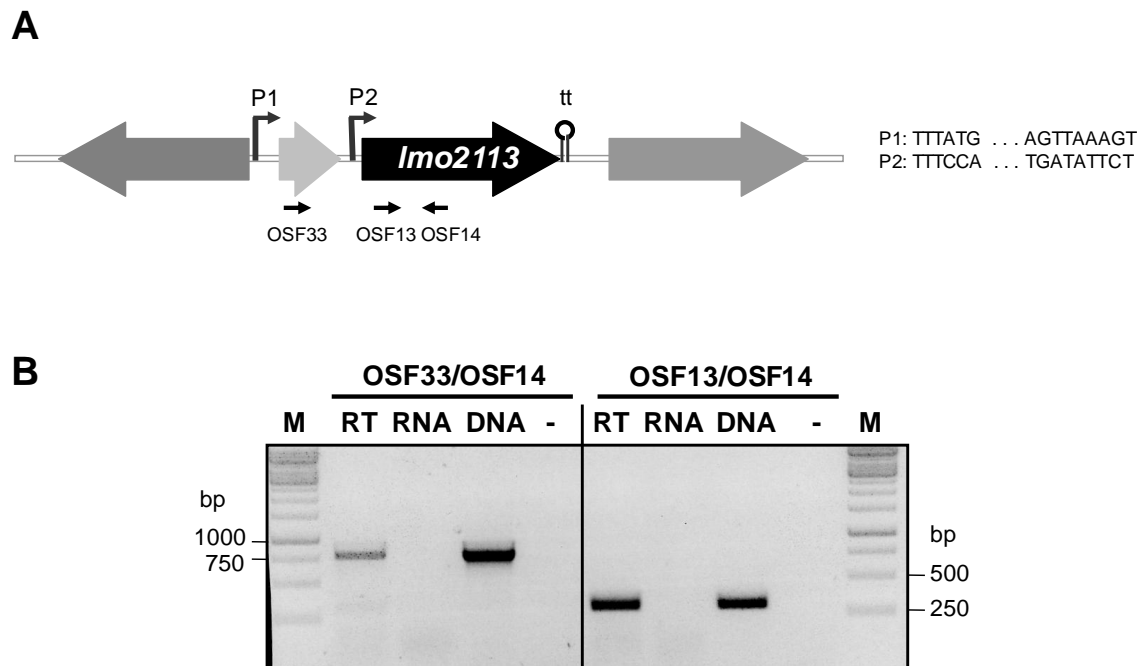


Fig. B.3: Transcriptional analysis of *Imo2113* in *L. monocytogenes*. (A) Schematic illustration of the *clt* homologue (*Imo2113*) located downstream of the putative DNA-binding domain of the excisionase family (*Imo2112*). The predicted promoters (P1 and P2) and transcriptional terminator (tt) of *Imo2113* are shown. Binding positions of the applied PCR primers are indicated. (B) RT-PCR analysis of *Imo2113* transcription. Left panel, PCRs performed with primers OSF33/OSF14 to detect the bicistronic transcript consisting of *Imo2112* and *Imo2113*. Right panel, PCRs performed with primers OSF13/OSF14 to detect a monocistronic *Imo2113* transcript. M, size marker (1 kb DNA ladder, Fermentas); RT, cDNA was used as template; RNA, total RNA was used as template; DNA, genomic DNA was used as template; (-), negative control for the PCR reactions (no template added).

Section B

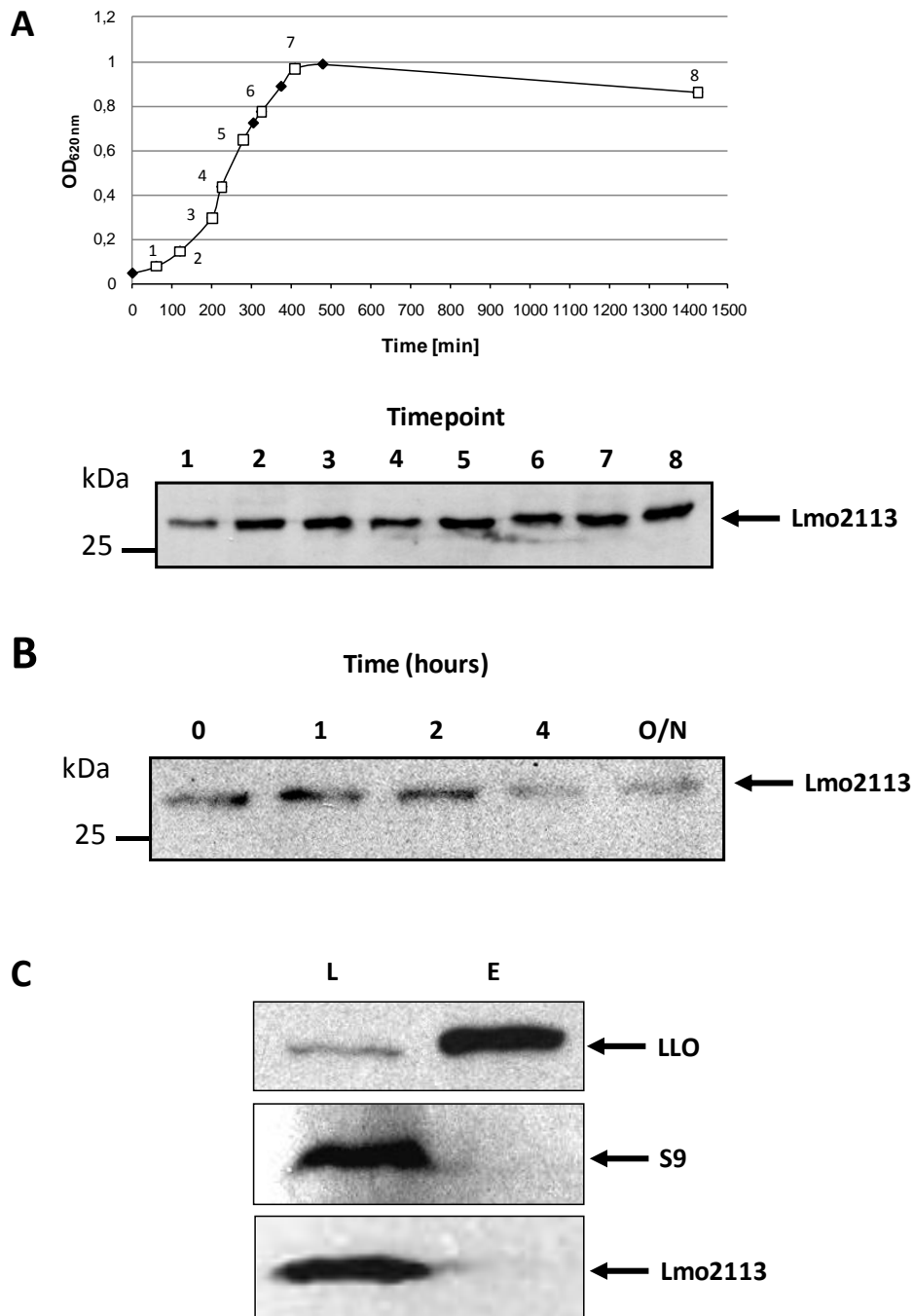


Fig. B.4: Protein expression analysis of Lmo2113 in *L. monocytogenes*. (A) Top panel: growth curve of *L. monocytogenes* LO28 cultured in liquid BHI medium at 37°C. Numbers indicate times of sampling for Western blot analyses. Bottom panel: Western blot detection of Lmo2113 in total cell lysates of *L. monocytogenes* LO28 cultured in liquid BHI medium at 37°C throughout the entire growth curve. Loading of equal protein amounts was ensured as described in the Materials and Methods section. TP, time points of sampling (refer to the growth curve, top panel). (B) Lmo2113 stability assay by Western blot detection. Protein synthesis was inhibited by adding spectinomycin to cultures of *L. monocytogenes* LO28 at the mid-logarithmic growth phase. Samples were withdrawn at regular time intervals. O/N, over-night. Loading of equal protein amounts was ensured as described in the Materials and Methods section. (C) Sub-cellular localization of Lmo2113. Western blot analysis of total cell lysates (L) and secreted exoproteins (E) of *L. monocytogenes* LO28 cultured in liquid BHI medium at 37°C to the late-logarithmic phase. Antibodies specific for Lmo2113, LLO and ribosomal protein S9 of *L. monocytogenes* were used. Loading of equal protein amounts was ensured as described in the Materials and Methods section.

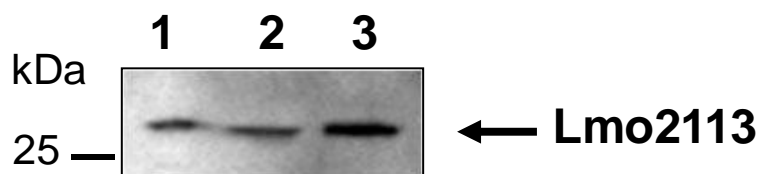


Fig. B.5: *L. monocytogenes* Lmo2113 expression under aerobic or anaerobic conditions. Western blot detection of Lmo2113 in total cell lysates of *L. monocytogenes* LO28 cultured in liquid BHI medium under various growth conditions to the late stationary phase. Representative results of 3 independent experiments are shown. Lane 1, aerobic growth in 100 ml Erlenmeyer flasks containing 50 ml of medium with shaking (150 rpm) at 37°C; Lane 2, aerobic growth in 100 ml glass bottles containing 50 ml of medium with shaking (150 rpm) at 37°C; Lane 3, anaerobic growth under N₂ atmosphere (100 ml glass bottles containing 50 ml of medium) at 37°C. Band intensity quantification by image analysis revealed a 4.9-fold increase of the Lmo2113 level under anaerobic conditions. Equal loading of samples was ensured as described in the Materials and Methods section.

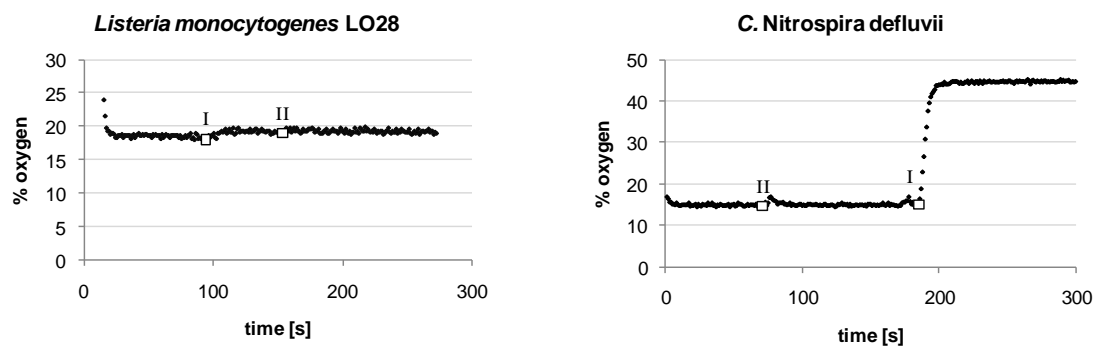


Fig. B.6: Measurements of oxygen production by Cld-like proteins. Oxygen production was measured using a Clark-type oxygen sensor and sodium chlorite as substrate. Left panel, heme reconstituted and purified, recombinant Lmo2113 protein of *L. monocytogenes* LO28 expressed in *E. coli*; right panel, purified recombinant Cld of "*Candidatus N. defluvii*" expressed in *E. coli*. (I), addition of the respective Cld-like protein and (II), addition of NaClO₂. For technical reasons the addition of enzyme and sodium chlorite was performed in reversed order for "*C. N. defluvii*".

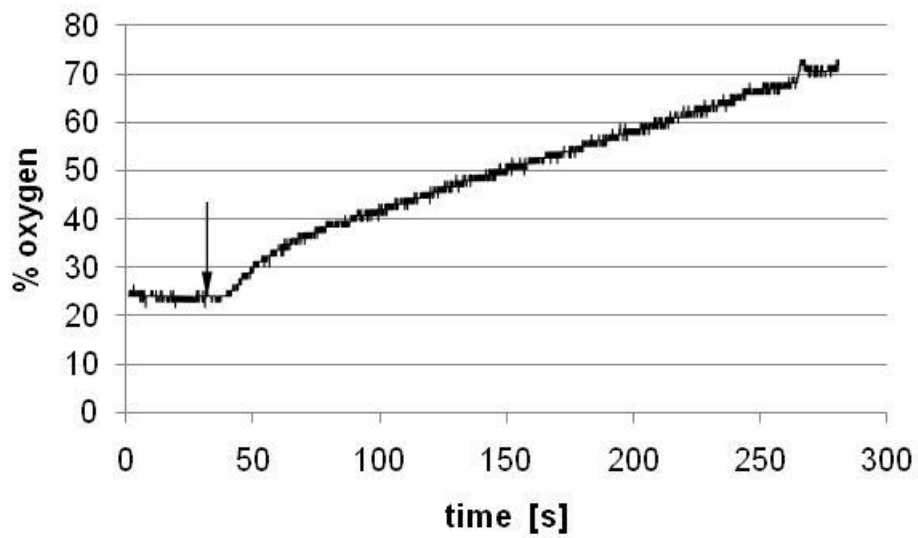


Fig. B.7: Measurement of catalase activity of Lmo2113. Oxygen production was measured using a Clark-type oxygen electrode and H_2O_2 as substrate. Lmo2113 shows a weak catalase activity as indicated by the slow oxygen formation. The arrow indicates the addition of Lmo2113 to the reaction mixture.

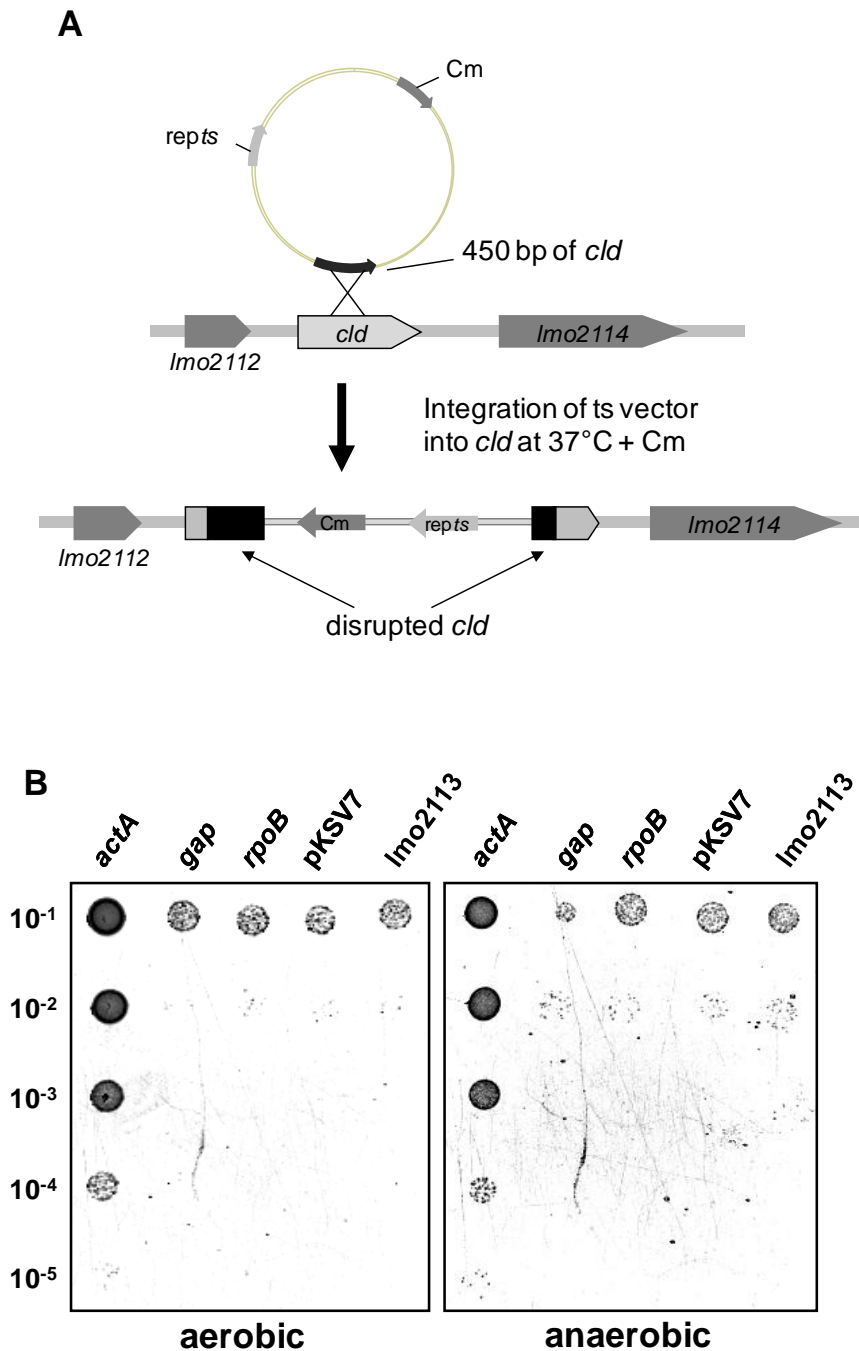


Fig. B.8: Gene disruption by plasmid integration. (A) Gene disruption is mediated by integration of a thermosensitive vector, which harbours a 450-500 bp internal fragment of the gene of interest, at the non-permissive temperature (37°C) into the respective gene copy on the chromosome. *repts*: thermosensitive origin of replication, *Cm*: chloramphenicol resistance gene. (B) Growth test showing that disruption of the *cld*-like gene in *L. monocytogenes* is lethal. Growth occurred at the lowest dilution (10^{-1}) in experiments where essential genes had been disrupted, most likely due to the presence of some *Listeria* cells that contained non-integrated vector (which did not lead to gene disruption). Such cells were diluted out at the higher dilution factors. Please refer to the main text for further details. *actA*, actin-assembly inducing protein, non-essential; *gap*, glyceraldehyde-3phosphatase dehydrogenase, essential; *rpoB*, DNA-directed RNA polymerase beta subunit, essential; *pKSV7*, thermo-sensitive vector control that cannot integrate into the chromosome due to the lack of homologous regions; *Imo2113*, *cld*-like gene, growth phenotype comparable to that of essential genes.

Supplementary Material

Supplementary Table S1: List of bacterial strains used in this study.

Strain	Characteristics	Reference(s) or source
<i>E. coli</i>		
TOP10	F- <i>mcrA</i> Δ (<i>mrr-hsdRMS-mcrBC</i>) ϕ 80 <i>lacZ</i> Δ M15 Δ <i>lacX74</i> <i>recA1</i>	Invitrogen
C43(DE3)	<i>araD139</i> Δ (<i>araleu</i>) 7697 <i>galU galK rpsL</i> (StrR) <i>endA1 nupG</i> <i>ompT hsdS</i> (<i>r_B m_B</i>) <i>gal</i> λ (DE3) (containing at least two non-characterized mutations, derived from C41(DE3))	(4)
SF58	TOP10 (pSF6)	This study
SF61	TOP10 (pSF7)	This study
SF78	TOP10 (pSF8)	This study
SF79	TOP10 (pSF9)	This study
SF89	TOP10 (pSF10)	This study
SF90	TOP10 (pSF11)	This study
SF103	TOP10 (pSF14)	This study
SF109	TOP10 (pSF15)	This study
SF130	TOP10 (pSF16)	This study
SF22	C43(DE3) (pSF24)	This study
SF2	TOP10 (pSF25)	This study
SF7	TOP10 (pSF26)	This study
<i>L. monocytogenes</i>		
LO28	wild-type strain	(3)
SF14	LO28 (pSF26 replicating at 28°C)	This study
SF25	LO28 (pSF26 integrated in the genome)	This study
SF70	LO28 (pSF7 replicating at 28°C)	This study
SF116	LO28 (pSF7 integrated in the genome)	This study
SF93	LO28 (pSF11 replicating at 37°C)	This study
SF104	LO28 (pSF5 / pSF11 replicating at 28°C)	This study
SF107	LO28 (pSF5 integrated in the genome / pSF11 replicating at 37°C)	This study
SF91	LO28 (pSF10 replicating at 37°C)	This study
SF110	LO28 (pSF15 replicating at 37°C)	This study
SF133	LO28 (pKSV7 replicating at 28°C)	This study
SF134	LO28 (pSF16 replicating at 28°C)	This study
SF135	LO28 (pKSV7- <i>actA</i> (internal fragment) replicating at 28°C)	This study
SF136	LO28 (pKSV7- <i>gap</i> (internal fragment) replicating at 28°C)	This study
SF137	LO28 (pKSV7- <i>rpoB</i> (internal fragment) replicating at 28°C)	This study

Supplementary Table S2: List of plasmids used in this study.

Plasmid	Characteristics	Purpose	Reference(s) or source
pET21b(+)	F1 ori, Amp ^R , <i>lacI</i> , His-Tag	Heterologous expression of proteins in <i>E. coli</i>	Novagen
pSF24	pET21b(+) Ω <i>lmo2113</i> (<i>L. monocytogenes</i> LO28)	Heterologous expression of <i>L. monocytogenes</i> <i>lmo2113</i> in <i>E. coli</i>	This study
pCN38	pT181 <i>copw</i> <i>trepC-cat194-amp</i> ColE1 ori	Source for Cm ^R cassette	(2)
pEC64	<i>repF</i> (pE194) <i>ts-ermC-amp</i> ColE1 ori	Source for <i>repF</i> ts cassette	E. Charpentier
pEC84	<i>repAts</i> -ColE1- <i>aphIII</i>	Source for back-bone thermo-sensitive vector	E. Charpentier
pSF25	pEC84 Ω <i>lmo2113up-lmo2113dw</i>	Source for thermo-sensitive plasmid used for in-frame deletion of <i>lmo2113</i> in <i>L. monocytogenes</i>	This study
pSF26	pEC84(<i>repAts::repF</i> (pE194) <i>ts</i>) Ω <i>lmo2113up-lmo2113dw</i>	Thermo-sensitive plasmid for in-frame deletion of <i>lmo2113</i> in <i>L. monocytogenes</i>	This study
pSF5	pEC84(<i>repAts::repF</i> (pE194) <i>ts</i>) Ω <i>bgaB</i> Ω <i>lmo2113up-lmo2113dw</i>	Modified thermo-sensitive plasmid for in-frame deletion of <i>lmo2113</i> in <i>L. monocytogenes</i>	This study
pSF6	pEC84(<i>repAts::repF</i> (pE194) <i>ts</i>) Ω <i>lmo2113up-cat194-lmo2113dw</i>	Thermo-sensitive plasmid for gene replacement of <i>lmo2113</i> in <i>L. monocytogenes</i>	This study
pSF7	pEC84(<i>repAts::repF</i> (pE194) <i>ts</i>) Ω <i>bgaB</i> Ω <i>lmo2113up-cat194-lmo2113dw</i>	Modified thermo-sensitive plasmid for gene replacement of <i>lmo2113</i> in <i>L. monocytogenes</i>	This study
pMAD	ori pE194 <i>ts-ermC-bla</i> -ori pBR322-P <i>clpB-bgaB</i>	Source for β -galactosidase gene	(1)
pLIV1	oriT- <i>ts</i> ori- <i>cam</i> -ColE1- <i>amp-orfZ'</i> -(T1) terminators-PSPAC/ <i>lacOid-erm-Pp60-lacI-orfZ'</i>	Shuttle thermo-sensitive backbone vector for inducible gene expression in <i>L. monocytogenes</i>	D. Higgins
pSF9	pLIV1 Ω <i>lmo2113</i>	Shuttle thermo-sensitive plasmid expressing IPTG inducible <i>lmo2113</i> for use in conditional knock-out strategy of <i>lmo2113</i> in <i>L. monocytogenes</i>	This study
pAM401	<i>rep-cop-cat-tet</i>	Shuttle replicating plasmid for gene expression <i>in trans</i> in <i>L. monocytogenes</i>	(7)
pSF11	pAM401 Ω PSPAC/ <i>lacOid</i> Ω <i>lmo2113</i>	IPTG inducible <i>lmo2113</i> cassette	This study
pSF8	pLIV1 Ω as <i>lmo2113</i>	IPTG inducible <i>lmo2113</i> asRNA cassette	This study
pSF10	pAM401 Ω PSPAC/ <i>lacOid</i> Ω as <i>lmo2113</i>	Shuttle replicating plasmid for <i>lmo2113</i> gene silencing via inducible expression of <i>lmo2113</i> asRNA	This study

Section B

Plasmid	Characteristics	Purpose	Reference(s) or source
pSF14	pLIV1 Ω as <i>llo</i>	IPTG inducible <i>llo</i> asRNA cassette	This study
pSF15	pAM401 Ω pSPAC/lacOid Ω as <i>llo</i>	Shuttle replicating plasmid for <i>llo</i> gene silencing via inducible expression of <i>llo</i> asRNA	This study
pKSV7	Not available	Shuttle thermo-sensitive vector for gene disruption by plasmid integration in <i>L. monocytogenes</i>	(6)
pSF16	pKSV7 Ω <i>lmo2113</i> (internal fragment)	Shuttle thermo-sensitive plasmid for <i>lmo2113</i> gene disruption by plasmid integration in <i>L. monocytogenes</i>	This study
pKSV7 Ω <i>actA</i>	pKSV7 Ω <i>actA</i> (internal fragment)	Shuttle thermo-sensitive plasmid for <i>actA</i> gene disruption by plasmid integration in <i>L. monocytogenes</i>	(5)
pKSV7 Ω <i>rpoB</i>	pKSV7 Ω <i>rpoB</i> (internal fragment)	Shuttle thermo-sensitive plasmid for <i>rpoB</i> gene disruption by plasmid integration in <i>L. monocytogenes</i>	(5)
pKSV7 Ω <i>gap</i>	pKSV7 Ω <i>gap</i> (internal fragment)	Shuttle thermo-sensitive plasmid for <i>gap</i> gene disruption by plasmid integration in <i>L. monocytogenes</i>	(5)

Supplementary Table S3: List of primers used in this study.

Primer	F/R ^a	Sequence (5'-3') ^b	Specificity
OSF13	F	GCATTCTTGGTCAAAAAG	<i>lmo2113</i> (RT-PCR; Northern blot)
OSF33	F	CGCCAACAACAAATAGAT	<i>lmo2112</i> (RT-PCR)
OSF14	R	CGTTCTTCCATTGGAAGC	<i>lmo2113</i> (RT-PCR; Northern blot)
OSF15	F	GCGACCTACTCTCGCAGG	5S rRNA (Northern blot, loading control)
OSF16	R	GTTATGGCGAGAAGGTCA	5S rRNA (Northern blot, loading control)
OSF17	F	CGAGCG CATATGA ATGAAGCAGTAAAAACG (NdeI)	His-tagged <i>Lmo2113</i> expression
OSF18	R	GCGCG ACTCGAGA AATAGTAAATAATTTAGA (XhoI)	His-tagged <i>Lmo2113</i> expression
OLEC253	F	TACAAT GGATCCGA AATAATCTCTTGGTCATATGCTT (BamHI)	<i>lmo2113up</i> cassette
OLEC254	R	AATCA AGGTACCT ATGTATCACTCCTTGTTTAGAAT (KpnI)	<i>lmo2113up</i> cassette
OLEC255	F	TAATC AGGTACCT AATATAAGTAAAACTGGAATTC (KpnI)	<i>lmo2113down</i> cassette
OLEC256	R	ATTCAT GAGCTCAA AATAAGTAGAATGACTGATGAG (SacI)	<i>lmo2113down</i> cassette
OSF31	F	TAGCGT GGTACCT TATTATCAAGATAAGAAAG (KpnI)	<i>cat194</i> cassette
OSF32	R	ATCTA AGGTACCT AAACCTTCTTCAACTAACGGGG (KpnI)	<i>cat194</i> cassette
OLEC644	F	ATGCAC CTCGAGT TAGCATATTATGTTGCCAACTG (XhoI)	<i>β-gal</i> cassette
OLEC645	R	ATGCAC CCGCGGGT CTAGTTAATGTGTAACGTAAC (SacII)	<i>β-gal</i> cassette
OSF43	F	GAC CTCTAGAA ACAAGGAGTGATACATAATGAATGAAG (XbaI)	<i>lmo2113</i> and <i>aslmo2113</i> cassettes
OSF44	R	GG ACTCTAGAT TAAATAGTAAATAATTTAGAAAGT (XbaI)	<i>lmo2113</i> and <i>aslmo2113</i> cassettes
OSF48	F	ATAG TTCTAGAAA ATGTAGAAGGAGAGTGAAACC (XbaI)	<i>llo</i> cassette
OSF49	R	GACAG TCTAGAT TATTTCGATTGGATTATCTACT (XbaI)	<i>llo</i> cassette
OSF54	F	GCG CTGCAGG CTGCATGGCGTGAATAAA (PstI)	450 bp internal <i>lmo2113</i> fragment
OSF55	R	GCG TCTAGAG CGAATAAGTTGTTGGCGTT (XbaI)	450 bp internal <i>lmo2113</i> fragment

^a F, forward; R, reverse.

^b Bold sequences indicate restriction sites.

References

1. **Arnaud, M., A. Chastanet, and M. Debarbouille.** 2004. New vector for efficient allelic replacement in naturally nontransformable, low-GC-content, gram-positive bacteria. *Appl Environ Microbiol* **70**:6887-6891.
2. **Charpentier, E., A. I. Anton, P. Barry, B. Alfonso, Y. Fang, and R. P. Novick.** 2004. Novel cassette-based shuttle vector system for gram-positive bacteria. *Appl Environ Microbiol* **70**:6076-6085.
3. **Kocks, C., E. Guin, M. Tabouret, P. Berche, H. Ohayon, and P. Cossart.** 1992. *L. monocytogenes*-induced actin assembly requires the actA gene product, a surface protein. *Cell* **68**:521-531.
4. **Miroux, B., and J. E. Walker.** 1996. Over-production of proteins in *Escherichia coli*: mutant hosts that allow synthesis of some membrane proteins and globular proteins at high levels. *Journal of Molecular Biology* **260**:289-298.
5. **Port, G. C., and N. E. Freitag.** 2007. Identification of novel *Listeria monocytogenes* secreted virulence factors following mutational activation of the central virulence regulator, PrfA. *Infect Immun* **75**:5886-5897.
6. **Smith, K., and P. Youngman.** 1992. Use of a new integrational vector to investigate compartment-specific expression of the *Bacillus subtilis* spoIIIM gene. *Biochimie* **74**:705-711.
7. **Wirth, R., F. Y. An, and D. B. Clewell.** 1986. Highly efficient protoplast transformation system for *Streptococcus faecalis* and a new *Escherichia coli*-*S. faecalis* shuttle vector. *J Bacteriol* **165**:831-836.

Section C

The true function of the putative
chlorite dismutase from
L. monocytogenes remains concealed

Abstract

In section B it was shown that *clid* is an essential gene in *L. monocytogenes* and that, unexpectedly, it does not exhibit a chlorite degrading function. This section describes further experiments performed in order to elucidate the true function of Cld in *L. monocytogenes*. We investigated the influence of the two-component system ResDE on *clid* expression as it was shown for *B. subtilis* (19) and, furthermore, we analyzed the influence of Cld on the pathogenicity of *L. monocytogenes* and *S. typhimurium* in RAW264.7 macrophages. When describing the mechanism of chlorite degradation by Cld, Lee *et al.* (17) also investigated the interaction of Cld with various substrates of peroxidases and halogenases. As Cld of *L. monocytogenes* did not show any chlorite degrading function, one aim was to verify a putative peroxidase, halogenase or catalase function. Additionally, the heterologous expression of *clid* in *E. coli* revealed a very interesting phenotype comparable to the expression of hemoglobin in *E. coli*. However, none of the conducted experiments revealed the true function of this gene.

Introduction

ResDE is a two-component system in *B. subtilis* and *L. monocytogenes*

Two-component systems are well known regulatory systems in both prokaryotes and eukaryotes. They usually consist of a sensor kinase that autophosphorylates after receiving environmental stimuli. The phosphoryl group is then transferred to a response regulator that modulates expression of a defined set of genes (29).

ResDE is a typical two-component system well described in *Bacillus subtilis* but also known from other species. ResE thereby acts as the sensor kinase responding to a yet unknown signal which is most likely correlated with a change in oxygen tension. After autophosphorylation of ResE, the phosphoryl group is transferred to the aspartate at position 57 of the response regulator ResD (10). ResD acts on the transcriptional level regulating different genes like the redox regulator *fnr*

Section C

(14, 24), *cydABCD*, which encodes products for the production of cytochrome bd oxidase (28), the nitrite reductase operon *nasDE* (22), the flavohemoglobin encoding *hmp* (14), *ctaA* and *ctaB* (18) - both required for synthesis of heme A - and *plcR*, coding for the major virulence gene regulator (8). Although ResDE is seen as a classical two-component system, it has been shown that phosphorylation of ResD is not a pre-requisite for gene activation (10). Unphosphorylated as well as mutated ResD (D57A) can activate gene expression at low levels (10). Furthermore, it has been suggested that the phosphorylation state of ResD triggers the activation of Fnr by direct interaction (8). Analyses of the regulatory promoter regions from *fnr*, *hmp* and *nasD* revealed highly variant regions that are bound tandemly by ResD (10, 23). However, Nakano *et al.* proposed a short sequence to act as a putative ResD box (5' – TTTGTGAAT – 3'), although this needs to be further investigated (23).

In 2000, Marino *et al.* (19) investigated the influence of anaerobic growth conditions on protein synthesis in *B. subtilis* using 2D gel electrophoresis. First of all, they reported a significant upregulation of the *cld*-homolog *ywfl* under different anaerobic growth conditions (Fig. C.1).

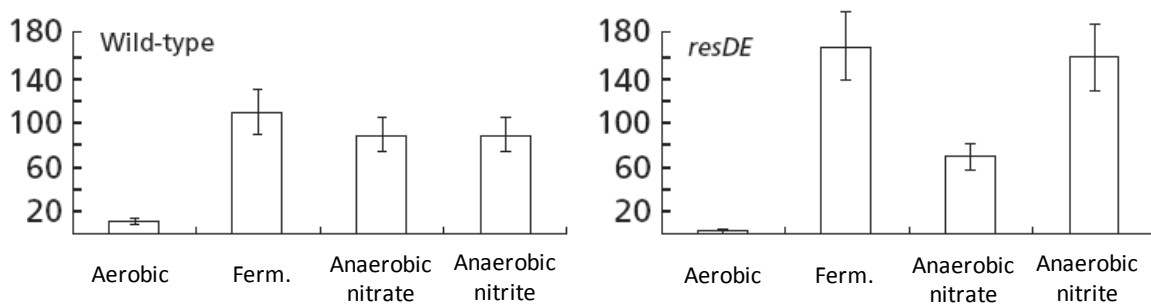


Fig. C.1: Marino *et al.* (19) show that expression of the *cld*-homolog *ywfl* in *B. subtilis* is upregulated in a *resDE* mutant strain under fermentative and anaerobic nitrite conditions indicating a direct or indirect regulation of *resDE* on *ywfl* (with permission of (19)).

Furthermore, in a *resDE* deficient mutant strain of *B. subtilis* the authors could show that *ywfl* is even more upregulated under fermentative and anaerobic nitrite conditions indicating that ResD directly or indirectly represses *cld* expression under anaerobic conditions (Fig. C.1). The general upregulation under anaerobic conditions correlates well with a similar phenotype observed in

PCRBs (see section B), although no information is present on the regulators involved in *clid* expression in PCRBs until now. The described two-component system ResDE is also present in *Listeria monocytogenes*. There, recently, a *resD* mutant and its phenotypic characterization had been published (15) where the authors showed major differences in the target genes of ResDE-mediated regulation. First, ResD influenced the expression of a functional glucose/mannose PTS system by positively regulating *mptA* (encoding the EIIAB^{Man} component) expression. Due to the impaired glucose/mannose uptake, the mutant showed a reduced growth rate that could be minimized by the addition of 25 mM carbohydrates. It must be noted, that *L. monocytogenes* harbours 3 mannose-specific enzyme II permeases (11). Thus, the organism is not dependent on ResD-regulated *mptA* expression for mannose uptake. In case of glucose the situation is different. Besides the high affinity PTS system described above, *L. monocytogenes* encodes only one other low-affinity proton motive force mediated system specific for glucose uptake (25). Therefore, the growth deficient phenotype of the *resD* mutant can be more efficiently reduced by the addition of mannose than glucose.

It is well known that *L. monocytogenes* induces virulence gene expression under the presence of activated charcoal (7), an effect that is repressed by the addition of fermentable carbohydrates to the medium (20). As already expected, due to the impaired carbohydrate uptake system, the *resD* mutant is not able to repress the induced virulence gene expression. Next, the influence of ResD on respiration in *L. monocytogenes* was investigated under aerobic conditions (as no anaerobic respiration is performed in *Listeria*) and it could be shown that *cydA* (encoding cytochrome bd-I oxidase subunit I) expression is dependent on *resD* expression. Finally, the authors investigated the internalization and intracellular survival of *L. monocytogenes* in different eukaryotic cell lines. No difference was observed concerning the intracellular survival of mutant cells, but a reduced internalization was monitored. This could result from an altered cell surface observed by the authors.

Degradation of chlorite by Cld

As mentioned earlier, Lee *et al.* showed that the chlorite degrading mechanism of chlorite dismutase is a O-O bond forming mechanism similar to that of photosystem II (17). The authors also tested the reactivity of Cld in the presence of oxidation and halogenation co-substrates. For this purpose, Cld was incubated with guaiacol or 2,2'-Azino-bis(3-ethylbenzothiazoline-6-sulfonic acid) (ABTS) alone, two diagnostic substrates for peroxidases, but no formation of an 1e⁻ oxidized product was measured. Only if peracetic acid (PAA) was added to the reaction, catalytic activity was observed. Using stopped-flow UV-vis spectroscopy, the authors could then show that, after the addition of PAA, Cld forms compound I which is further decaying to compound II within 20 ms. Sequential addition of ascorbate regenerated the ferric state of the heme. In experiments with monochlorodimedon (MCD), no halogenation ability of Cld was seen. These results indicate a high specificity of Cld to chlorite with no side reaction.

The overall aim of the different experiments described in this section was to identify the true function of Cld which is not the degradation of chlorite as shown in section B. Therefore, every hint found through-out the literature was followed, explaining the seemingly unconnected nature of the described approaches. Among these were infection assays using RAW264.7 macrophages, expression analyses of *cld* in a *L. monocytogenes* mutant deficient of the two-component system ResDE and functional analyses of a putative peroxidase, halogenase and/or catalase activity of Cld from *L. monocytogenes*. Part of the latter experiments have already been briefly described in section B, but are presented here in more detail.

Material and Methods

Bacterial strains, media and growth conditions

A list of bacterial strains used in this study is presented in Table C.1. Handling of *E. coli* and *L. monocytogenes* was performed as described in section B. *Salmonella typhimurium* was grown and transformed as described for *E. coli*. Minimal medium for *L. monocytogenes* was prepared as described in the appendix.

Table C.1: Bacterial strains used in this study

Strain	Plasmid (antibiotic resistance)	Source/Reference
<i>E. coli</i> C43 (DE3)		(21)
SF22	pSF24 (Amp)	This study
SF194	pET21b(+) (Amp)	Novagen
SF197	pET22b(+) + <i>a/eIF2α</i> (Amp)	D. Hasenöhrl
<i>Listeria monocytogenes</i> EGD		(15)
<i>Listeria monocytogenes</i> EGD Δ resD		(15)
<i>Salmonella typhimurium</i> 14028s		E. Charpentier
SF138	pSF24 (Amp)	This study
SF151	pET21b(+) (Amp)	This study

DNA manipulations

For heterologous expression of *cl*d, plasmid pSF24 as described in section B was used.

Oligonucleotides used as primers in this study are listed in Table C.2.

Table C.2: Primers used in this study

Primer code	Primer name	Oligonucleotide sequence (5' - 3')	Specificity
OSF56	cldRNARcF	CCTGGATTTAATTCACGCCATGCA	<i>cl</i> d
OSF57	cldRNARcR	TTGGCTCTTTCTTTATTGGAAACCTG	<i>cl</i> d
OSF58	16SRNARcF	GCCACACTTTATCATTCCGGTATTAGC	16S <i>rRNA</i>
OSF59	16SRNARcR	GCCTTGACACACCGCCCGTCAC	16S <i>rRNA</i>

RNA manipulations

Self-circularisation of RNA for simultaneous determination of 5'- and 3'- ends

RNA from *L. monocytogenes* LO28 cells was isolated as described in section B and checked for complete removal of DNA. Then, 6 µg RNA was treated with 10 U Tobacco Acid Pyrophosphatase (TAP) (Biozym) to remove pyrophosphates at the 5' – end, which resulted in the formation of 5' – monophosphates in a 50 µl reaction. A subsequent acidic phenol/chloroform/isoamylalcohol extraction was performed to purify the TAP-treated RNA for the following ligation reaction. After denaturation of the purified RNA, RNA ligase I (New England Biolabs) was used to self-ligate different amounts of RNA in a 25 µl reaction each. The purified and self-ligated RNA was then used in a RT-PCR reaction using primer pair OSF56/OSF57 for *clt* and primer pair OSF58/OSF59 for 16S rRNA and the OneStep RT-PCR kit (Qiagen) according to the manufacturer's instructions. The method is described by Gonzales *et al.* (unpublished) and shown in Figure C.2.

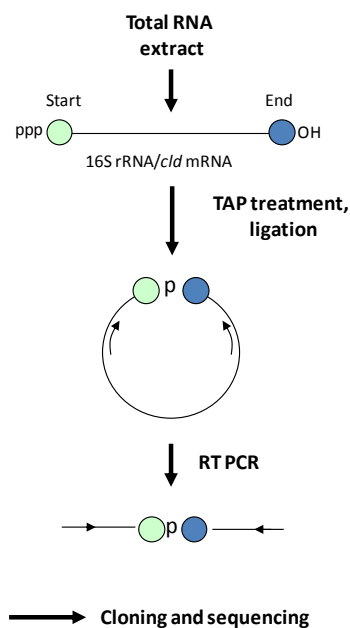


Fig. C.2: self-circularisation of mRNA to determine 5'- and 3'- ends

Protein manipulations

Heterologous expression and protein purification

Cld was expressed and purified as described in section B.

Growth curves and colony forming units (cfu) of SF22 and controls

SF22 (*E. coli* C43 harbouring pSF24) and *E. coli* C43

SF22 and *E. coli* C43 were grown in 30 ml LB in two 100 ml flask including the respective antibiotic if necessary. One of the flasks from each strain was induced using 0.5 mM IPTG at $OD_{600} = 0.8 - 1$.

SF22 and SF194 (*E. coli* C43 harbouring pEt21b(+))

Either strain was inoculated in duplicates in 40 ml LB in two 100 ml flask including the respective antibiotic and grown until $OD_{600} = 0.8-1$, when one of the flasks was induced with 0.5 mM IPTG. Starting 2h after inoculation, three times 100 μ l of a 10^{-6} dilution of each culture were plated hourly on LB + Amp plates and incubated overnight at 37°C. Colony forming units were counted the next day and compared with the obtained OD_{600} values.

SF194 and SF197 (*E. coli* C43 harbouring pET22b(+)) + *a/eIF2 α*)

SF194 and SF197 were grown in 30 ml LB in 100 ml flasks including the respective antibiotic and handled as described above for SF22 and SF194 with one modification: after 2h, 100 μ l of a 10^{-4} dilution was plated.

Cell size determination:

Strains SF22, SF194 and SF197 were grown in 30 ml LB in 100 ml flasks until $OD_{600} = 0.9 - 1$, when protein expression was induced with 0.5 mM IPTG. Samples were withdrawn 3.5h after induction and 2 μ l of each sample were analysed under the microscope. Using a LSM 510 Meta (Carl Zeiss), two pictures of each sample were obtained and the length of 50 cells was determined using the inbuilt LSM 510 Meta software (Zeiss). Average length values and standard deviation of the obtained values were then implemented into a diagram.

Immunofluorescence

Cells of *L. monocytogenes* LO28 were grown in BHI medium until the early mid-log phase, when 4 ml were harvested by centrifugation and washed with 1 ml 1xPBS. Then, cells were fixed using 500 μ l 4% PFA for 45 min on ice, washed again with 1xPBS and resuspended in 750 μ l 1xPBS/EtOH

Section C

(1:1) for further storage at -20°C. For labelling of fixed cells with a specific antibody, 100 µl were washed with 1xPBS and incubated in 0.05% Tween20/H₂O for 10 min at room temperature (RT) to increase membrane permeability. After a second washing step in 1xPBS, cells were blocked with 100 µl 2% BSA/1xPBS for 30 min at RT to decrease unspecific binding of the antibody. Labelling of the cells was performed by independent incubation with a 1:100 dilution of a Cld-specific monoclonal antibody as well as a S9-specific antibody in 100 µl 2% BSA/1xPBS for 1h at RT. A subsequent washing step with 1xPBS was followed by incubation in the dark with the following secondary antibodies: Cy2-labelled anti-rabbit antibody (1:1000) and Alexis-labelled chicken anti-goat antibody (1:1500) for Cld and S9, respectively. To remove unbound antibodies, cells were washed again with 1xPBS. Five µl of the cell suspension were applied onto the well of a Teflon-coated 10-well slide. After coating with Moviol (2.4 g Moviol 4-88 from Sigma, 6 g glycerine, 6 ml ddH₂O, and 12 ml 0.2M Tris-HCl pH 8.5 were stirred at 50-60°C for several hours; then the solution was centrifuged at 7,700 x g for 15 minutes at room temperature to remove air bubbles and undissolved matter, and the supernatant was stored at -20°C until further use), the slide was sealed with a coverslip and stored at 4°C in the dark. Embedded samples were examined by confocal laser scanning microscopy (LSM 510 Meta, Carl Zeiss).

Macrophage infection assays

To determine the impact of Cld on the survival of *L. monocytogenes* LO28 and *S. typhimurium* 14028s during infection, RAW264.7 macrophage infection assays were performed. Therefore, 100 µl of DMEM (Dulbecco's Modified Eagle Medium) medium including 10% fetal calf serum (FCS) containing 2×10^4 mouse-derived RAW264.7 macrophages were seeded in 6 wells of a flat-bottom 96-well plate and incubated ON at 37°C with 5% CO₂. From an overnight culture of *L. monocytogenes* LO28, cell numbers were determined using a Vi-cell cell viability analyzer (Beckman Coulter) and dilutions of 4×10^5 cells in 10 µl sterile 1xPBS final volume were prepared to infect the macrophages with a multiplicity of infection (MOI) of 10 in duplicates. For the infection with *L. monocytogenes* and exogenously added Cld, protein was purified as described in section B,

Section C

dialysed against 1xPBS and 5.8 µg were added to 4×10^5 *L. monocytogenes* cells in a final volume of 10 µl. Again, macrophages were infected with this suspension in duplicates. As controls in this experiment, macrophages were incubated with 5.8 µg pure Cld protein in 10 µl 1xPBS and with 10 µl 1xPBS only. For each time point, one 96-well plate with 6 infected wells was prepared and incubated at 37°C and 5% CO₂. After 1h of incubation, all media were removed by decanting or aspiration and 100 µl fresh media including 50 µg gentamycin were added to kill remaining extracellular bacteria. One hour later, the medium was removed again and 100 µl fresh medium including 10 µg gentamycin was added. Samples were taken after 1h, 2h, 4h, 6h and 8h by lysing macrophages with 100 µl dH₂O and vigorous pipetting. After transfer of the suspension to a 1.5 ml tube, each well was washed again with 100 µl dH₂O to ensure complete harvest of macrophages and intracellular bacteria. The supernatant was then combined with the first 100 µl. The suspension was then further diluted 1:20 – 1: 20 000, of which 100 µl were plated two times on BHI. Following overnight incubation at 37°C, cfu on the plates were determined the next day. The mean cfu value for each timepoint and infection was determined and implemented into a diagram together with the respective standard deviation.

For the infection of macrophages with *Salmonella typhimurium* 14028s the same protocol with minor modifications was applied. First, *S. typhimurium* 14028s was transformed with plasmid pSF24 leading to strain SF138. SF138 is expressing *cld* constitutively and independently from the addition of IPTG. As a control for the effect of the plasmid backbone, the empty pET21b(+) was also transformed into *S. typhimurium* 14028s (leading to strain SF151) and used as control in the infection. RAW264.7 macrophages were prepared as described above and infected with MOI 20 in duplicates with the wild-type strain *S. typhimurium* 14028s, strain SF138 expressing *cld* from plasmid pET21b(+) and strain SF151 harbouring the empty plasmid pET21b(+) as a control. Samples were taken after 1h, 4h and 21h by lysing infected macrophages with 200 µl sterile 0.5% DOC. Dilutions of 1:20 and 1:200 were then plated in duplicates in 100 µl aliquots on LB and LB

plus ampicillin plates. Evaluation of the data was performed as described. All infections were performed in triplicates.

Analyses of *cld* expression in *Listeria monocytogenes* EGD Δ resD

To investigate the expression pattern of *cld* on the protein level in a *L. monocytogenes* EGD Δ resD strain (15), the mutant as well as its isogenic wild-type were grown in 50 ml BHI medium under aerobic or anaerobic conditions as described in section B. Samples for Western blot analyses were taken during the late stationary phase and were processed as described in section B.

Peroxidase function of Cld

Protein was purified by Georg Mlynek from the group of Kristina Djinovic-Carugo. Total protein concentration was determined to be 4 mg/ml (= 140 μ M) using the Bradford assay as described in section B.

Photometric Analysis

A diode Array UV-VIS spectrophotometer (HP 8453, Agilent) was used to determine the Soret peak of Cld.

H₂O₂ electrode measurements:

Reactions were performed at RT in a 4 ml volume containing compounds at different concentrations as indicated in table C.3. Solutions of H₂O₂ and NaClO₂ were prepared freshly. To ensure homogenous distribution of the reagents, measurements were performed under constant stirring.

Table C.3: H₂O₂ measurements

Assay	Phosphate-buffer, pH 7	H ₂ O ₂	Cld	NaClO ₂
1	100 mM	100 μ M	5 μ M	
2	100 mM	100 μ M	5 μ M	50 μ M
3	100 mM	100 μ M	5 μ M	100 μ M
4	100 mM	100 μ M	5 μ M	200 μ M

Clark electrode (O₂) measurements:

Reactions were performed in 5 ml volume using the indicated concentrations in table C.4. H₂O₂ and NaClO₂ were used simultaneously in assays 1 and 2 to investigate if compound I produced by either H₂O₂ or NaClO₂ enables production of oxygen via the other substrate.

Before starting the measurements, the phosphate buffer was flushed with N₂ for 5 min to remove all oxygen. Again, reactions were performed at RT under constant stirring of the solution.

Table C.4: O₂ measurements

Assay	Cld	Phosphate buffer pH 7	H ₂ O ₂	NaClO ₂
1	500 nM	50 mM	1 mM	1 mM
2	1 μM	50 mM	1 mM	2 mM
3	1 μM	50 mM		10 mM
4	1 μM	50 mM	10 mM	

Peroxidase-activity test with guaiacol and ABTS:

The oxidation of guaiacol and 2,2'-Azino-bis(3-ethylbenzothiazoline-6-sulfonic acid) (ABTS) can be monitored by an increased absorbance at 470 nm and 414 nm, respectively, after the addition of the enzyme. Cld was mixed with different compounds as listed in table C.5 and table C.6 and the absorbance was monitored using a diode Array UV-VIS spectrophotometer (HP 8453, Agilent).

Table C.5: guaiacol assay

Assay	Cld	Myelo-peroxidase	Phosphate buffer pH 7	Guaiacol	H ₂ O ₂	NaClO ₂
1	50 nM		100 mM	100 μM	100 μM	
2		100 μg	100 mM	100 μM	100 μM	
3	50 nM		100 mM	100 μM		100 μM

Table C.6: ABTS assay

Assay	Cld	Myelo-peroxidase	Phosphate buffer pH 7	ABTS	H ₂ O ₂
1	50 nM		100 mM	1 μM	100 μM
2	50 nM	100 μg	100 mM	1 μM	100 μM

MCD Assay:

The MCD assay is indicative for the halogenase activity of a certain enzyme. Thereby, monochlorodimedon (=MCD) is halogenated via compound I deriving from the reaction of the enzyme with H₂O₂. In this study, the halogen should be transferred from NaCl or KBr halogen to MCD which would be indicated by a reduced signal at 290 nm. The absorbance was monitored using a diode Array UV-VIS spectrophotometer (HP 8453, Agilent). For used substrates or substrate combinations see table C.7. Control experiments using highly purified myeloperoxidase from Planta Natural Products (<http://www.planta.at>) or no enzyme were performed in parallel.

Table C.7: MCD assay

Assay	Cld	Phosphate buffer pH 5	MCD	H ₂ O ₂	NaCl	KBr	NaClO ₂
1	100 nM	100 mM	100 µM	100 µM	100 mM		
2	100 nM	100 mM	100 µM	100 µM		100 mM	
3	100 nM	100 mM	100 µM				100 µM
4	100 nM	100 mM	100 µM	100 µM			100 µM
5	100 nM	100 mM	100 µM	100 µM	100 µM		100 µM
6	100 nM	100 mM	100 µM	100 µM		100 mM	100 µM

Stopped flow experiments:

To investigate a putative peroxidase activity, the influence of certain known peroxidase substrates on the absorbance of Cld was determined by different stopped flow experiments. Thereby, different substrates are mixed in a defined order and time frame and the change in absorbance is recorded over time. The formation of compound I, as suggested by the publication of Lee *et al.* (17), would appear as a shift in the Soret peak to a higher absorbance. The applied substrate combinations are listed in table C.8. All measurements were performed using a Stopped Flow spectrophotometer/fluorimeter SX-18MV (Applied Photophysics). Assays containing only Cld and H₂O were used as controls.

Section C

Table C.8: Stopped flow experiments. Final assay concentrations are indicated

Assay	Cl ₂	H ₂ O ₂	NaClO ₂	Peracetic acid	HOCl	KNO ₂	Ascorbic acid
1	14 μM	20 μM					
2	14 μM	200 μM					
3	14 μM	2 mM					
4	14 μM		20 μM				
5	14 μM		200 μM				
6	14 μM		2 mM				
7	14 μM			200 μM			
8	14 μM			2 mM			
9	7 μM				10 μM		
10	7 μM				100 μM		
11	7 μM				1 mM		
12	28 μM			200 μM			
13	28 μM			200 μM	100 μM		
14	28 μM			200 μM	1 mM		
15	28 μM			200 μM		100 μM	
16	28 μM			200 μM		1 mM	
17	28 μM	2 mM				1mM	
18	28 μM	2 mM					100 μM
19	28 μM	2 mM					1 μM
20	28 μM	2 mM		200 μM			1 μM

Results and discussion

Self-circularisation of *cld* mRNA to determine 5'- and 3' – ends of *cld* mRNA

Sequence analysis of genes surrounding *cld* revealed two potential promoters for the transcription of *cld* (see section B). To determine the 5' – and 3'- end of *cld* mRNA, the self-circularisation method described by Gonzales *et al.* (unpublished) was used. As a control, the 16S rRNA was used showing a single band at the expected size after RT-PCR, indicating a correct experimental set-up. Unfortunately, for *cld* mRNA no product was obtained due to unknown reasons.

Immunofluorescence

To confirm the suggested cytosolic localization, immunofluorescence experiments were performed by hybridizing *L. monocytogenes* cells with a polyclonal Cld-specific antibody. This experiment should confirm the cytoplasmic localization of Cld that was already suggested due to the absence of a signal peptide and the results obtained by Western blot (see section B). To investigate the background fluorescence signal of the specific antibody, the pre-serum obtained before antibody production was used and unfortunately showed high background fluorescence using the Cy2-labelled secondary antibody. Nevertheless, the signal clearly occurred only from the cells and not from other substances in the cell solution. To exclude unspecific signals deriving from the secondary antibody, one possibility would have been to test a differently labelled antibody using another channel for detection.

IPTG induction of SF22 leads to higher OD₆₀₀ but lower cfu number

When growth curves measuring OD₆₀₀ of induced and non-induced SF22 strains were obtained, a much higher growth was observed for cells heterologously expressing *cld* (= induced SF22) than for non-induced SF22 or the *E. coli* host strain C43 alone (Fig. C.3). To investigate the reason of

this apparently increased growth when *clb* was expressed, cfu assays were performed to analyse if the seemingly higher growth rate also manifests in a higher cfu number or if cells are only physically enlarged, which as well would lead to a higher OD₆₀₀.

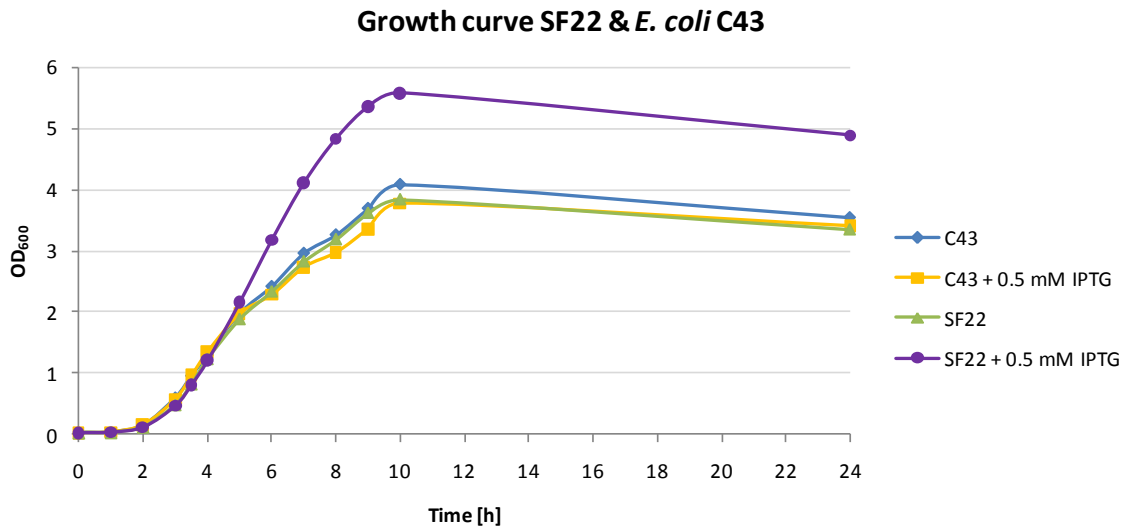


Fig. C.3: Growth curve of SF22 and *E. coli* C43 showing a longer log-phase of induced SF22 cells

A similar increased growth has been described during heterologous overexpression of bacterial hemoglobins in *E. coli*. These bacterial hemoglobins/globin-coupled sensors are described as mediators of cellular responses to metabolic and environmental stimuli such as NO, CO and oxygen (4, 9). Cells e.g. expressing the hemoglobin of *Vitreoscilla* outgrew the non-induced control strains as well as cells without plasmid (13). Furthermore, the expression of hemoglobins of *Vitreoscilla* was shown to be upregulated under diminished oxygen concentrations (5) similar to the expression of *clb*. Comparable to *Clb*, hemoglobins are heme-proteins. Another interesting observation was the identification of a chimeric protein consisting of a globin domain coupled to an antibiotic monooxygenase (ABM) (3). A similar chimera was described for a putative *clb* and an ABM domain in *H. volcanii* (1). Speculatively, these striking similarities might indicate a related function of *Clb* and hemoglobins.

Section C

First, SF22 was compared to *E. coli* C43 carrying the empty expression plasmid pET21b(+) (= strain SF194) under induced and non-induced conditions. As described, cells were induced at $OD_{600} \approx 0.8 - 1$, (3.5h post inoculation). Already 1.5h later, at timepoint 5h, a reduced cfu count of induced SF22 compared to non-induced SF22 and SF194 was observed. This difference became even more pronounced later during the experiment (Fig. C.4) The ratio between determined cfu and measured OD_{600} for induced SF22 decreased over time, clearly showing that the observed cfu number, which was reduced compared to the control strains did not correlate with the measured OD_{600} (Fig. C.5). Monitoring the cells under the microscope revealed an increased cell size of induced SF22 compared to the control strains (Fig. C.8). A possible explanation could be the high amounts of Cld produced. Thereby, cells use all their resources to express the protein and almost completely abolish cell division. However, the comparison with results from hemoglobin studies is difficult in this case since in these studies growth was only monitored by measuring OD_{600} or dry-cell weight (2, 13) and not by cfu numbers.

In a control experiment, pET22b(+) harbouring the gene *a/eIF2 α* from the archaeon *Sulfolobus solfataricus* (26) was transformed into *E. coli* C43 (= strain SF197) encoding a protein of 30 kDa. *a/eIF2 α* is a translation initiation factor in *Archaea* and was chosen as a control protein because it is comparably well expressed in *E. coli* and is described to not show any function in *E. coli* (26). In this experiment, growth rate and cfu were determined as described (Fig. C.6). Similarly to the first experiment, SF197 was compared to SF194 under induced and non-induced conditions. Induction occurred at 4h post inoculation and led to an arrest in cell division until timepoint 5h. Here, all strains showed similar OD_{600} values (Fig. C.6). However, the ratio between cfu and OD_{600} was considerably lower for induced SF197 than for the control strains, indicating that cfu counts were lower when the protein was expressed (Fig. C.7). This suggests that cells again redirected their resources from cell division to heterologous expression of *a/eIF2 α* . The lower cfu number of induced SF197 compared to the OD_{600} measurements can similarly to the situation in induced SF22 be explained by clearly enlarged cells as seen under the microscope (Fig. C.8).

Growth curve and cfu of SF22 and SF194 +/- IPTG

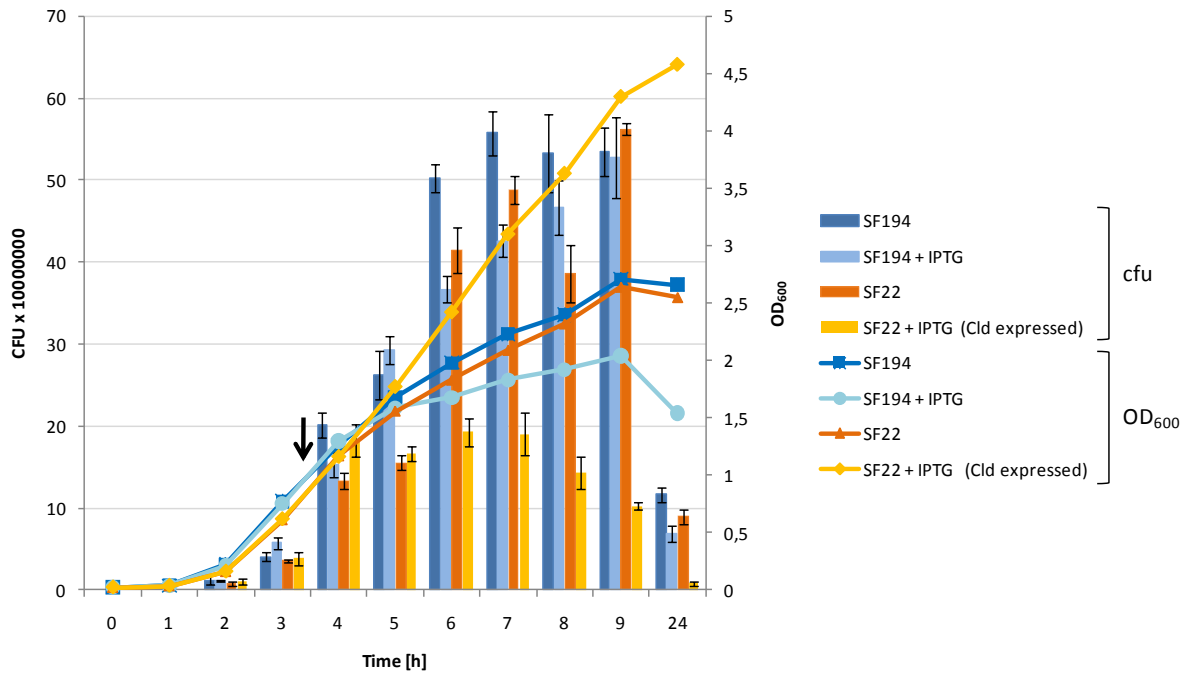


Fig. C.4: Growth curve and cfu of SF22 and SF194 under induced and non-induced conditions. Induced SF22 which heterologously expresses Cld reaches a higher OD₆₀₀ than non-induced SF22 and the control strain SF194 carrying empty pET21b(+). However, induced SF22 shows a highly reduced cfu number compared to the controls. The black arrow indicates time of induction with 0.5 mM IPTG.

Ratio SF22 and SF194 cfu/OD₆₀₀

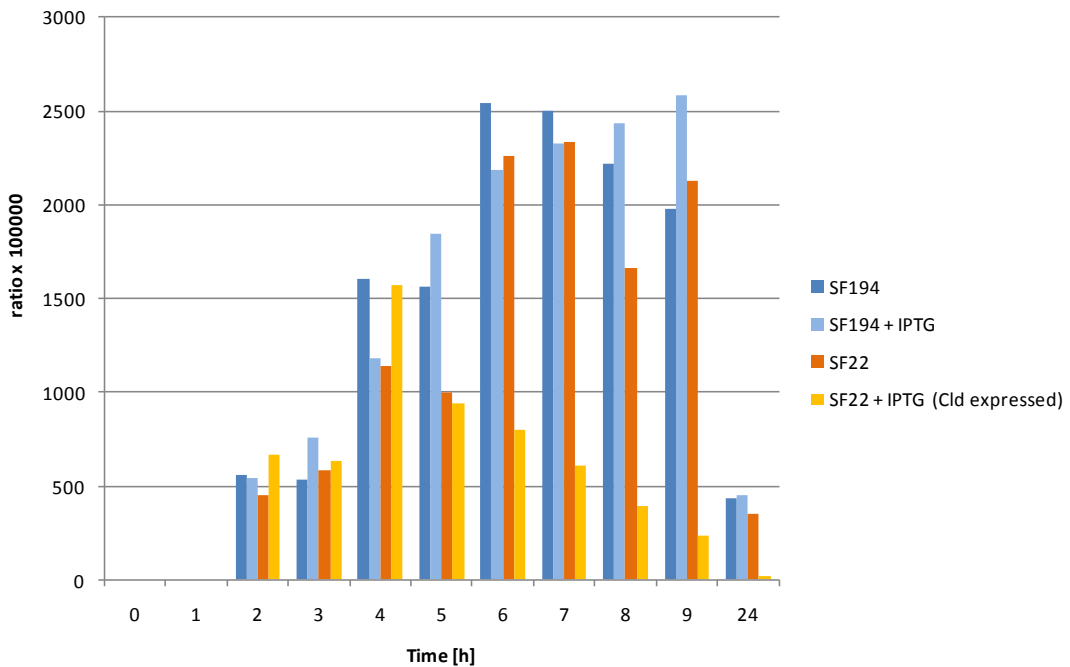


Fig. C.5: Ratio of cfu and OD₆₀₀ values shown in Fig.C.4. The reduced ratio for induced SF22 shows that OD₆₀₀ values are increasing while cfu counts are reduced during the course of the experiment.

Growth curve and cfu SF194 and 197 +/- IPTG

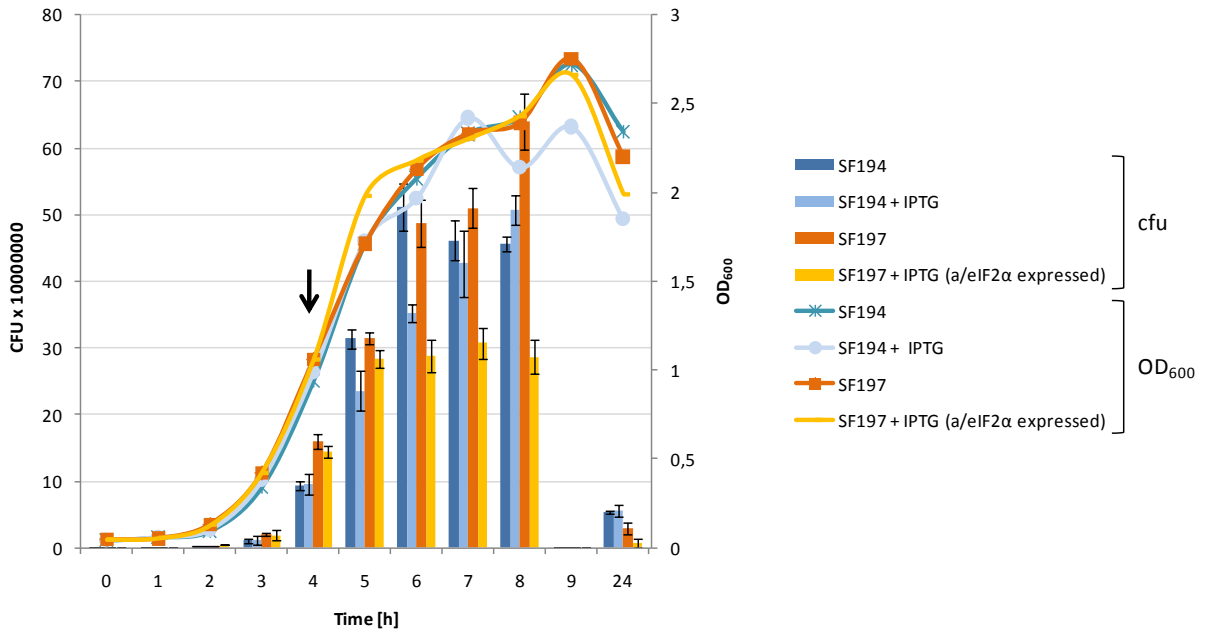


Fig. C.6: Growth curve of SF194 and SF197 under induced and non-induced conditions. All strains show a similar growth curve independent of IPTG addition. Compared to the control strain SF194 and non-induced SF197, the expression of *a/eIF2α* in SF197 leads to a reduction in cfu counts starting at time point 5h. The black arrow indicates time point of induction with 0.5 mM IPTG.

Ratio SF194 and SF197 cfu/OD₆₀₀

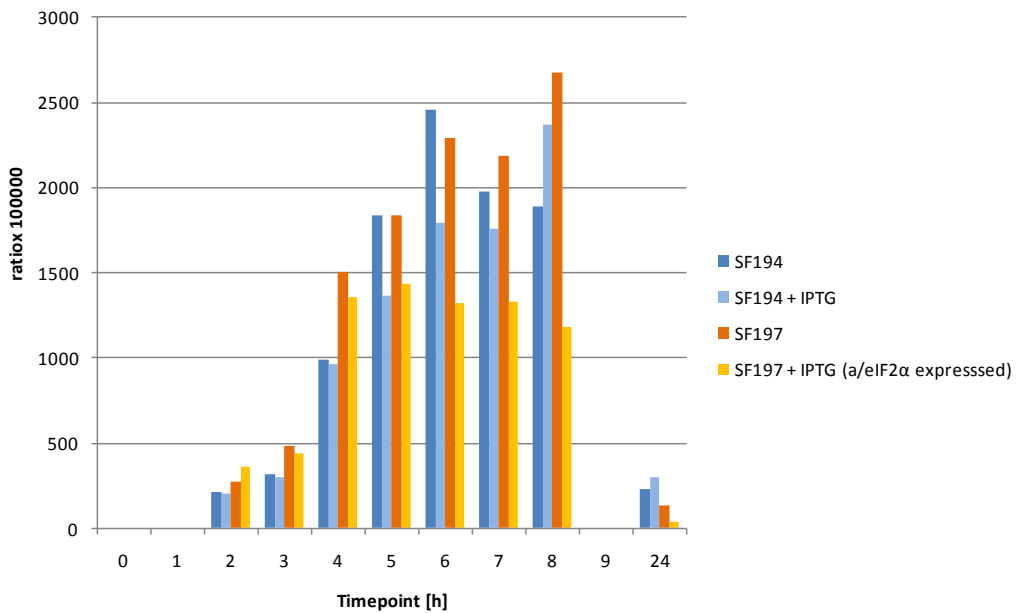


Fig. C.7: Ratio of cfu and OD₆₀₀ values shown in Fig.C.5. The expression of *a/eIF2α* in SF197 starting at 4h after inoculation clearly reduces the ration between cfu counts and OD₆₀₀. This is comparable although less pronounced to the effect observed for induced SF22.

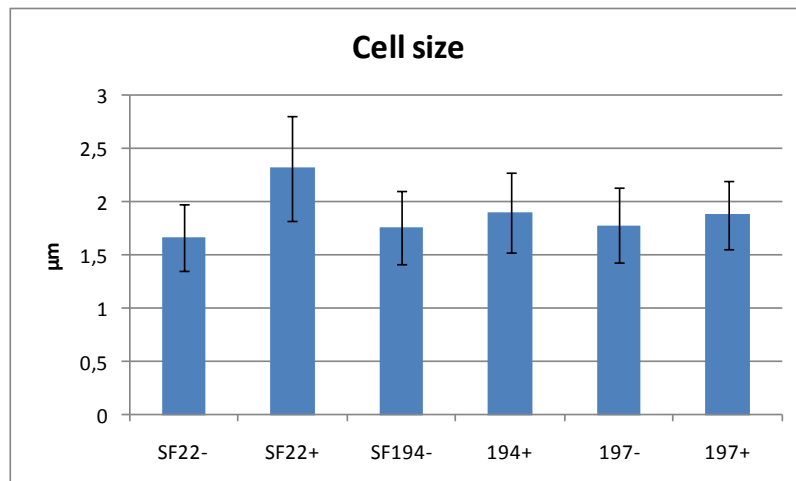


Fig. C.8: Average cell sizes of strains SF22, SF194 and SF197 under induced and non-induced conditions as determined by microscopic analyses. Induced SF22 shows increased cells sizes compared to non-induced SF22 and other control strains. The increased cell size is reflected in an increased OD_{600} as shown in Figures C.5 and C.7.

To compare the amount of *cld* expression and expression of *a/eIF2 α* in *E. coli*, samples were taken at timepoint 8h and analyzed by SDS-PAGE (Fig. C.9). The gel pictures show that *cld* (Fig. C.9 (A)) is stronger expressed than *a/eIF2 α* (Fig. C.9 (B)). This would explain why the ratio of cfu to OD_{600} is much lower in induced SF22 (*Cld*) then in SF197 (*a/eIF2 α*) assuming that the increased protein content leads to a larger cell size.

The results obtained here suggest that the at first observed phenotype of an increased OD_{600} seems to derive from a more general phenomenon. The high protein production leads to a larger cell size which is reflected in a higher OD_{600} . However, a possible influence of an unknown *Cld* function can at this point not be excluded. The results obtained with the control strain SF197 indicate that an increase in OD_{600} is primarily due to physical enlargement of the bacterial cell.

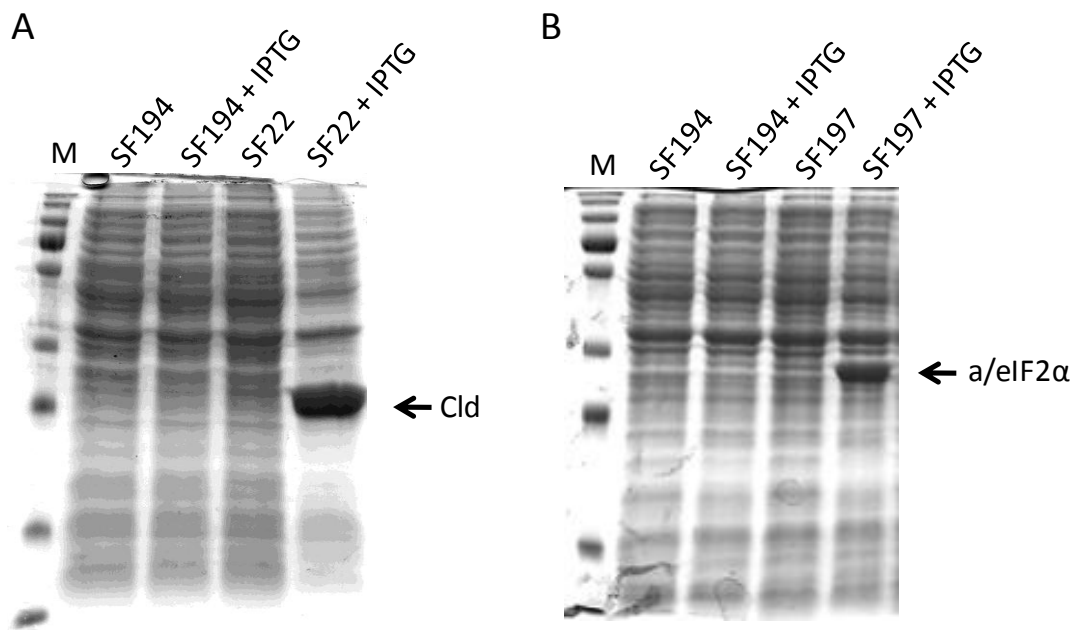


Fig. C.9: Protein gels of the SF194/SF22 and SF194/SF197 growth curve experiments. Samples were taken at 8h, loaded on an SDS-PAGE and stained with colloidal Coomassie blue. Overexpression of *clد* (A) is higher than overexpression of *a/eIF2α* (B)

Addition of Cld during infection of RAW 264.7 macrophages does not alter survival of *Listeria* and *Salmonella*

Listeria is a very potent pathogen that is able to survive the harsh environment of the phagolysosome in high numbers. Nevertheless, some cells are killed and lysed, thereby releasing their content. According to personal discussion with Prof. Thomas Decker, it is widely discussed in the scientific community that enzymes released from these lysed cells might further help the remaining bacteria to better cope with the bactericidal compounds. Therefore, RAW264.7 macrophages were infected with *L. monocytogenes* LO28 and purified Cld was added simultaneously, thereby simulating the release of Cld by lysed *Listeria* cells. In a control experiment, macrophages were infected with *Listeria* cells only or incubated with purified sole Cld as described in the materials and methods section. Figure C.10 shows that there was no significant difference in survival of *L. monocytogenes* with (black bar) and without (grey bar) the

Section C

addition of Cld. Therefore we concluded that Cld does not have a direct influence on the virulence of *L. monocytogenes*. However, it must be noticed that the internalization of exogenous Cld by macrophages could not be directly shown as the used protein amounts were too low for Western blot analysis. Moreover, it cannot be excluded that the heterologous expression and purification of Cld did not lead to a fully functional protein.

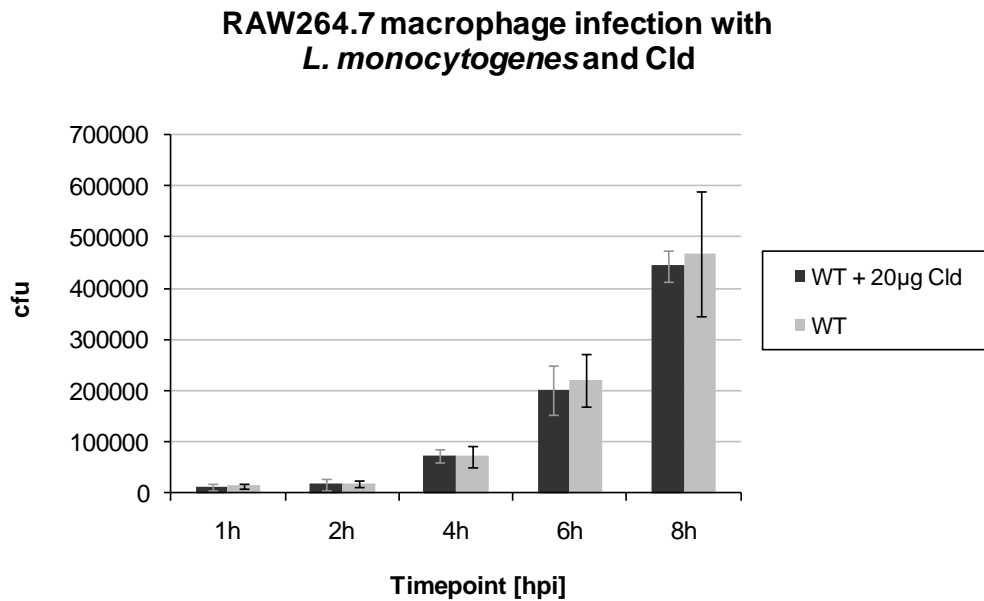


Fig. C.10: Summary of three independent RAW 264.7 macrophage infection experiments with *L. monocytogenes* LO28 (wt) and *L. monocytogenes* LO28 with exogenously added Cld (WT+20g Cld). No significant change in survival rate could be observed

In an additional experiment the influence of *S. typhimurium* 14028s expressing *cld* from plasmid pSF24 in the infection of RAW264.7 macrophages was tested. As *Salmonella* does not possess a homolog of *cld*, no interference with a host-derived Cld could be expected and due to the high similarity of *Salmonella* with *E. coli*, expression of *cld* from pET21b(+) was easily achievable. RAW264.7 macrophages were then infected with wt *S. typhimurium* 14028s, SF138 and SF151 as described. Again, no difference was observed in survival of *Salmonella* while expressing *cld* (= SF138) compared to the wt or SF151. Interestingly, the introduction of an empty copy of pET21b(+) already increased the survival of *Salmonella* without the addition of antibiotics as a selective agent (Fig. C.11). Finally, it cannot be excluded that the expression of *cld* was not correct

concerning post-translational modification or co-factor binding in *Salmonella*. Furthermore, the absence of *clid* from the genome of *Salmonella* could also be compensated by the presence of an alternative gene. Then, no change in infectivity or survival rate would be expected.

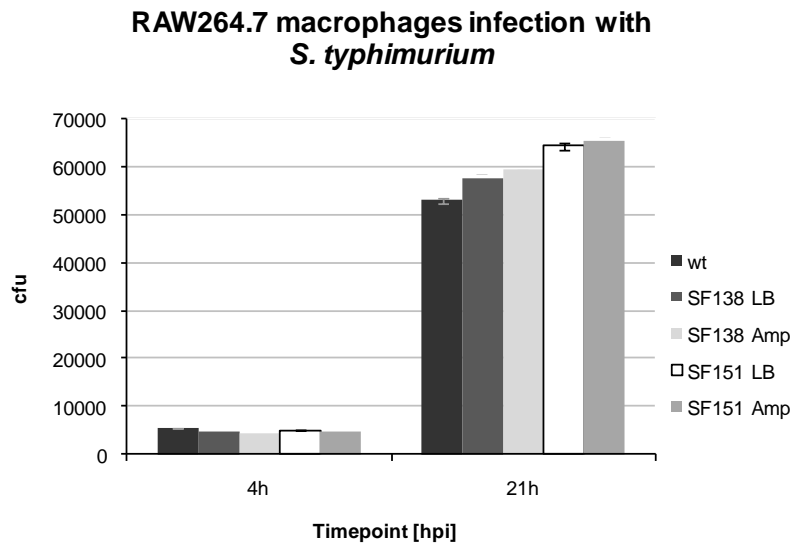


Fig. C.11: Representative result of a RAW264.7 macrophage infection with *S. typhimurium* 14028s (wt), a *clid*-expressing *S. typhimurium* 14028s strain (SF138) and SF151 as control. Samples from strains SF138 and SF151 were plated on LB and LB+ampicillin plates to investigate a putative loss of plasmid during the course of the assay. No significant difference in survival rate was monitored between wild type and *clid*-expressing strains.

Does ResD influence *clid* expression in *L. monocytogenes*?

As described in the Introduction, an altered expression of *ywfl*, a *clid*-homolog in *B. subtilis*, was reported under different anaerobic growth conditions in *B. subtilis* Δ *resD*. The aim of this experiment was to study the effect of a *resD* knock-out in *L. monocytogenes* on *clid* expression in the mutant *L. monocytogenes* strain EGD Δ *resD* (obtained from M. Larsen (15)). It must be noted that *L. monocytogenes* LO28, the strain used in other experiments of this study, was not used here because it only encodes a truncated version of *resD* (12). Here, cells were first grown under aerobic and anaerobic conditions in rich BHI medium with and without the addition of 25 mM mannose.

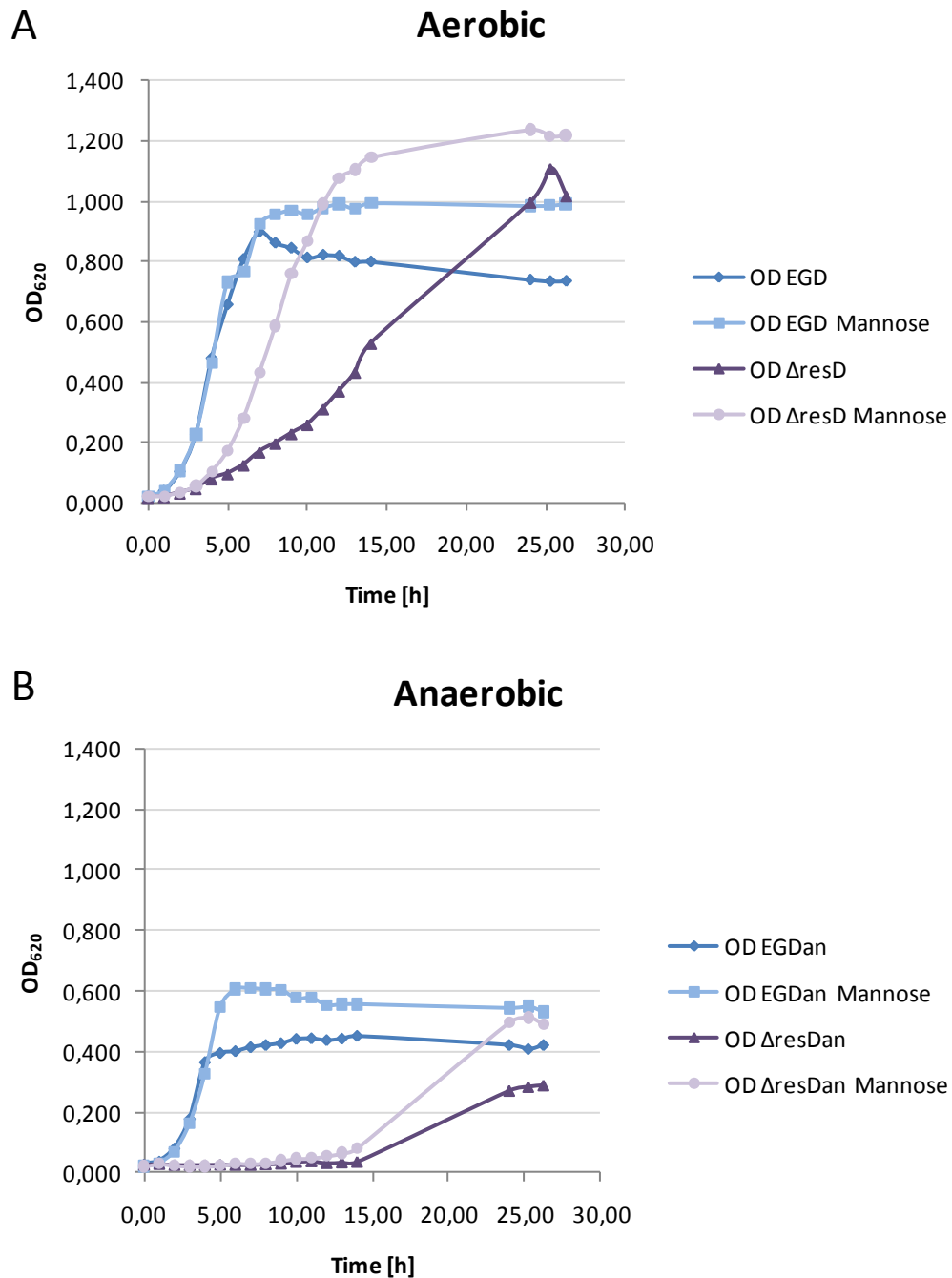


Fig. C.12: Aerobic and anaerobic growth curves of *L. monocytogenes* EGD wt and Δ resD in BHI with/without 25 mM mannose. (A) aerobic growth curve showing that 25 mM mannose can compensate the reduced growth of the *resD* mutant leading to a even higher growth than the wt. Addition of mannose to the wt prolongs the stationary phase. (B) Anaerobic growth curve: The *resD* mutant has a largely increased lag-phase under anaerobic growth conditions compared to the wt. Similarly to aerobic conditions, 25 mM mannose can compensate the reduced growth rate. Under anaerobic conditions, the wt shows a much more pronounced response to 25 mM mannose leading to a higher OD₆₂₀ than the wt without mannose.

Section C

The reason to use mannose was the presence of two other mannose-specific PTS dependent uptake systems that were not affected by the lack of ResD, whereas for glucose, the low-affinity uptake system could not fully compensate the lack of the PTS system (15). The response of both strains to the different conditions was first monitored by recording growth curves (Fig. C.12). Under aerobic conditions, the addition of mannose could compensate the reduced growth rate of the *resD* mutant strain leading to a slightly increased lag-phase and a higher growth than the wt. The response of the wt to mannose became visible as a prolonged stationary phase. Under anaerobic growth conditions, *L. monocytogenes* generally reaches a 50% lower OD₆₂₀ than under aerobic conditions. However, wt cells exhibited an approximately 30% higher OD₆₂₀ with 25 mM mannose than without mannose. The *resD* mutant shows a highly increased lag-phase under anaerobic conditions, but the increased growth effect with the addition of mannose is similar to the aerobic growth conditions. The results obtained here clearly confirm the observations of Larsen *et al.* (15). The addition of increased amounts of carbohydrates compensates the lack of a functional glucose/mannose-specific PTS system in the *resD* mutant under aerobic conditions and stimulates growth in the wt. Additionally, under anaerobic conditions the mutant has a comparably longer lag-phase with and without mannose but reaches wt level at stationary phase when mannose is added.

To analyse the expression pattern of *cld* under aforementioned conditions, cells were harvested at late stationary phase and protein extracts were analysed by Western blot as described in materials and methods. *L. monocytogenes* EGDΔ*resD* grown in BHI under aerobic conditions did not show any *cld* expression without mannose in the medium. This changed after the addition of mannose to the medium. Under anaerobic conditions, low *cld* expression was visible which again was increased to wt level by the addition of mannose (Fig. C.13). These results clearly show an important direct or indirect effect of ResD on *cld* expression, although it is in strong contrast to the indicated essential phenotype of *cld* (section B). The assay was repeated three times but, unexpectedly, this result could not be reproduced.

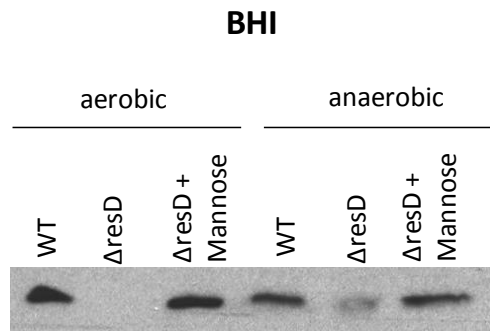


Fig. C.13: Cld-specific Western blot of *L. monocytogenes* EGD and *L. monocytogenes* EGD $\Delta resD$ grown aerobically/anaerobically in BHI medium. Growth of *resD* mutant was supplemented with 25 mM mannose. Under aerobic conditions, *cld* expression was not observed in the *resD* mutant, although the addition of mannose reversed this effect. Under anaerobic conditions, the *resD* mutant has a weak *cld* expression. This finding contradicts the strongly indicated essential phenotype of *cld*. Repetitive experiments did not confirm this finding due to unknown reasons.

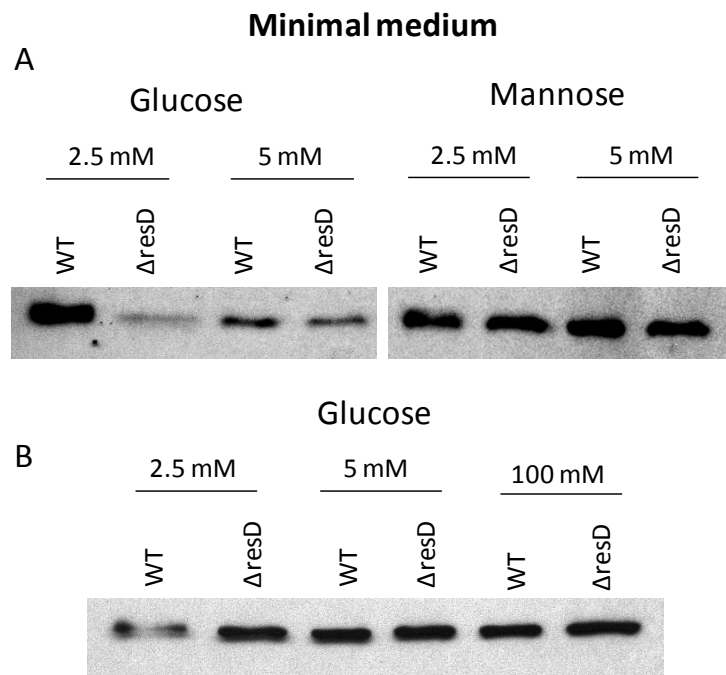


Fig. C.14: Cld-specific Western blot of *L. monocytogenes* EGD and *L. monocytogenes* EGD $\Delta resD$ grown aerobically in minimal medium. (A) Growth with 2.5 mM glucose shows a reduced expression of *cld* which is again compensated if cells are grown in the presence of mannose. The reduction in *cld* expression is diminished if 5 mM glucose are added indicating a glucose dependent expression pattern. Comparable to the experiments with BHI, the phenotype could not be reproduced (B).

As indicated, the amount of carbohydrates in the medium could be an important factor in *cld* regulation and could also vary over a certain range in the commercially available medium BHI. Therefore, in a next attempt, cells were grown in minimal medium according to Phan-Thanh *et al.* (27) with defined amounts of glucose and mannose. First growth experiments under aerobic conditions using 2.5 mM and 5 mM glucose indicated that truly, *cld* expression was triggered by glucose in a dose-dependent manner (Fig. C.14 (A)). Addition of similar amounts of mannose increased *cld* expression again to wt level. Similar to the experiments with BHI, the same phenotype could not be reproduced in three independent experiments when cells were grown in minimal medium (Fig. C.14 (B)). However, it is interesting that the reduced *cld* expression could be seen in both BHI and minimal medium grown cells. Although the assays were not reproducible, a certain effect of ResD on *cld* cannot be excluded.

Cld does not possess a peroxidase function but shows a weak catalase activity

When screening available databases like Genbank for members of COG3253, different functions like chlorite dismutase, chlorite O₂-lyase, (conserved) hypothetical protein or putative heme peroxidase are assigned to these proteins. Remarkably, a putative heme peroxidase function of the chlorite dismutase homolog TT1485 of *T. thermophilus* HB8 was already suggested by Ebihara *et al.* (6) but not shown. However, the authors show a weak catalase activity of the *cld*-homolog using an oxygen electrode. Lee *et al.* (17) as well tested different known peroxidase substrates like guaiacol and ABTS but did not observe any reactivity of Cld from *D. aromatica* RCB to these compounds.

In this study we first recorded the absorption spectrum of purified Cld, revealing a Soret peak at 412 nm and two additional peaks at 540 nm and 570 nm (Fig. C.15) characteristic for the heme ligand as already mentioned in section B.

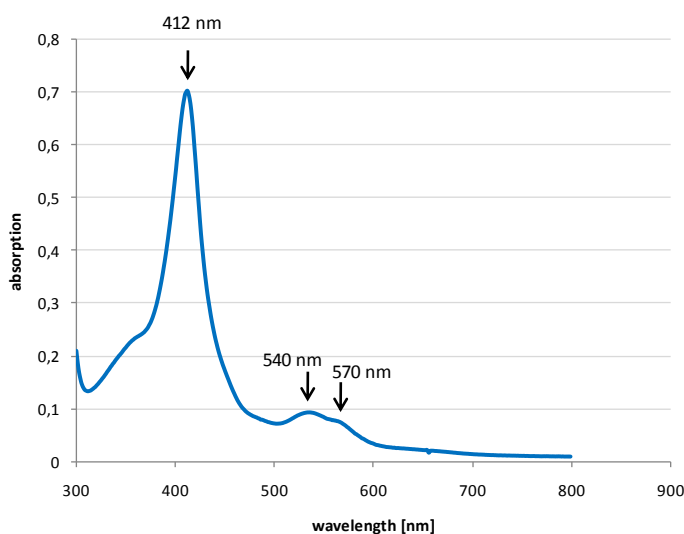
Absorption spectrum of *L. monocytogenes* Cld

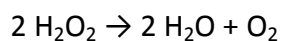
Fig. C.15: Absorption spectrum of *L. monocytogenes* Cld. Three distinct peaks are visible at 412 nm (Soret peak), 540 nm and 570 nm.

Peroxidase and halogenase activity

The known peroxidase substrates guaiacol and ABTS were used to investigate the reaction of Cld with H_2O_2 and/or $NaClO_2$ in different combinations as shown in table C.5 and table C.6. No reaction to any of the compounds used in this experiment could be shown. Next, the ability of Cld to halogenate MCD was tested using NaCl and KBr in different combinations with H_2O_2 and/or $NaClO_2$ similar to the study of Lee *et al.* (17). Again, no reactivity was observed. For a more detailed view on the reaction of Cld with H_2O_2 , $NaClO_2$, peracetic acid, HOCl, KNO_2 and ascorbic acid, stopped-flow experiments were performed (for more details see table C.8). As shown by Lee *et al.* (17), Cld of *Dechloromonas aromatica* RCB, is able to form compound I from peracetic acid, but, although the authors proposed a mechanism for the degradation of $NaClO_2$, they did not provide any experimental evidence for compound I formation out of $NaClO_2$. Here, with none of the mentioned substrates or substrate combinations, compound I or even compound II formation could be shown for the Cld of *L. monocytogenes*.

Catalase activity

Lee *et al.* (17) also stated that the Cld mechanism predicted by them is reminiscent of the catalase reaction. Thus, H₂O₂ and oxygen electrode measurements were performed using H₂O₂ and/or NaClO₂ (table C.3 and table C.4) to investigate if Cld can perform the following catalase reaction:



Using the H₂O₂ electrode, H₂O₂ decay without NaClO₂ was first shown to be exponential, followed by a continuous linear decline in H₂O₂ (Fig. C.16). Next, NaClO₂ was additionally added to the reaction. We hypothesized that although Cld cannot complete the reaction from ClO₂⁻ to O₂ and Cl⁻, an intermediate compound could react with H₂O₂ and increase oxygen formation from both substrates. However, the addition of NaClO₂ to a mixture of Cld and H₂O₂ reduced the efficiency of Cld to decay H₂O₂ with increasing concentrations, especially over 100 mM NaClO₂ (Fig. C.16). This bleaching effect can be addressed to destruction of the heme by NaClO₂.

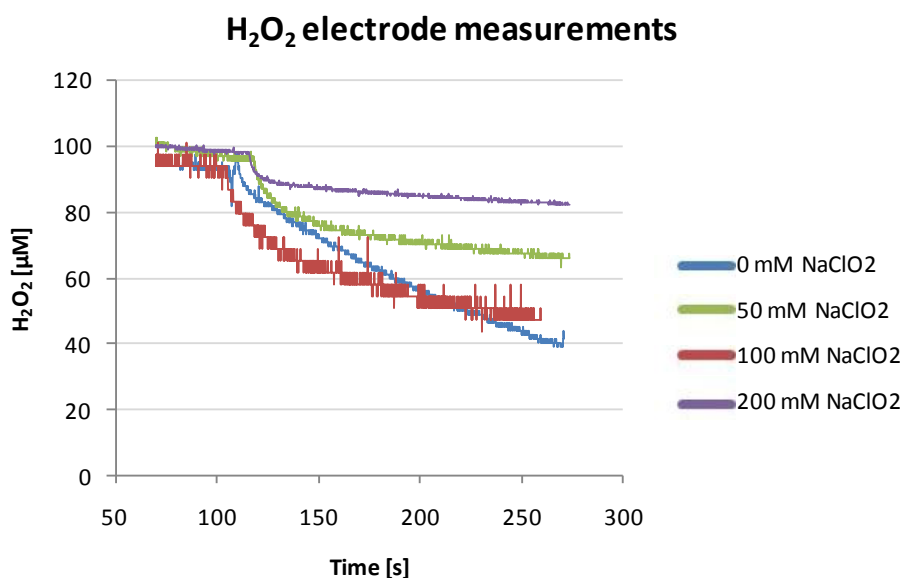


Fig. C.16: H₂O₂ electrode measurements. 5 µM Cld and 100 µM H₂O₂ were mixed with increasing amounts of NaClO₂ and the reduction in H₂O₂ concentration was monitored over time. NaClO₂ reduced the ability of Cld to decay H₂O₂, which can be seen by a flattening of the curves compared to the control experiment without NaClO₂.

Section C

As already briefly described in section B, measurements with a Clark-type oxygen electrode were performed thereby mixing 1 μM Cld with 10 mM H_2O_2 . A linear increase in oxygen formation was observed which increased with further addition of 1 μM Cld (see Fig. B.7) suggesting a decay of H_2O_2 caused by Cld. Similarly to the measurements with the H_2O_2 electrode, the addition of NaClO_2 to the reaction blocked oxygen formation due to bleaching of the heme center.

However, to clearly evaluate this indicated weak catalase activity, further calibration of the electrode and more replicates of these experiments would be necessary. Indeed, considering the abundance of a validated catalase in *L. monocytogenes* (16), there seems to be no need given for such weak and inefficient catalase activity as seen for Cld.

Conclusive remarks

In section B it was shown that *clt* of *L. monocytogenes* is an essential gene and that its product does not exhibit a chlorite degrading function. Therefore, the aim of the experiments shown here, was to further investigate *clt* and elucidate the true function of this gene. First, it was interesting to see that the strong heterologous expression of a protein like Cld has a crucial effect on the growth of the host. In first experiments a similar increase in growth after expression of *clt* in *E. coli* compared to heterologous overexpression of hemoglobins was observed. However, a more detailed investigation using cfu assays and microscopic evaluation of the different cell sizes showed that the increased OD_{600} derived from enlarged cells and seems to be a more general effect of protein overexpression. Nevertheless, it would be interesting to see how the situation is during heterologous hemoglobin expression as during these studies only OD_{600} and dry-weight measurement had been performed. Is the increased OD_{600} there also reflected in cfu number? As these two proteins show other striking similarities like the constitutive expression in the host and the chimeric occurrence of hemoglobins and *clt* with an antibiotic monooxygenase domain, it would be worth to further analyse these two proteins.

Section C

One of the hypotheses concerning the function of Cld was a putative ROS/RNS detoxifying activity during persistence in the phagolysosome. Therefore, infection studies with RAW264.7 macrophages were performed but did not show any effect on the survival of *Listeria* or *Salmonella*.

In another approach, the expression of *cld* in a *resD* mutant strain of *L. monocytogenes* EGD was investigated but gave very contradictory results. Although first growth experiments in both BHI and minimal medium showed a significant decrease in *cld* expression in the *resD* mutant, the results were not reproducible due to unknown reasons. However, a certain influence of ResD on *cld* cannot be excluded as the phenotype had been observed in two different media. Assuming that there is an influence of ResD on *cld* in *L. monocytogenes*, ResD must positively regulate *cld* expression in a direct or indirect manner. This is in contrast to the negative regulation shown for ResD on the *cld*-homolog *ywfl* in *B. subtilis* (19). Furthermore, the observed phenotype is contradicting the strongly indicated essential feature of *cld* as shown in section B. One explanation for this inconsistency could be that in the *resD* mutant Cld is not necessary anymore due to a complete shut-down of the respective pathway, Cld is involved in. Another possibility could be that Cld is important for the removal of toxic side products that are not produced in the mutant. As the knowledge about ResD in *L. monocytogenes* is restricted to only one study, nothing is known about the regulatory mechanisms or the binding motif of ResD. The proposed ResD box of *B. subtilis* was not found in close proximity to *cld* in *L. monocytogenes*. However, it would not be surprising if ResD binds to an alternative motif in *L. monocytogenes* considering the different target genes of ResD compared to *B. subtilis*. To completely clarify a putative interaction of ResD with *cld*, further experiments on the DNA, RNA and protein level are necessary.

Finally, putative peroxidase, halogenase and catalase activities were examined. These functions have already been investigated in former studies on different Cld-like proteins (6, 17). Here, it could not be shown that Cld of *L. monocytogenes* is able to form compound I from chlorite or any other known peroxidase substrate. As the degradation of chlorite by Cld was also suggested to

Section C

occur via compound I formation, this observation is in accordance with the lack of a measurable chlorite degrading function of Cld as shown in section B. Furthermore, a possible halogenase activity as known for other peroxidases could not be shown either.

Although a weak catalase activity was measured, this can hardly be considered as the main function of Cld, especially as a validated catalase in *L. monocytogenes* is described. However, it cannot be excluded that a catalase activity was the former or is an emerging function of Cld-like proteins. Nevertheless, the obtained results strongly indicate that the true function of Cld in *L. monocytogenes* lies elsewhere.

References

1. **Bab-Dinitz, E., H. Shmuely, J. Maupin-Furlow, J. Eichler, and B. Shaanan.** 2006. *Haloferax volcanii* PitA: an example of functional interaction between the Pfam chlorite dismutase and antibiotic biosynthesis monooxygenase families? *Bioinformatics* **22**:671-5.
2. **Bollinger, C. J., J. E. Bailey, and P. T. Kallio.** 2001. Novel hemoglobins to enhance microaerobic growth and substrate utilization in *Escherichia coli*. *Biotechnol Prog* **17**:798-808.
3. **Bonamore, A., A. Attili, F. Arengi, B. Catacchio, E. Chiancone, V. Morea, and A. Boffi.** 2007. A novel chimera: the "truncated hemoglobin-antibiotic monooxygenase" from *Streptomyces avermitilis*. *Gene* **398**:52-61.
4. **Chan, M. K.** 2001. Recent advances in heme-protein sensors. *Curr Opin Chem Biol* **5**:216-22.
5. **Dikshit, K. L., R. P. Dikshit, and D. A. Webster.** 1990. Study of *Vitreoscilla* globin (vgb) gene expression and promoter activity in *E. coli* through transcriptional fusion. *Nucleic Acids Res* **18**:4149-55.
6. **Ebihara, A., A. Okamoto, Y. Kousumi, H. Yamamoto, R. Masui, N. Ueyama, S. Yokoyama, and S. Kuramitsu.** 2005. Structure-based functional identification of a novel heme-binding protein from *Thermus thermophilus* HB8. *J Struct Funct Genomics* **6**:21-32.
7. **Ermolaeva, S., S. Novella, Y. Vega, M. T. Ripio, M. Scotti, and J. A. Vazquez-Boland.** 2004. Negative control of *Listeria monocytogenes* virulence genes by a diffusible autorepressor. *Mol Microbiol* **52**:601-11.
8. **Esbelin, J., J. Armengaud, A. Zigha, and C. Duport.** 2009. ResDE-dependent regulation of enterotoxin gene expression in *Bacillus cereus*: evidence for multiple modes of binding for ResD and interaction with Fnr. *J Bacteriol* **191**:4419-26.
9. **Freitas, T. A., S. Hou, and M. Alam.** 2003. The diversity of globin-coupled sensors. *FEBS Lett* **552**:99-104.
10. **Geng, H., S. Nakano, and M. M. Nakano.** 2004. Transcriptional activation by *Bacillus subtilis* ResD: tandem binding to target elements and phosphorylation-dependent and -independent transcriptional activation. *J Bacteriol* **186**:2028-37.
11. **Glaser, P., L. Frangeul, C. Buchrieser, C. Rusniok, A. Amend, F. Baquero, P. Berche, H. Bloecker, P. Brandt, T. Chakraborty, A. Charbit, F. Chetouani, E. Couve, A. de Daruvar, P. Dehoux, E. Domann, G. Dominguez-Bernal, E. Duchaud, L. Durant, O. Dussurget, K. D. Entian, H. Fsihi, F. Garcia-del Portillo, P. Garrido, L. Gautier, W. Goebel, N. Gomez-Lopez, T. Hain, J. Hauf, D. Jackson, L. M. Jones, U. Kaerst, J. Kreft, M. Kuhn, F. Kunst, G. Kurapkat, E. Madueno, A. Maitournam, J. M. Vicente, E. Ng, H. Nedjari, G. Nordsiek, S. Novella, B. de Pablos, J. C. Perez-Diaz, R. Purcell, B. Rimmel, M. Rose, T. Schlueter, N. Simoes, A. Tierrez, J. A. Vazquez-Boland, H. Voss, J. Wehland, and P. Cossart.** 2001. Comparative genomics of *Listeria* species. *Science* **294**:849-52.

12. **Kallipolitis, B. H., and H. Ingmer.** 2001. *Listeria monocytogenes* response regulators important for stress tolerance and pathogenesis. *FEMS Microbiol Lett* **204**:111-5.
13. **Khosla, C., and J. E. Bailey.** 1988. Heterologous expression of a bacterial haemoglobin improves the growth properties of recombinant *Escherichia coli*. *Nature* **331**:633-5.
14. **LaCelle, M., M. Kumano, K. Kurita, K. Yamane, P. Zuber, and M. M. Nakano.** 1996. Oxygen-controlled regulation of the flavohemoglobin gene in *Bacillus subtilis*. *J Bacteriol* **178**:3803-8.
15. **Larsen, M. H., B. H. Kallipolitis, J. K. Christiansen, J. E. Olsen, and H. Ingmer.** 2006. The response regulator ResD modulates virulence gene expression in response to carbohydrates in *Listeria monocytogenes*. *Mol Microbiol* **61**:1622-35.
16. **Leblond-Francillard, M., J. L. Gaillard, and P. Berche.** 1989. Loss of catalase activity in Tn1545-induced mutants does not reduce growth of *Listeria monocytogenes* in vivo. *Infect Immun* **57**:2569-73.
17. **Lee, A. Q., B. R. Streit, M. J. Zdilla, M. M. Abu-Omar, and J. L. DuBois.** 2008. Mechanism of and exquisite selectivity for O-O bond formation by the heme-dependent chlorite dismutase. *Proc Natl Acad Sci U S A* **105**:15654-9.
18. **Liu, X., and H. W. Taber.** 1998. Catabolite regulation of the *Bacillus subtilis* ctaBCDEF gene cluster. *J Bacteriol* **180**:6154-63.
19. **Marino, M., T. Hoffmann, R. Schmid, H. Mobitz, and D. Jahn.** 2000. Changes in protein synthesis during the adaptation of *Bacillus subtilis* to anaerobic growth conditions. *Microbiology* **146 (Pt 1)**:97-105.
20. **Milenbachs, A. A., D. P. Brown, M. Moors, and P. Youngman.** 1997. Carbon-source regulation of virulence gene expression in *Listeria monocytogenes*. *Mol Microbiol* **23**:1075-85.
21. **Miroux, B., and J. E. Walker.** 1996. Over-production of proteins in *Escherichia coli*: mutant hosts that allow synthesis of some membrane proteins and globular proteins at high levels. *Journal of Molecular Biology* **260**:289-298.
22. **Nakano, M. M., T. Hoffmann, Y. Zhu, and D. Jahn.** 1998. Nitrogen and oxygen regulation of *Bacillus subtilis* nasDEF encoding NADH-dependent nitrite reductase by TnrA and ResDE. *J Bacteriol* **180**:5344-50.
23. **Nakano, M. M., Y. Zhu, M. Lacelle, X. Zhang, and F. M. Hulett.** 2000. Interaction of ResD with regulatory regions of anaerobically induced genes in *Bacillus subtilis*. *Mol Microbiol* **37**:1198-207.
24. **Nakano, M. M., P. Zuber, P. Glaser, A. Danchin, and F. M. Hulett.** 1996. Two-component regulatory proteins ResD-ResE are required for transcriptional activation of *fnr* upon oxygen limitation in *Bacillus subtilis*. *J Bacteriol* **178**:3796-802.
25. **Parker, C., and R. W. Hutkins.** 1997. *Listeria monocytogenes* Scott A transports glucose by high-affinity and low-affinity glucose transport systems. *Appl Environ Microbiol* **63**:543-6.

Section C

26. **Pedulla, N., R. Palermo, D. Hasenohrl, U. Blasi, P. Cammarano, and P. Londei.** 2005. The archaeal eIF2 homologue: functional properties of an ancient translation initiation factor. *Nucleic Acids Res* **33**:1804-12.
27. **Phan-Thanh, L., and T. Gormon.** 1997. A chemically defined minimal medium for the optimal culture of *Listeria*. *Int J Food Microbiol* **35**:91-5.
28. **Puri-Taneja, A., M. Schau, Y. Chen, and F. M. Hulett.** 2007. Regulators of the *Bacillus subtilis* cydABCD operon: identification of a negative regulator, CcpA, and a positive regulator, ResD. *J Bacteriol* **189**:3348-58.
29. **Stock, A. M., V. L. Robinson, and P. N. Goudreau.** 2000. Two-component signal transduction. *Annu Rev Biochem* **69**:183-215.

Section D

The truncated chlorite dismutase of
Nitrobacter winogradskyi is a fully
functional chlorite degrading enzyme

Abstract

In this study, the truncated chlorite dismutase of *Nitrobacter winogradskyi* was heterologously expressed, purified and characterized. Spectroscopic analysis revealed the expected Soret peak at 406 nm indicating the presence of the heme ligand. The temperature and pH optima of purified Cld were shown to be 20°C and pH 5.5. V_{max} and K_M determination classified Cld performance of *Nitrobacter* close to other validated Clds. Comparison of *Nitrobacter* Cld aa sequence with the recently published crystal structure of Cld from *A. oryzae* showed the presence of the three main residues important for chlorite dismutase function. The missing N-terminal part of Cld in *N. winogradskyi* does therefore not interfere with heme coordination and substrate binding. Further sequence analysis revealed the absence of a signal peptide at the N-terminus, suggesting that Cld is probably localized in the cytoplasm. The suggested co-localization of a nitrite-oxidoreductase and Cld in the cytoplasm might indicate a functional relationship that needs to be further investigated.

Introduction

Aerobic nitrification is a key process in the microbial nitrogen cycle and of biological waste water treatment and consists of two steps. First ammonia is oxidized to nitrite by ammonia-oxidizing bacteria (AOB) or archaea (AOA) (14, 15). Subsequently, nitrite (NO_2^-) is further oxidized by nitrite-oxidizing bacteria (NOB) to nitrate (NO_3^-) by the following reaction (12):



Nitrite functions as an electron donor for the reduction of NAD via reverse electron flow and the generation of ATP by oxidative phosphorylation (24). The functional guild of NOB comprise until now 5 genera including *Nitrospira* and *Nitrobacter* (1, 4).

Section D

Nitrobacter winogradskyi is a gram-negative, facultative chemolithoautotrophic, nitrite-oxidizing alphaproteobacterium. It gains energy by the oxidation of nitrite and fixes carbon dioxide as its main source of carbon (24). Recently the genome sequences of *N. winogradskyi* Nb-255 (24) and of *N. hamburgensis* X14 (25) have been published giving a more detailed insight into the physiological capabilities and unique features of *Nitrobacter* spp..

Chlorate reduction by microorganisms involved in the nitrogen cycle had first been linked to nitrate reduction (5, 11). Mutants deficient in chlorate reduction were also unable to reduce nitrate, thereby connecting the two mechanisms (27). For nitrite-oxidizing bacteria (NOB) like *Nitrospira* and *Nitrobacter*, it was shown that the nitrite-oxidizing enzyme system can as well oxidize nitrite using chlorate as electron acceptor (21, 22). Especially for cultures of *Nitrobacter* it was shown that nitrite-oxidation can be linked with chlorate reduction under aerobic as well as anaerobic conditions (11, 17). Interestingly, the resulting chlorite seemed to strongly inhibit further nitrite-oxidation (11, 17) and no evidence was given that *N. winogradskyi* could detoxify the accumulating chlorite. However, Hynes *et al.* (11) only measured the amount of chlorite produced (0.25 mM) from 10 mM chlorate by *N. winogradskyi* but did not investigate the remaining amounts of chlorate in the medium. Therefore, it is unknown how much chlorate was reduced to chlorite, which subsequently could have been processed by Cld to chloride and oxygen.

The recent publication of Maixner *et al.* (19) was the first report that experimentally linked a nitrite oxidizing bacterium (NOB) to chlorite degradation. The authors showed that '*C. Nitrospira defluvi*' encodes a functional chlorite dismutase gene, albeit showing a lower affinity to chlorite than other Clds from validated PCRB. This might be a hint to a different main function of the Cld-homolog. The proven occurrence of a functional Cld in a NOB without any identified (per)chlorate reductase genes induced discussion about the origin and the purpose of this gene. As Maixner *et al.* (19) stated, the reduction of perchlorate or chlorate by *Nitrospira* would provide almost similar amounts of $\text{ATP}^*(\text{mol NO}_2^-)^{-1}$ than aerobic nitrite oxidation. This leads to the assumption that

Section D

perchlorate or chlorate could be alternative electron acceptors for *Nitrospira* although growth would be expected to be slower (19). The reduction of (per)chlorate could presumably be mediated by the enzyme nitrite-oxidoreductase (Nxr). Working in both directions (29), Nxr might mediate the oxidation of nitrite to nitrate under aerobic conditions (32) and the reduction of nitrate to nitrite under anaerobic conditions (9, 13). For nitrate reductase, it has already been shown that chlorate can be reduced to chlorite (16). Thus similarly, Nxr could use chlorate instead of nitrate and reduce it to chlorite.

Nxr is the key enzyme for nitrite-oxidation and belongs to the molybdopterin-dependent enzymes of the DMSO reductase family (18) comparably to perchlorate reductase (2). It consists of at least three subunits (alpha to gamma) (18) thereby forming a heteromer. In *Nitrospira*, Nxr seems to be present in the periplasm where it is attached to the cytoplasmic membrane via its gamma subunit (22). In contrast to that, Nxr in *Nitrobacter* is directed to the cytoplasm but is as well attached to the membrane (23).

As already mentioned by Maixner *et al.* (19), *N. winogradskyi* also harbours a *cld*-homolog that differs from that of *Nitrospira*. Thus, the aim of this study was to heterologously express *cld* of *N. winogradskyi* and investigate its predicted chlorite degrading function. The obtained results should then be compared with the characteristics of Cld from '*Candidatus N. defluvii*' described by Maixner *et al.* (19) and with other validated Clds.

Material and Methods

Bacterial strains, media and growth conditions

E. coli was handled as described in section B. *E. coli* BL21 tuner strain ($F^- ompT hsdS_B (r_B^- m_B^-) gal dcm lacY1$, Novagen) was used for heterologous over-expression of *cld*. Therefore, plasmid pSF29 was transformed into *E. coli* BL21 tuner leading to strain SF170. SF170 was grown in rich TB medium (12 g trypton, 24 g yeast extract, 4 ml glycerol per 1 l dH₂O; 10x KHPO₄: 23.14 g KH₂PO₄, 164.3 g K₂HPO₄*3H₂O per 1 l dH₂O, used 1x final concentration) and handled as described in chapter "Protein manipulations".

DNA manipulations

Plasmid pSF29 was obtained from F. Maixner. Shortly, the 552 bp gene sequence of *cld* of *Nitrobacter winogradskyi* was amplified using primers CldNBV (5'-CGAGC GCATATGACGTTACAGTCTTCACC-3')/CldNBR (5'-GCGCGAGGATCCCCTATCGCGCGCCAATCG-3'), purified and cloned into expression plasmid pET21b(+) via its NdeI/BamHI restriction sites.

Protein manipulations

For heterologous expression and purification of Cld from *Nitrobacter winogradskyi*, pSF29 was transformed into *E. coli* BL21 tuner resulting in strain SF170. For optimal expression of *cld*, 3 l of TB medium in a 5 l flask were inoculated 1:50 with an ON culture of SF170 and incubated for 6h at 28°C with agitation. Then, 0.5 mM IPTG was added to induce protein expression during further ON incubation at 28°C. Cells were harvested on the next day and proteins were purified as described in section B with one exception: before sonication, cells were incubated with appropriate amounts of DNaseI and lysozyme for 30 min on ice. Total protein was pooled and dialysed against 20 mM HEPES/ 100 mM NaCl/ 0.5 % glycerol pH 7.4 . To increase the concentration of the protein, Amicon Ultra-4, PLGC Ultracel-PL Membran, 10 kDa columns (Millipore) were used as described

Section D

by the manufacturer. Heme reconstitution of the purified Cld was performed by addition of hemin (50 mg/ml in 0.1 M NaOH) to the suspension. Via gel filtration (Hiload 2660 Superdex 200, GE Healthcare) most of the excessive hemin was removed. As additional purification of Cld from SF170 was necessary, all purification steps were repeated and the resulting protein mixed with the gel-filtered protein suspension. Finally, the total protein extract was re-purified using a 5 ml HisTrap column in an ÄKTA explorer chromatography system (GE Healthcare Life Sciences). Red/brownish-coloured fractions were harvested and pooled. Final protein concentration was 32 mg/ml resulting in 57.6 mg total protein.

Protein concentration and integrity was determined as described in section B.

Functional assay

The Soret peak of purified Cld was determined spectroscopically using a Nanodrop ND-1000 (PeqLab). To determine putative bleaching effects on the heme ligand, absorbance was measured after the addition of 100 mM NaClO₂. Furthermore, the influence of the reducing agent Na-dithionite on the heme ligand was determined.

Determination of the production rate of chloride by Cld from *Nitrobacter winogradskyi* was carried out as described by Maixner *et al.* (19). Briefly, a chloride electrode (DX235-Cl connected to a Seven Multi station; Mettler-Toledo) was used to measure emerging Cl⁻ in 50 ml of reaction buffer (10 mM sodium phosphate, adjusted to the respective pH) containing the respective concentration of NaClO₂ and 100 mM NaNO₃. The solution was stirred in a 100 ml beaker in a heated water bath at the respective temperature. To ensure equal conditions for all triplicates measured, temperature inside the beaker was taken manually. Measurements below 25°C, were performed in a 4°C room. After the enzymatic reaction had been started by adding 450 µg of purified Cld, the Cl⁻ concentration was recorded every second until no further change in Cl⁻ concentration could be monitored. Subsequently, the measured Cl⁻ concentrations were plotted against time and the rate of Cl⁻ formation was calculated based on the linear part of the curve.

Section D

Specific enzyme activity was expressed in U (mg protein)⁻¹, where one unit (U) is defined as the amount of Cl⁻ produced per minute (μmol min⁻¹; (30)). For determination of pH and temperature optima, 1 mM NaClO₂ was used as substrate, whereby every data point was measured 3 times independently. Based on these verified optimal conditions for ClD, activities for increasing amounts of NaClO₂ were measured and all specific activities were plotted against the respective NaClO₂ concentrations. Curve fitting was performed using the Michaelis Menten equation and the substrate inhibition equation of the GraphPad Prism software package (GraphPad Software Inc.). Based on the latter equation, K_M and V_{max} values were determined. The turnover number k_{cat} was calculated by multiplying V_{max} with the molar mass of one subunit. Furthermore, the ratio of k_{cat}/K_M indicates the substrate specificity of a certain substrate-enzyme combination.

Sequence analysis

Sequence analysis was carried out as described in section B. Molecular mass determination was performed using the DNA/RNA/Protein/Chemical Molecular Weight Calculator from Chang Biosciences (<http://www.changbioscience.com/genetics/mw.html>).

Results and Discussion

Annotation of *cld* and its surrounding genomic region

The genomic proximity of *cld* in *N. winogradskyi* is very diverse (Fig. D.1). Upstream of *cld* two genes involved in DNA replication (DNA primase Nwi_2440) and transcription (RNA polymerase sigma factor, Nwi_2441) are encoded on the opposite strand. The *cld* gene itself is a 552 bp long gene that has an overlapping ORF with the downstream gene Nwi_2443. The product of Nwi_2443 is a N-formylglutamate amidohydrolase, known to catalyse the terminal reaction in the five-step pathway for histidine utilisation in *Pseudomonas putida*. In this reaction, N-formyl-L-glutamate (FG) is hydrolysed to produce L-glutamate plus formate. Further downstream two hypothetical genes (Nwi_2444, Nwi_2445) are located followed by a carbamoyl-phosphate synthase (Nwi_2446), which catalyzes the production of carbamoyl-phosphate from bicarbonate and glutamine in the pyrimidine and arginine biosynthesis pathways. Genes Nwi_2447 and Nwi_2448 encode for a DNA-binding ferritin-like protein and an undetermined tRNA, respectively.

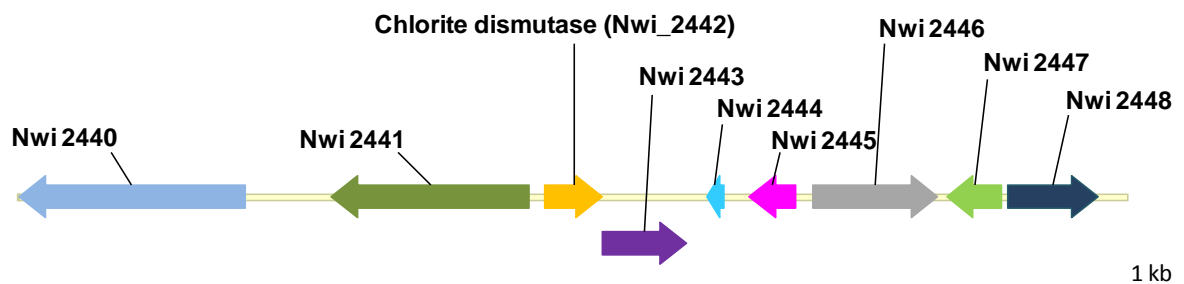


Fig. D.1: Annotation of genomic region surrounding *cld*. Nwi_2440: RNA polymerase sigma factor, Nwi_2441: DNA primase, Nwi_2442: chlorite dismutase, Nwi_2443: N-formylglutamate amidohydrolase, Nwi_2444: hypothetical protein, Nwi_2445: hypothetical protein, Nwi_2446: carbamoyl-phosphate synthase small subunit, Nwi_2447: DNA-binding ferritin-like protein (Dps), Nwi_2448: undetermined tRNA. 5'- region of Nwi2443 is overlapping with 3' - region of *cld*.

No reasonable functional link between *cld* and its surrounding genes could be hypothesized. None of the genes are organized in an operon and no functional relationship could be deduced for any

of these genes. Comparing the genomic region surrounding *cld* in *N. winogradskyi* with the organization in '*C. N. defluvii*' (19), no similarities can be observed as in '*C. N. defluvii*', *cld* is embedded in genes encoding for the purine synthesis pathway.

Alignment of Cld and determination of important residues

Compared to other *cld* or *cld*-like genes, chlorite dismutase of *N. winogradskyi* is a very short gene of only 552 bp. It lacks a signal-peptide at the 5' – end as determined by SignalP (3) together with a major part of the N-terminus of the protein leading to a reduced protein size of 20.4 kDa. This indicates that Cld is probably not transported outside the cytoplasm. In clear contrast to this, the Cld of *Nitrospira* does encode a signal peptide and therefore is assumed to be located in the periplasm (19).

The latest results on important residues for chlorite dismutase function were published by Geus *et al.* (6) for Cld of *Azospira oryzae* Gr-1. The obtained results were implicated in a multiple sequence alignment (Fig. D.2). The authors identified a highly important arginine residue at position 183 to be involved in substrate positioning and activation (red, Fig. D.2). Furthermore, a histidin (His170) was described to be necessary for the coordination of the iron atom in the heme (turquoise, Fig. D.2). The highly conserved tryptophan (Trp155) is involved in binding one of the propionate groups of the heme ligand and could as well act as an electron donor during the formation of compound II (black, Fig. D2). These three residues are highly conserved in all validated Clds and were shown to occupy similar positions in the active sites of cytochrome *c* peroxidase. The amino acids marked in blue in Figure D.2 (asparagine, tyrosine, isoleucine) show residues that are also involved in binding of the propionate groups of the heme, but they seem to be less conserved. Despite its truncated N-terminus, Cld of *N. winogradskyi* harbours the three highly important and conserved residues described above but encodes an arginine and a valine instead of the asparagine and isoleucine involved in heme binding.

Section D

reduced the Soret peak signal indicating bleaching of the heme center by excessive substrate concentrations. Reduction of the heme center from Fe(III) to Fe(II) by Na-di-thionite was not visible in the assay which would be indicated by a shift of the curve to the right. This could be due to a highly unstable Fe(II) phase that is immediately recurring to its oxidized state.

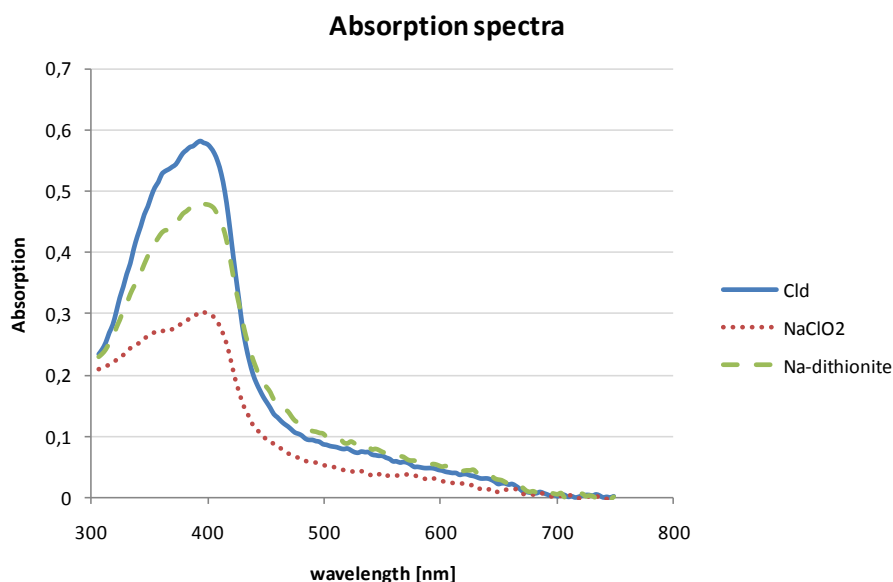


Fig. D.3: Absorption spectra of *N. winogradskyi* Cld. The Soret peak was determined to be at 406 nm (continuous line). Characteristic additional peaks at around 550 nm are most likely hidden in the decreasing slope of the curve. Addition of 100 mM NaClO₂ decreased the Soret peak due to bleaching of the heme center (dotted line). The strong reductant Na-dithionite should shift the Soret peak to a higher wavelength. No shift could be observed for *N. winogradskyi* Cld (stippled line).

The method for the activity measurements of Cld has already been described by Maixner *et al.* (19). Using 1 mM NaClO₂ as substrate, temperature and pH optima were determined to be 20°C and pH 5.5, respectively (Fig. D.4 and D.5). This temperature optimum is the lowest of all so far characterized characterized Clds, which have their optima at 25°C (*Candidatus* *N. defluvii*, *P. chloritidismutans*) or 30°C (*A. oryzae* GR-1). The optimal pH of *Nitrobacter* Cld is slightly lower than for other Clds (pH 6). For a comparison of values for all validated Clds see table D.1. Specifically comparing the obtained values with the second Cld of a nitrite-oxidizer shows that the Cld of *Nitrobacter* has a lower pH optimum and a lower temperature optimum than that of *Nitrospira*. Interestingly, the two nitrite-oxidizers are optimally cultivated between 28°C and 31°C (31). Hence, in both cases the temperature optima for Cld of *Nitrobacter* and *Nitrospira* are lower

Section D

than their respective growth optima. Therefore, it is rather difficult to explain the difference in Cld performance optima.

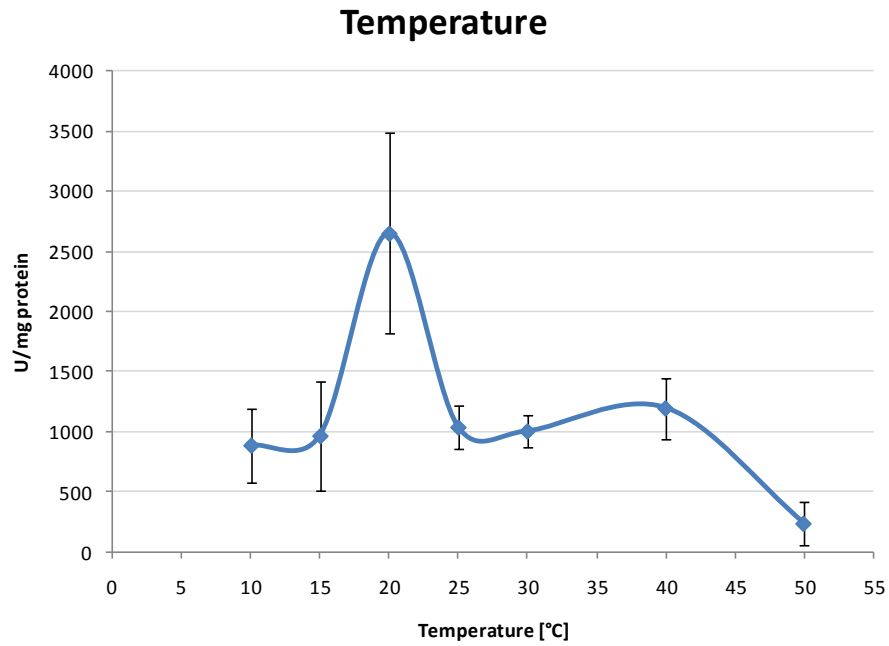


Fig. D.4: Specific activities for Cld using 1 mM NaClO₂ at different temperatures from 10°C to 50°C; optimum for Cld activity is at 20°C.

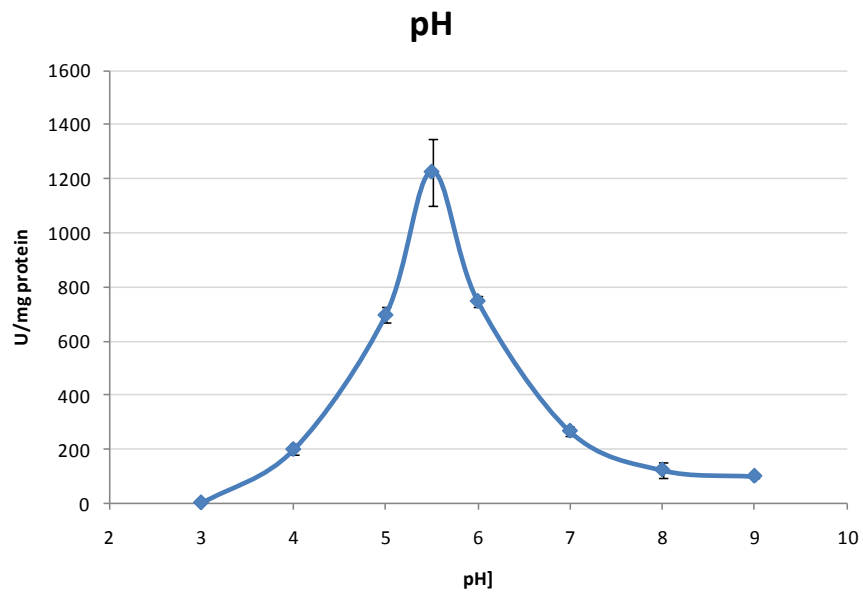


Fig. D.5: Specific activities for Cld using 1 mM NaClO₂ at different pH ranging from pH 3 to pH 9; optimum for Cld activity is at pH 5.5

Under the obtained optimal conditions, specific activities of Cld at increasing amounts of NaClO_2 were determined and blotted against the respective concentrations. The data was then fit to the Michaelis-Menten equation using the program GraphPad Prism. The plotted curve did not fit to values at higher NaClO_2 concentrations due to a decrease in specific activity (stippled line, Fig. D.6). This could be explained by inactivation of Cld due to bleaching of the heme center by high amounts of NaClO_2 (28). Therefore, the substrate inhibition equation was applied, perfectly fitting to the values obtained (full line, Fig. D.6). In fact, the mechanism of heme bleaching is more a suicide inhibition than a substrate inhibition. It is not reversible (28) but leads to the same reduction in specific activity.

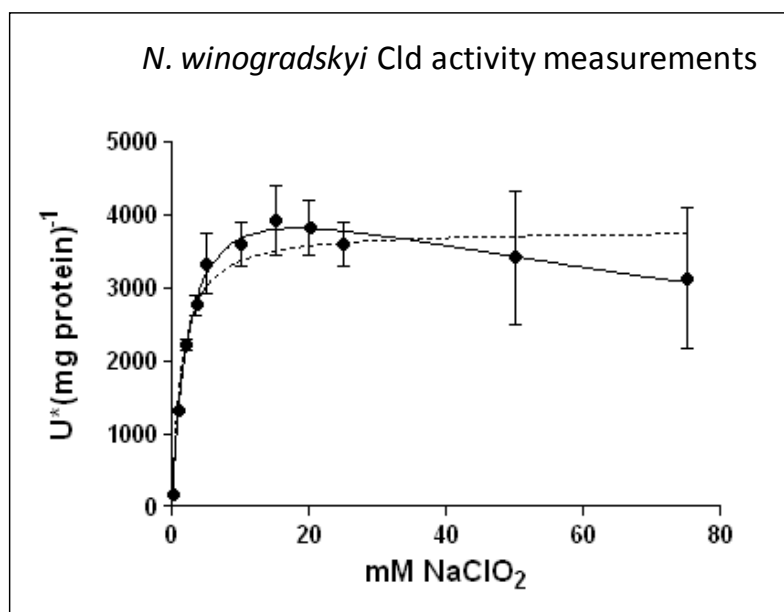


Fig. D.6: Specific activity as function of the NaClO_2 concentration. Curve fitting is based on the Michaelis-Menten equation (stippled line) and on the substrate inhibition equation of the GraphPad Prism program (full line). Due to the suicide inhibition effect of increased substrate amounts, the specific activity is reduced at higher chlorite concentrations. For more details refer to the text.

Section D

The K_M value of Cld was determined to be 2.384 ± 0.2515 mM and V_{max} to be 4796 ± 177.6 U*(mg protein)⁻¹ under optimal reaction conditions. The obtained K_M is lower than for the Cld of 'Candidatus *N. defluvii*' (15.8) but still higher than the values deriving from Clds of validated PCRB (0.08 – 0.26). This indicates that the Cld of *N. winogradskyi* has a much higher affinity to chlorite than the homolog in 'Candidatus *N. defluvii*'. Nevertheless, its affinity is lower than that of the Clds of PCRB. This could have different reasons like for example: (i) the primary substrate of Cld of *N. winogradskyi* might be a similar compound but not chlorite itself; (ii) heterologous expression systems can never resemble the exact host synthesis system resulting in different catalytic properties of the enzyme; (iii) not all active centers contain a heme ligand.

Table D.1: Summary of various characteristics determined for all validated chlorite dismutases

	<i>Nitrobacter winogradskyi</i> ¹	<i>Candidatus Nitrospira defluvii</i> ²	<i>Azospira oryzae</i> GR-1 ³	<i>Ideonella dechloratans</i> ⁴	<i>Dechloromonas aromatica</i> RCB ⁵	<i>Thermus thermophilus</i> HB8 ⁶	<i>Pseudomonas chloritidismutans</i> AW-1 ⁷
Subunit size (kDa)	20.391	30	32	25	27	26	31
Relative molecular mass (kDa)	ND	ND	140	115	116	130	110
T optimum (°C)	20	25	30	ND	ND	ND	25
pH optimum	5.5	6	6	ND	ND	ND	6
V_{max} (Umg ⁻¹)	4.796×10^3	1.9×10^3	2.2×10^3	4.3×10^3	4.7×10^3	1.6	0.44×10^3
K_M (mM)	2.384	15.8	0.17	0.26	0.22	13	0.08
k_{cat} (s ⁻¹)	1.695×10^3	0.96×10^3	1.2×10^3	1.8×10^3	1.88×10^3	0.77	0.23×10^3
k_{cat}/K_M (M ⁻¹ s ⁻¹)	7.1×10^5	6.1×10^4	7.1×10^6	6.9×10^6	35.4×10^6	59	2.7×10^6
Heme content	ND	ND	1.7	2.4	3.7	0.6	1.5
Soret band (Fe ³⁺)	406	415	394 ⁸	392	388	403	411
Soret band (Fe ²⁺)	ND	433	432 ⁸	434	434	429	433

¹This study

²Maixner *et al.* (19)

³van Ginkel *et al.* (30)

⁴Stenklo *et al.* (26)

⁵Streit *et al.* (28)

⁶Ebihara *et al.* (7)

⁷Mehboob *et al.* (20)

⁸Hagedoorn *et al.* (10)

ND, not described

The ratio k_{cat}/K_M reflects the performance constant of a certain enzyme/substrate combination. It was used in different publications to compare the efficiency of Cld in converting chlorite (19, 20). However, the use of the k_{cat}/K_M ratio to compare different enzymes reacting with the same substrate is incorrect. Eisenthal *et al.* (8) clearly showed that an enzyme having a higher catalytic efficiency (i.e. k_{cat}/K_M value) can, at certain substrate concentrations, actually catalyze an identical reaction at lower rates than one having a lower catalytic efficiency. The ratio of the two reaction rates is not a constant but rather depends on the value of substrate concentration and K_M . Therefore, the values are shown in table D.1 but are not discussed.

Conclusive remarks

This study clearly shows that chlorite dismutase of *N. winogradskyi* is a fully functional chlorite degrading enzyme with K_M and V_{max} values comparable to other validated chlorite dismutases. It is the second report about a Cld from a nitrite-oxidizing bacterium showing that the number of validated Clds from non-perchlorate reducing bacteria is increasing. Compared to the Cld of '*C. N. defluvii*', significant differences in length and sequence were found. The absence of an N-terminal part of Cld in *N. winogradskyi* did not influence the overall chlorite degrading activity of the protein. In fact, the Cld of *N. winogradskyi* showed an even higher affinity to chlorite and a better performance than the Cld of *Nitrospira*. A multiple sequence alignment showed that the important residues suggested by de Geus *et al.* (6) for Cld are also present in Cld of *Nitrobacter*. To fully uncover the importance of the N-terminal part of Cld on the specific activity, additional studies including partial deletion of different parts of a full length active Cld would be necessary. Furthermore, it would be interesting to determine the "minimal needed unit" for an active Cld as well as the optimal amino acid composition of Cld for chlorite degradation considering future biotechnological applications of Cld.

When specifically comparing Cld from the two nitrite-oxidizers *Nitrobacter* and *Nitrospira*, it is interesting to notice that in *Nitrobacter*, Cld and Nxr are both assumed to be located in the

Section D

cytoplasm, whereas in *Nitrospira* they are suggested to be located in the periplasm. Due to this co-localization it can be speculated that Nxr could indeed reduce chlorate to chlorite which is then further degraded to chloride and oxygen by Cld. To confirm this speculation, further studies on a putative chlorate reducing activity of Nxr would be needed.

Taken together, *Nitrobacter* is able to use chlorate as an electron acceptor and encodes a functional chlorite dismutase. Nevertheless, chlorate or the product of chlorate reduction, chlorite, respectively, are known inhibitors of nitrite-oxidation and growth in NOB. One explanation for this phenomenon could be that the amounts of chlorate and therefore chlorite used in previous studies were too high to be degraded by chlorite dismutase of *Nitrobacter*. As shown, chlorite can act as a suicide inhibitor for chlorite dismutase, destroying the heme ligand by bleaching. Further studies investigating the response of *Nitrobacter* to physiological amounts of chlorate would be needed to see if and how much of emerging chlorite can be removed by chlorite dismutase *in vivo*.

Additionally to the functional studies mentioned above, several other questions concerning Cld of *N. winogradskyi* remain open: (i) is *cld* expressed *in vivo* in *N. winogradskyi*, (ii) under which conditions is *cld* expressed, (iii) what are the regulators of *cld* expression and (iv) is chlorite the only substrate of Cld or can it convert other substrates or substrate combinations. It would be highly interesting and important to answer these questions in further studies to complete the present picture of Cld in NOB thereby determining the purpose of this chlorite-degrading enzyme in *Nitrobacter winogradskyi*.

References

1. **Alawi, M., A. Lipski, T. Sanders, E. M. Pfeiffer, and E. Spieck.** 2007. Cultivation of a novel cold-adapted nitrite oxidizing betaproteobacterium from the Siberian Arctic. *ISME J* **1**:256-64.
2. **Bender, K. S., C. Shang, R. Chakraborty, S. M. Belchik, J. D. Coates, and L. A. Achenbach.** 2005. Identification, characterization, and classification of genes encoding perchlorate reductase. *J Bacteriol* **187**:5090-6.
3. **Bendtsen, J. D., H. Nielsen, G. von Heijne, and S. Brunak.** 2004. Improved prediction of signal peptides: SignalP 3.0. *J Mol Biol* **340**:783-95.
4. **Bock, E., and M. Wagner.** 2001. Oxidation of inorganic nitrogen compounds as an energy source, p. 457-495. *In* M. Dworkin, S. Falkow, E. Rosenberg, K. H. Schleifer, and E. Stackebrandt (ed.), *The Prokaryotes: An Evolving Electronic Resource for the Microbiological Community (Volume 2)*. Springer Verlag, New York, USA.
5. **Chaudhuri, S. K., S. M. O'Connor, R. L. Gustavson, L. A. Achenbach, and J. D. Coates.** 2002. Environmental factors that control microbial perchlorate reduction. *Appl Environ Microbiol* **68**:4425-30.
6. **de Geus, D. C., E. A. J. Thomassen, P. Hagedoorn, N. S. Pannu, E. van Duijn, and J. P. Abrahams.** 2009. Crystal structure of chlorite dismutase, a detoxifying enzyme producing molecular oxygen. *Journal of Molecular Biology* **387**:192-206.
7. **Ebihara, A., A. Okamoto, Y. Kousumi, H. Yamamoto, R. Masui, N. Ueyama, S. Yokoyama, and S. Kuramitsu.** 2005. Structure-based functional identification of a novel heme-binding protein from *Thermus thermophilus* HB8. *J Struct Funct Genomics* **6**:21-32.
8. **Eisenthal, R., M. J. Danson, and D. W. Hough.** 2007. Catalytic efficiency and k_{cat}/K_M : a useful comparator? *Trends Biotechnol* **25**:247-9.
9. **Freitag, A., M. Rudert, and E. Bock.** 1987. Growth of *Nitrobacter* by dissimilatory nitrate reduction. *FEMS Microbiol Lett*:105-109.
10. **Hagedoorn, P. L., D. C. De Geus, and W. R. Hagen.** 2002. Spectroscopic characterization and ligand-binding properties of chlorite dismutase from the chlorate respiring bacterial strain GR-1. *Eur J Biochem* **269**:4905-11.
11. **Hynes, R. K., and R. Knowles.** 1983. Inhibition of Chemoautotrophic Nitrification by Sodium Chlorate and Sodium Chlorite: a Reexamination. *Appl Environ Microbiol* **45**:1178-1182.
12. **Jetten, M. S.** 2008. The microbial nitrogen cycle. *Environ Microbiol* **10**:2903-9.
13. **Kiesow, L.** 1964. On the Assimilation of Energy from Inorganic Sources in Autotrophic Forms of Life. *Proc Natl Acad Sci U S A* **52**:980-8.
14. **Konneke, M., A. E. Bernhard, J. R. de la Torre, C. B. Walker, J. B. Waterbury, and D. A. Stahl.** 2005. Isolation of an autotrophic ammonia-oxidizing marine archaeon. *Nature* **437**:543-6.

15. **Koops, H. P., U. Purkhold, A. Pommerening-Roser, G. Timmermann, and M. Wagner.** 2003. The lithoautotrophic ammonia-oxidizing bacteria, p. 778-811. In M. Dworkin, S. Falkow, E. Rosenberg, K. H. Schleifer, and E. Stackebrandt (ed.), *The Prokaryotes: An Evolving Electronic Resource for the Microbiological Community (Volume 5)*. Springer Verlag, New York, USA.
16. **Kucera, I.** 2006. Interference of chlorate and chlorite with nitrate reduction in resting cells of *Paracoccus denitrificans*. *Microbiology* **152**:3529-34.
17. **Lees, H., and J. R. Simpson.** 1957. The biochemistry of the nitrifying organisms. V. Nitrite oxidation by *Nitrobacter*. *Biochem J* **65**:297-305.
18. **Maixner, F., H. Koch, S. Hauzmayer, E. Spieck, D. Le Paslier, M. Wagner, and H. Daims.** Nitrite oxidoreductase (Nxr) - the metabolic key enzyme of nitrite-oxidizing *Nitrospira*: Characterization of an unusual Nxr and its application as a novel functional and phylogenetic marker gene. Unpublished.
19. **Maixner, F., M. Wagner, S. Lucker, E. Pelletier, S. Schmitz-Esser, K. Hace, E. Spieck, R. Konrat, D. Le Paslier, and H. Daims.** 2008. Environmental genomics reveals a functional chlorite dismutase in the nitrite-oxidizing bacterium '*Candidatus Nitrospira defluvii*'. *Environ Microbiol* **10**:3043-56.
20. **Mehboob, F., A. F. Wolterink, A. J. Vermeulen, B. Jiang, P. L. Hagedoorn, A. J. Stams, and S. W. Kengen.** 2009. Purification and characterization of a chlorite dismutase from *Pseudomonas chloritidismutans*. *FEMS Microbiol Lett* **293**:115-21.
21. **Meincke, M., E. Bock, D. Kastrau, and P. M. H. Kroneck.** 1992. Nitrite oxidoreductase from *Nitrobacter hamburgensis* redox centers and their catalytic role. *Arch Microbiol*:127-131.
22. **Spieck, E., S. Ehrich, J. Aamand, and E. Bock.** 1998. Isolation and immunocytochemical location of the nitrite-oxidizing system in *Nitrospira moscoviensis*. *Arch Microbiol* **169**:225-30.
23. **Spieck, E., S. Muller, A. Engel, E. Mandelkow, h. Patel, and E. Bock.** 1996. Two-dimensional structure of membrane-bound nitrite-oxidoreductase from *Nitrobacter hamburgensis*. *J. Struct. Biol.*:117-123.
24. **Starkenburger, S. R., P. S. Chain, L. A. Sayavedra-Soto, L. Hauser, M. L. Land, F. W. Larimer, S. A. Malfatti, M. G. Klotz, P. J. Bottomley, D. J. Arp, and W. J. Hickey.** 2006. Genome sequence of the chemolithoautotrophic nitrite-oxidizing bacterium *Nitrobacter winogradskyi* Nb-255. *Appl Environ Microbiol* **72**:2050-63.
25. **Starkenburger, S. R., F. W. Larimer, L. Y. Stein, M. G. Klotz, P. S. Chain, L. A. Sayavedra-Soto, A. T. Poret-Peterson, M. E. Gentry, D. J. Arp, B. Ward, and P. J. Bottomley.** 2008. Complete genome sequence of *Nitrobacter hamburgensis* X14 and comparative genomic analysis of species within the genus *Nitrobacter*. *Appl Environ Microbiol* **74**:2852-63.
26. **Stenklo, K., H. D. Thorell, H. Bergius, R. Aasa, and T. Nilsson.** 2001. Chlorite dismutase from *Ideonella dechloratans*. *J Biol Inorg Chem* **6**:601-7.
27. **Stewart, V.** 1988. Nitrate respiration in relation to facultative metabolism in enterobacteria. *Microbiol Rev* **52**:190-232.

Section D

28. **Streit, B. R., and J. L. DuBois.** 2008. Chemical and steady-state kinetic analyses of a heterologously expressed heme dependent chlorite dismutase. *Biochemistry* **47**:5271-80.
29. **Sundermeyer-Klinger, H., W. Meyer, B. Warninghoff, and E. Bock.** 1984. Membrane-bound nitrite oxidoreductase of *Nitrobacter*: evidence for a nitrate reductase system. *Arch Microbiol*:153-158.
30. **van Ginkel, C. G., G. B. Rikken, A. G. Kroon, and S. W. Kengen.** 1996. Purification and characterization of chlorite dismutase: a novel oxygen-generating enzyme. *Arch Microbiol* **166**:321-6.
31. **Watson, S. W.** 1971. Taxonomic Considerations of the Family *Nitrobacteraceae* Buchanan: Requests for Opinions. *Int J Syst Evol Microbiol* **21**:254 - 270.
32. **Yamanaka, T., and Y. Fukumori.** 1988. The nitrite oxidizing system of *Nitrobacter winogradskyi*. *FEMS Microbiol Rev* **4**:259-70.

Appendix

Minimal Medium for *L. monocytogenes*

after Phan-Thanh and Gormon - IJFM (1997) 35 :91 :95

Solution 1 : Phosphate salts 10X – store at RT			
Name	Amount	Provider	Remark
Na ₂ HPO ₄	81,6 g	Fluka 71507	
KH ₂ PO ₄	3.28 g	Alpha Aesar 011594	
dH ₂ O	Fill up to 500 ml		1L bottle
Dissolve in dH ₂ O and autoclave			

Solution 2 : Magnesium salt 100X – store at RT			
Name	Amount	Provider	Remark
MgSO ₄ .7 H ₂ O	4.09 g	Merck 1.05886- 500g	
dH ₂ O	Fill up to 100 ml		250 ml bottle
Dissolve in dH ₂ O and autoclave			

Solution 3 : Ferric citrate solution (C₆H₅O₇,FeIII) 50 X – store at 4°C (use for 6 month max)			
Name	Amount	Provider	Remark
Ferric citrate	878 mg	SIGMA F-6129.250kg	In this solution there are 22,8% Fe III
dH ₂ O (warm)	200 ml		Use 250 ml bottle for final storage
Dissolve in 200 ml warm dH ₂ O - filter			

Solution 4 : 20% glucose – store at RT			
Name	Amount	Provider	Remark
Glucose	20 g	Fluka 49140	Keep for 1 month maximum
dH ₂ O	Fill up to 100 ml		Use 250 ml bottle for final storage
Dissolve in 100 ml warm dH ₂ O - filter			

Solution 5 : Amino acids 100 X – store at 4°C			
Name	Amount	Provider	Remark
L-Leucine	200 mg	SIGMA L-800-25g	LEU
L-Isoleucine	200 mg	SIGMA I-7403-25g	ILE
L-Valine	200 mg	SIGMA V-6504-25g	VAL
L-Methionine	200 mg	SIGMA M-2893-25g	MET
L-Arginine	200 mg	SIGMA A-5131-25g	ARG
L-Histidine	200 mg	SIGMA H-9511-25g	HIS
L-Tryptophane	200 mg	SIGMA T-0271-25g	TRY
L-Phenylalanine	200 mg	SIGMA P-2126-100g	PHE
dH ₂ O	Fill up to 20 ml		Falcon 50 ml
Dissolve aa mixture (200 mg each) in 20 ml sH ₂ O. Warm for dissolving and let cool down again. Filter.			

Solution 6 : Cysteine + Glutamine solution 100 X – store at 4°C - prepare freshly			
Name	Amount	Provider	Remark
Cysteine	100 mg	SIGMA C-7352 -25g	Préparer extemporanément
Glutamine	600 mg	SIGMA G-5763 - 25g	Préparer extemporanément
dH ₂ O	Fill up to 10 ml		Falcon 10 ml
Warm for dissolving and let cool down again. Filter.			

Solution 7 : Adenine solution 100 X – store at 4°C – prepare freshly			
Name	Amount	Provider	Remark
Adenin	25 mg	SIGMA A-8626-5g	Préparer extemporanément
HCl 0,2N	20 ml (19,67 ml dH ₂ O + 0,332 ml HCL 37%)	Reidel de Haën 30723 (1L)	50 ml bottle
Dissolve in 20 ml HCl 0,2N			

SOLUTION 8 : Vitamin solution 100 X – store at 4°C :
Prepare solutions 8A, 8B and 8C separately and mix after (10 ml 8A +10 ml 8B + 1ml 8C); fill up to 100ml with dH₂O and store at 4°C.

Solution 8A			
Name	Amount	Provider	Remark
Biotin	5 mg	SIGMA B-4501	Stored at 4°C
Riboflavin	5 mg	SIGMA R-9504-25g	
dH ₂ O (warm)	10 ml		Falcon
Dissolve in 10 ml warm dH ₂ O. Let cool down.			

Solution 8B			
Name	Amount	Provider	Remark
Thiamine HCl	10 mg	SIGMA T-1270-25g	
D-panthotetic acid hemicalcium salt	10 mg	SIGMA P-2250-5g	Store at 4°C
Niacinamid	10 mg	SIGMA N-5535-100g	
Pyridoxal HCl	10 mg	SIGMA P-9130-1g	Stored at -20°C
dH ₂ O (warm)	10 ml		Falcon
Dissolve in 10 ml warm dH ₂ O. Let cool down.			

Solution 8C			
Name	Amount	Provider	Remark
<i>p</i> -aminobenzoic acid	100 mg	SIGMA A-9878-1g	Stored at 4°C
Thioctic acid =lipoic acid	5 mg	Merck 5645	
Ethanol 95°	10 ml		Falcon
Dissolve in 10ml 98% Ethanol			

Preparation of minimal medium

For 1l of medium :

Solution 1 : Phosphate salts 10X	100 ml
Solution 2 : Magnesium salt 100X	10 ml
Solution 3 : Ferric citrate solution (C₆H₅O₇,FeIII) 50 X	20 ml
Solution 4 : 20% glucose	5 ml
Solution 5 : Amino acids 100 X	10 ml
Solution 8 : Vitamin solution 100 X	10 ml
dH₂O	845 ml

Sterilisation : filter solution in sterile bottle
Divide medium in 200 ml per bottle and store at 4°C

Just before use :
Add to 200 ml of medium:

Solution 6 : Cysteine + Glutamine solution 100 X (sterile)	2 ml
Solution 7 : Adenin solution 100 X (sterile)	2 ml

Abbreviations

aa	amino acids
ABM	antibiotic monooxygenase
ABTS	2,2'-Azino-bis(3-ethylbenzothiazoline-6-sulfonic acid)
cfu	colony forming units
ORF	open reading frame
Cl ⁻	chloride
<i>cl</i> <i>d</i>	chlorite dismutase
ClO ₂ ⁻	chlorite
ClO ₃ ⁻	chlorate
ClO ₄ ⁻	perchlorate
DMEM	Dulbecco's Modified Eagle Medium
He	helium
HOCl	hypochlorite
IPTG	Isopropyl-β-D-thiogalactopyranosid
KNO ₂	potassium nitrite
llo	listeriolysin O
MCD	Monochlorodimedon
MOI	multiplicity of infection
NOB	nitrite oxidizing bacterium/bacteria
NO ₂ ⁻	nitrite
NO ₃ ⁻	nitrate
<i>n</i> <i>x</i> <i>r</i>	nitrite-oxidoreductase
ON	over-night
PAA	peracetic acid
Pcr	perchlorate reductase
PCRB	(per)chlorate reducing bacterium/bacteria
RT	room temperature

TAP	Tobacco Acid Pyrophosphatase
wt	wild type

Zusammenfassung

Die Chlorit-Dismutase (Cld) ist ein Chlorit-degradierendes Enzym im (Per)Chlorate-Reduktionsweg. Durch die Reduktion von Chlorat (ClO_3^-) entsteht toxisches Chlorit (ClO_2^-), das von Cld zu harmlosem Chlorid (Cl^-) und Sauerstoff (O_2) zerlegt wird. Bis vor kurzem war die Anwesenheit eines funktionellen *cld*-Homologs auf Organismen beschränkt, die alle Gene für den kompletten (Per)Chlorat-Reduktionsweg exprimieren. Eine groß angelegte Sequenzanalyse zeigte jedoch, dass *cld*-ähnliche Gene ubiquitär auch in verschiedenen prokaryotischen Organismen vorkommen, denen die Gene für eine vollständige Reduktion von (Per)Chlorat fehlen.

In dieser Studie wurde das *cld*-ähnliche Gen aus dem human-pathogenen, gram-positiven Bakterium *Listeria monocytogenes* untersucht. *L. monocytogenes* ist ein weit verbreitetes Bakterium, das aus Erde, Silage, Wasser und anderen Umwelthabitaten isoliert werden kann. Des Weiteren, kann dieser pathogene Mikroorganismus verschiedene Wirtszellen infizieren, in deren Zytoplasma es repliziert und sich dann von einer Zelle zur nächsten Zelle bewegt, um den Angriffen des Immunsystems zu entkommen. *L. monocytogenes* ist ein sehr gut erforschter Mikroorganismus, für den zahlreiche experimentelle Techniken zur Verfügung stehen. Deshalb und aufgrund seiner Vielseitigkeit ist *L. monocytogenes* ein idealer Kandidat, um die Funktion eines unbekanntes Gens zu untersuchen.

Eine Hypothese für die Anwesenheit eines *cld*-homologen Gens in *Listeria* war die funktionelle Notwendigkeit während der Infektion einer Wirtszelle. Dabei wird das Bakterium mit einer sehr feindlichen Umgebung konfrontiert. Cld könnte hierbei in der Detoxifizierung von reaktiven Sauerstoff- bzw. Stickstoffradikalen, die vom Immunsystem des Wirts produziert werden, involviert sein. Die Hauptaufgabe dieser Arbeit war die Deletion des *cld*-Homologs in *L.*

monocytogenes und eine Vergleichsanalyse der unterschiedlichen Phänotypen von Wildtyp und Mutante während der Infektion und unter anderen Stressbedingungen.

Sektion B beschreibt die unterschiedlichen Strategien zur Deletion des *clt*-Gens in *L. monocytogenes*. Da keine der angewandten Strategien zur Isolation einer *clt* Mutante geführt hatte, wurde ein Gen-Disruptionsexperiment durchgeführt. Dabei ergaben sich starke Hinweise, dass *clt* ein neues essentielles Gen in *L. monocytogenes* ist. Weitere Analysen auf Basis der DNS/RNS zeigten, dass *clt* monocistronisch und bicistronisch gemeinsam mit einem Excisionase-ähnlichen Gen transkribiert wird. Eine Expressionsanalyse auf Proteinebene zeigte, dass diese Clt im Zytoplasma lokalisiert ist, sehr stabil ist und konstitutiv bei 28°C und 37°C exprimiert wird. Weiters konnte unter anaeroben Wachstumsbedingungen eine Hochregulierung der *clt*-Expression beobachtet werden, wie sie auch von validierten Clts bekannt ist. Überraschenderweise besitzt die Clt von *L. monocytogenes* keine Chlorit-degradierende Aktivität. Es konnte jedoch eine schwache Katalase-Aktivität gezeigt werden.

In Sektion C werden weitere Experimente beschrieben, die durchgeführt wurden, um die wahre Funktion der Clt aus *L. monocytogenes* aufzuklären. Eine Verbindung zwischen dem 2-Komponenten System ResD und *clt* wie in *B. subtilis* konnte für *Listeria* nicht gezeigt werden. Ebenso konnte kein Einfluss von Clt auf die Infektivität und das Überleben von *L. monocytogenes* und *S. typhimurium* in RAW267.4 Makrophagen nachgewiesen werden. Im Jahr 2008 wurde ein Mechanismus für die Chlorit-Degradierung durch Clt vorgeschlagen, der dem der Peroxidase sehr ähnlich ist. Dabei kommt es zu einer Sauerstoffdoppelbindung und der Formierung eines „compound I“. Mittels verschiedenster spektroskopischer Methoden wurde eine mögliche Peroxidase und Halogenase-Aktivität von Clt untersucht. Bei keiner der verwendeten Substratkombinationen konnte jedoch eine Reaktion von Clt nachgewiesen werden. Wie schon erwähnt, zeigt Clt eine schwache Katalase-Aktivität. Da *L. monocytogenes* bereits für eine

funktionelle Katalase kodiert, wäre es höchst ungewöhnlich, dass dies die wahre Funktion von Cld ist.

Wie oben angeführt, sind *cld*-ähnliche Gene weit verbreitet in Mikroorganismen, die nicht zur Reduktion von (Per)Chlorat fähig sind. In einer Studie aus dem Jahre 2008 konnte gezeigt werden, dass das Nitrit-oxidierende Bakterium ‚*Candidatus Nitrospira defluvii*‘ eine voll-funktionsfähige Cld besitzt. Ein weiteres *cld*-Homolog konnte auch in *Nitrobacter winogradskyi*, einem weiteren Nitrit-Oxidierer, gefunden werden, welches im Rahmen dieser Arbeit auf eine Chlorit-degradierende Funktion untersucht (Sektion D) wurde. Die *cld* von *N. winogradskyi* kodiert für nur 183 Aminosäuren und ist damit verglichen mit anderen validierten Clds am N-terminalen Ende verkürzt. Unter Verwendung einer Chlorid-Elektrode konnte eine ausgeprägte Chlorit-degradierende Funktion bei einer optimalen Temperatur von 20°C und einem pH-Optimum von pH 5,5 nachgewiesen werden. Der K_M Wert der Cld aus *Nitrobacter* wurde mit $2,384 \pm 0,2515$ mM und V_{max} mit $4796 \pm 177,6$ U*(mg protein)⁻¹ unter optimalen Bedingungen bestimmt. Diese Werte weisen auf eine höhere Chlorit-Affinität der *Nitrobacter* Cld verglichen mit der Cld von ‚*C. N. defluvii*‘ hin. Interessanterweise ist Chlorit jedoch ein bekannter Inhibitor für Nitrit-oxidierende Bakterien. Deshalb benötigt es weitere Analysen, um die wahre Rolle der Cld in *N. winogradskyi* zu bestimmen.

Summary

Chlorite dismutase (Cld) is a chlorite degrading enzyme involved in the (per)chlorate reduction pathway. Thereby, it is important for the detoxification of highly reactive chlorite, originating from the reduction of chlorate, to harmless chloride and oxygen. The presence of a functional chlorite dismutase was until recently restricted to organisms capable of the energy-gaining respiration of (per)chlorate. Surprisingly, a large sequence analyses published in 2008 revealed an almost ubiquitous abundance of *cld*-like sequences in numerous organisms belonging to *Bacteria* and *Archaea*.

In this study, we investigated the putative *cld* gene of the well-described human pathogen *Listeria monocytogenes*. *L. monocytogenes* is a widely abundant bacterium that can be isolated from soil, silage, water and other environments. Furthermore, it can infect various host cells, where it replicates inside the cytosol and directly moves from one cell to the other to evade the host immune system. Due to its role as a human pathogen and its exquisite intracellular survival strategies, *L. monocytogenes* is well studied and, thus, numerous experimental techniques are available. This versatility of *L. monocytogenes* makes it an ideal candidate to study a gene with an unknown function.

The main hypothesis for the presence of a chlorite dismutase gene in *Listeria* was a functional requirement during host infection where these bacteria face a rather harsh environment. Thus, chlorite dismutase could be involved in the detoxification of reactive oxygen or nitrogen species produced by the host immune system. Therefore, one aim of this PhD thesis was to delete the putative chlorite dismutase gene in *L. monocytogenes* and compare the phenotype of the mutant and its isogenic wild type during infection and other stress conditions.

In section B, the different strategies to obtain a *cld*-mutant strain are described. As none of the applied strategies led to the deletion of *cld*, a conducted gene disruption experiment strongly indicated that *cld* is a novel essential gene in *L. monocytogenes*. Therefore, we suggest a more general metabolic function of *cld*. Furthermore, transcriptional analyses revealed that *cld* is transcribed monocistronically and polycistronically together with an excisionase-like gene encoded upstream. Further expression analysis on the protein level demonstrated that the Cld-like protein of *L. monocytogenes* is cytosolic, shows a high degree of stability, and is constitutively expressed in situ throughout growth at 28°C and 37°C. Furthermore, Cld expression is upregulated under anaerobic growth conditions which is in accordance with other validated *cld* genes. Surprisingly, Cld of *L. monocytogenes* does not have a chlorite degrading activity but shows a weak catalase activity.

Section C describes further experiments performed in order to elucidate the function of *cld* in *L. monocytogenes*. However, a link of *cld* expression to the two-component system ResDE as described for *B. subtilis* could not be confirmed for *L. monocytogenes*. Similarly, an influence of Cld on the infectivity and survival of *L. monocytogenes* and *S. typhimurium* in RAW267.4 macrophages could not be shown. In 2008, the mechanism of chlorite degradation by chlorite dismutase was suggested revealing a O-O bond forming mechanism involving compound I formation that is also produced during peroxidase activity. Using various spectroscopic techniques, I investigated the peroxidase and halogenase activity of Cld from *L. monocytogenes* using numerous substrate combinations. However, none of the chosen enzyme-substrate combinations showed any reactivity. As mentioned above, Cld exhibits a weak catalase activity although due to the presence of a highly functional catalase in *Listeria*, no need for such a weak catalase could be hypothesized.

As described above, *cld*-like genes are ubiquitously abundant in organisms not capable of (per)chlorate degradation. In 2008, the *cld* gene of the nitrite-oxidizer '*Candidatus Nitrospira*

defluvii has been shown to encode a functional chlorite dismutase. Therefore, it was very interesting to see that *Nitrobacter winogradskyi*, another nitrite-oxidizer, also harbours a putative *cld*-gene. This *cld*-homolog was further investigated as described in section D. The *cld* gene encodes for only 183 aa thereby lacking the N-terminus. Using a chloride electrode, a strong chlorite degrading activity of *Nitrobacter Cld* was revealed, having an optimal temperature at 20°C and a pH optimum of 5.5. The K_M value of Cld was determined to be 2.384 ± 0.2515 mM and V_{max} to be 4796 ± 177.6 U*(mg protein)⁻¹ under optimal conditions. These values indicate a higher affinity of *Nitrobacter Cld* to chlorite than the aforementioned Cld of *N. defluvii*. Interestingly, chlorite is a known inhibitor for nitrite-oxidizing bacteria and therefore, the role of Cld in *N. winogradskyi* still needs to be determined.

Acknowledgements

When spending four years working on your PhD thesis, many people accompany you and support you through good and bad times. Therefore, I want to acknowledge the most important people I worked and lived with during this time:

- Holger Daims for the opportunity to do my PhD in his group, to be able to work with my favorite pathogen "*Listeria monocytogenes*" and for vivid discussions on the topic and beyond
- Michael Wagner for offering me a PhD position in his department and supporting my work with numerous ideas
- Emmanuelle Charpentier for hosting me in her lab for the last 3.5 years and supplying me with important information and tricks on how to handle *Listeria*
- Angela Witte for numerous discussions, encouraging meetings and important survival strategies – and of course for being member of my PhD committee
- Thomas Decker for being part of the project as member of my PhD committee, for important input and for an always open door
- Udo Bläsi for taking part in my PhD committee, for his honest opinion and helpful discussion
- Nancy Freitag for a very nice and fruitful collaboration – I learned a lot and really enjoyed being in contact
- Frank Maixner for help with chlorite dismutase phylogeny, the chloride electrode measurements and any other question I had
- Kilian Stoecker for help with the microscope, reading this manuscript and answering any other question coming up
- Markus Schmid for help with sequences, alignments and more
- Christian Baranyi for help with statistics and various other "small" problems

- Georg Mlynek for purification of Cld and help with chromatography
- Katharina Ettwig and Marc Strous for hosting me in the lab in Nijmegen and for help with the oxygen electrode measurements
- Paul Georg Furtmüller and Christian Obinger for help with the peroxidase/catalase measurements
- Eva for encouraging me to fight for my rights
- Fanny, Silvia and Karine for helping me through the last 3.5 years. Thank you for everything, I really enjoyed being member of our group
- Doris for always listening to me, being there for me and for her support during all these stressy times. Other times will come and they will be ours!
- Hansi for an always open ear and annoying discussions – you know how to distract me
- My family for always being a safe haven and for supporting me endlessly through-out the last 30 years
- The ones closest are usually the ones that suffer the most when things are not going well. Therefore, I want to thank my husband David from the bottom of my heart that he never gave up on me. He supported me uncompromisingly - no matter what happened. You are everything to me!

Curriculum Vitae

<i>Name</i>	Mag. Stephanie Füreder
<i>Date of birth</i>	18 th October 1979
<i>Place of birth</i>	Linz, Austria
<i>Citizenship</i>	Austrian
<i>Family status</i>	married

Education

1985 – 1989	Adalbert Stifter – Übungsvolksschule, Linz
1989 – 1998	Gymnasium und Realgymnasium des Kollegiums Aloisianum, Linz
1998 – 2000	Studies „Wirtschaftsingenieurwesen Maschinenbau“ at the TU Vienna
2000 – 2005	Studies „Biology“, with specification in microbiology, at the University of Vienna
2004 – 2005	Diploma thesis at the department of microbial ecology at the University of Vienna, under the supervision of o.Univ.Prof.Dr. Michael Wagner Title: „ <i>Microarray-based diversity analyses of microorganisms involved in sulfur and nitrogen cycling</i> “
07/2005	Graduation
2005 – 2009	PhD thesis at the department of microbial ecology at the University of Vienna in cooperation with the department of microbiology and immunobiology under the supervision of o.Univ.Prof.Dr. Michael Wagner, Dr. Holger Daims and Dr. Emmanuelle Charpentier financed by the university focus “Molecular Interactions between Intracellular Bacteria and their Eukaryotic Host Cells” Title: „ <i>Functional analyses of chlorite dismutase-like proteins from Listeria monocytogenes and Nitrobacter winogradskyi</i> “

Publications

Füreder S, Wagner M, Furtmüller PG, Ettwig KF, Decker T, Freitag NE, Witte A, Daims H and Charpentier E (2009) "Characterization of the chlorite dismutase homologue in *Listeria monocytogenes*", submitted to AEM

Hesselsøe M, Füreder S, Schloter M, Bodrossy L, Iversen N, Roslev P, Nielsen PH, Wagner M, Loy A (2009). „Isotope array analysis of *Rhodocyclales* uncovers functional redundancy and versatility in an activated sludge", ISME Journal, Epub 2 July 2009.

Reipert BM, Ilas J, Carnewal C, Füreder S, Bözlbauer U, Teschner W, Fiedler C, Schwarz HP (2006). „Fc function of a new intravenous immunoglobulin product: IGIV 10% triple virally inactivated solution", Vox Sang. 2006 Oct; 91(3):256-63.

Poster presentation

Stephanie Füreder, Thomas Decker, Michael Wagner, Holger Daims and Emmanuelle Charpentier (2007) "Characterization of a putative chlorite dismutase gene in *Listeria monocytogenes*", IMP PHD symposium, Vienna